5-2001

An Externally-Synchronized Coherent Communication System Design

Gary R. Ragsdale
University of Tennessee - Knoxville

To the Graduate Council:

I am submitting herewith a dissertation written by Gary R. Ragsdale entitled "An Externally-Synchronized Coherent Communication System Design." I have examined the final electronic copy of this dissertation for form and content and recommend that it be accepted in partial fulfillment of the requirements for the degree of Doctor of Philosophy, with a major in Electrical Engineering.

Daniel B. Koch, Major Professor

We have read this dissertation and recommend its acceptance:

Michael J. Roberts, Paul B. Crilly, Balram S. Rajput

Accepted for the Council:

Carolyn R. Hodges

Vice Provost and Dean of the Graduate School

(Original signatures are on file with official student records.)

To the Graduate Council:

We are submitting herewith a dissertation written by Gary Ragsdale entitled "An Externally-Synchronized Coherent Communication System Design." We have examined the final copy of this dissertation for form and content and recommend that it be accepted in partial fulfillment of the requirements for the degree of Doctor of Philosophy, with a major in Electrical Engineering.

Daniel B. Koch, Major Professor

We have read this dissertation
and recommend its acceptance:

Michael J. Roberts

Paul B. Crilly

Balram S. Rajput

Accepted for the Council:

Dr. Anne Mayhew
Interim Vice Provost and
Dean of The Graduate School

(Original signatures are on file in the Graduate Admissions and Records Office.)

An Externally-Synchronized Coherent Communication System Design

A Dissertation
Presented for the
Doctor of Philosophy
Degree
The University of Tennessee, Knoxville

Gary L. Ragsdale
May 2001

DEDICATION

I dedicate this work to my creator, my savior, and my family. To God and his son Jesus Christ, I offer praise for giving me life and for giving my life direction according to His plan. (Psalm 118:8)

To my wife Joyce, I give my deepest affection for filling my life with enduring love and happiness. We have traveled many roads together. She is my friend.

To my daughters Holly and Shannon, I give a warm embrace that symbolizes the love and pride that I have for them. I pray for God's blessings and guidance upon them. May they know happiness, fulfillment, and peace for all of their lives.

ACKNOWLEDGEMENTS

I extend my deepest appreciation to Dr. Daniel B. Koch for his trust, advice, and leadership during my graduate program and the preparation of my dissertation. Dr. Koch has been an outstanding instructor and advisor. My thanks also goes to Dr. Michael J. Roberts, Dr. Paul B. Crilly, and Dr. Belram S. Rajput for serving on my doctoral committee and for their guidance in the refinement of the research. I take pride in my association with the University of Tennessee, its faculty, and its administration.

I gratefully acknowledge the contributions of my fellow research engineer Tom Warnagiris. His experience in radio frequency communications, suggestions, and insight was a frequent aid to me during the research.

I offer my thanks to Southwest Research Institute and its management for their active support during my doctoral program. I often used Institute tools, laboratory equipment, the Library, and facilities provided during the research and compilation of this dissertation. The Institute Library staff provided valuable literature research assistance and acquired much of my reference materials.

I wish to thank Dr. Walter L. Green for his counsel at a critical time in my life. His unselfish advice and words of encouragement brought me to the University of Tennessee.

ABSTRACT

The research described within this dissertation was initiated on October 1, 1997 to investigate communication link performance improvements made possible by using a frequency reference supplied by a residual carrier broadcast. The primary link types considered were radio frequency links, although prior research in externally-synchronized bistatic radar was also considered.

Conventional radio frequency communications links transfer information from transmitter to receiver by modulating a carrier signal at the transmitter and demodulating the received signal at the receiver. Demodulation can be done coherently or noncoherently. That is, the information on the received signal can be recovered by comparison of the received signal with an exact replica of the transmitter carrier (coherent demodulation) or by other methods that do not require a replica of the transmitter carrier (noncoherent demodulation).

Coherent demodulation provides superior link performance in the form of lower bit error rate (BER) for a received signal with a given signal-to-noise-ratio (SNR). Unfortunately, it is not always possible to produce a reliable replica of the carrier signal from the information-bearing signal.

The studied approach supplies a residual carrier reference signal as a synchronization reference common to both transmitter and receiver. Research shows that the common reference provides carrier synchronization and stabilizes the link carrier frequency.

The investigations performed under this research effort includes developing a model for a radio frequency (RF) link using an external reference signal, determining the effects of noise on the simulated reference signal, and comparing the simulated link performance with conventional links, which recover a carrier from the received signal. The model consists of three parts. The first part consists of a model using conventional synchronization in which the carrier is extracted from the information-bearing signal. The second part models the behavior of phase-locked loops (PLLs) when referenced to a residual carrier reference signal. The third part is a design tool for predicting the synchronization and bit error performance of a transmitter and a receiver synchronized to external residual carrier broadcast (a triad configuration). The models demonstrate that a transceiver referenced to a double-sideband residual carrier broadcast maintains synchronization at a very low received SNR.

Results of this research could be used in the development of externally-referenced wireless links for commercial and military applications. The models could serve as design aids to determine the expected performance of such systems.

TABLE OF CONTENTS

LIST OF FIGURES

LIST OF TABLES

LIST OF ACRONYMS

AGC	Automatic Gain Control
ALE	Automatic Link Establishment
AM	Amplitude Modulated
AWGN	Additive White Gaussian Noise
BER	Bit Error Rate
BFSK	Binary Frequency Shift Keying
BLPL	Band-pass Limiter Phase Lock Loop
BLSL	Bandeaus Limiter-Squaring Loop
BPSK	Binary Phase Shift Keying
CED	Communications Engineering Department
CNR	Carrier-to-Noise Ratio
CDMA	Code Division Multiple Access
DPSK	Differential Phase Shift Keying
DS	Direct Sequence
DSB-RC	Double-Sideband Residual Carrier
DSB-SC	Double-Sideband Suppressed Carrier
FCC	Federal Communications Commission
FDM	Frequency Division Multiplex
FH	Frequency Hopping
FSK	Frequency Shift Keying
GPS	Global Positioning System
HF	High Frequency
ISM	Instrumentation, Science, and Medical
LANs	Local Area Networks
LF	Low Frequency
MCD	Mathcad Document
NFSK	Noncoherent Frequency Shift Keying
NIST	National Institute of Standards and Technology
NTSC	National Television Standards Committee
PAL	Phase Alternating Line
PDF	Probability Density Function
PLL	Phase-Locked Loop
PN	Pseudo-random Number
PSK	Phase Shift Keying
QAM	Quadrature Amplitude Modulation
RC	Residual Carrier
RF	Radio Frequency
RMS	Root-Mean-Square
SC	Suppressed Carrier
SNR	Signal-to-Noise Ratio
SSB-SC	Single-Sideband Suppressed Carrier

SSB	Single-Sideband
TDM	Time Division Multiplex
TDMA	Time Division Multiple Access
TH	Time Hopping
TV	Television
UHF	Ultra High Frequency
VCO	Voltage-Controlled Oscillator
VI	Virtual Instrument
VSB-RC	Vestigial-Sideband Residual Carrier

CHAPTER 1 INTRODUCTION

This paper examines unique research regarding wireless modems synchronized to a double sideband-residual carrier (DSB-RC) broadcast signal. The research examines questions regarding the performance of externally-synchronized modems in comparison to conventional wireless modem synchronization. The following sections describe the unique aspects of externally-synchronized wireless modem research as it compares to prior research in various forms of communication synchronization.

1.1 Synchronization in Communication Systems

The word "synchronization" originates in the word "synchronous," which means "occurring at the same time" or "having identical period and phase" [1]. Synchronization is a fundamental requirement with radar, sonar, navigation, and communication systems. For example, radar systems require synchronization within their components as a prerequisite for accurately deriving range, velocity, and position from received signals [2].

"Frequency stabilization" is another form of synchronization found within frequency division multiplexed (FDM) systems. Frequency stabilization maintains constant relative spacing between FDM channels. It also maintains an absolute frequency reference for distinguishing individual channels within the FDM system.

Within digital communication systems, synchronization is a process of estimating frequency and time relationships among systems elements. Digital communication synchronization falls within five general categories: carrier, bit, codeword, frame, and

network [3, 4]. Carrier synchronization is necessary for phase coherent detection of modulated digital symbols. Bit synchronization, also referred to as "clock" synchronization, provides time demarcation of bit boundaries within digital transmission systems. Codeword synchronization defines the boundaries of symbol blocks used in encoded transmissions. Time division multiplexed systems maintain frame synchronization for proper time alignment of concatenated data samples in which each sample consists of multiple symbols. Network elements receiving information from and transmitting information to other network elements maintain network synchronization as means of reducing buffer requirements and simplifying the network design.

1.2 Problem Statement

The research described herein explores methods for analyzing and improving the performance of frequency stabilization and carrier synchronization within wireless digital communication systems. Radio frequency (RF) channel impairments and practical design constraints limit the effectiveness of wireless data transmission. Data transmission through an RF channel is subject to many forms of interference. Noise, Doppler shift, and multipath disturbances are inherent to the channel's physical characteristics. In addition, phase, frequency, and symbol synchronization errors develop from design limitations found within the transmitter and receiver synchronization components.

Technology and cost constraints bound the accuracy of coherent synchronization systems and the ability to stabilize FDM systems. Coherent and FDM systems frequently rely upon local oscillators as carrier or frequency references. Low cost oscillators drift

from their nominal frequency as a function of temperature variation and component aging. Highly accurate atomic oscillators and thermally stabilized oscillators provide much greater reference stability, but are too costly or bulky for many wireless applications. Consequently, wireless modems frequently employ carrier references that suffer from frequency and phase variations.

Coherent modems maintain frequency and phase synchronization as a necessary part of accurate symbol detection. Under conventional design, wireless transmitters and receivers contain local oscillators sufficiently stable to reduce frequency drift to a slow process. Wireless channel bandwidth allocations include bandwidth allowances for oscillator drift called "guard bands." The guard bands must be sufficiently large to allow for normal transmitter oscillator drift without impinging upon an adjoining channel.

Wireless receivers compensate for slow variations in the transmitter oscillator by tracking the received signal carrier using a PLL. Received noise causes time variations in the PLL phase estimate, an impairment referred to as “phase jitter.” Phase jitter greater than 0.4 radians leads to a large, nonreducible error within the receiver symbol detector and substantially reduces the effective SNR of the received signal with an attendant increase in the probability of a symbol error [5]. Carrier phase reference inaccuracies force modulation design compromises within the remainder of the transmitter-receiver architecture.

Coherent modulation offers inherently better transmission performance when compared with noncoherent modulation schemes. Even so, coherent modulation may not be suitable for some channel types due to carrier reference limitations. Considerable

research already exists regarding optimum modulation design using an internal carrier reference, i.e., carrier synchronization references embedded within the transmitter and receiver.

Developments in externally-referenced synchronization may change the paradigm of optimum transmitter-receiver design and suggest the need for new research. Recent Southwest Research Institute (SwRI) internal research and development (IR&D) efforts created frequency references derived from an external source, such as Amplitude Modulation (AM), National Television Standards Committee (NTSC), or National Institute of Standards and Technology (NIST) time reference broadcasts. The derived reference is inherently accurate, and in some cases, is less complex than the equivalent internal reference. The receiver and transmitter derive their reference from the same external source, thereby reducing problems of internal reference drift. This new concept in synchronization calls for new research for optimum transmitter-receiver design.

Until recently, the NIST and other international organizations operated the only recognized reference broadcasts [6]. Their broadcasts occur at HF (e.g., 2.5 MHz, 5 MHz, 10 MHz, 15 MHz, etc.) and suffer from multiple propagation problems (fading, multipath, etc.). In the past, the additional circuit complexity required to deal with HF propagation problems was costly for most applications. Consequently, little attention has been given to the use of these signals for direct frequency generation of transmitter and receiver carrier references.

Today the GPS signal serves as a synchronization reference for radar, communication networks, and many other complex systems [7, 8]. GPS is available

essentially worldwide without significant propagation degradation. At the same time, the cost of hardware for using the GPS or other signals has dropped significantly. Although GPS references are still expensive for some applications, they are being designed into commercial wireless communications systems as external synchronization references. The advent of an accurate external reference coupled with reduced hardware cost creates new opportunities for externally-referenced synchronization. The GPS precedent suggests other references might be opportunistically used as synchronization references.

1.2.1 Externally-Synchronized Wireless Modems

This research investigates a wireless modem transmitter-receiver pair (transceiver) operating in the presence of a commercial grade, AM radio broadcast as regulated by the Federal Communications Commission (FCC). Under regulation, the AM broadcast frequency must be accurate to within 20 Hz of the FCC-assigned center frequency [9, 10]. As such, an AM broadcast represents a potentially stable source of frequency and phase synchronization for the transceivers. If PLLs embedded within the transmitter and receiver track the AM carrier, then theoretically, their PLLs will maintain relative frequency and phase synchronization

Research conducted by the author explores a technique in which wireless transmitter and receiver PLLs track the AM carrier frequency and phase. Investigation attempts to show that the transmitter-receiver pair operate at the same frequency and at a constant phase offset for any stationary configuration of AM broadcast station, transmitting modem, and receiving modem. Under the scheme shown in Figure 1–1,

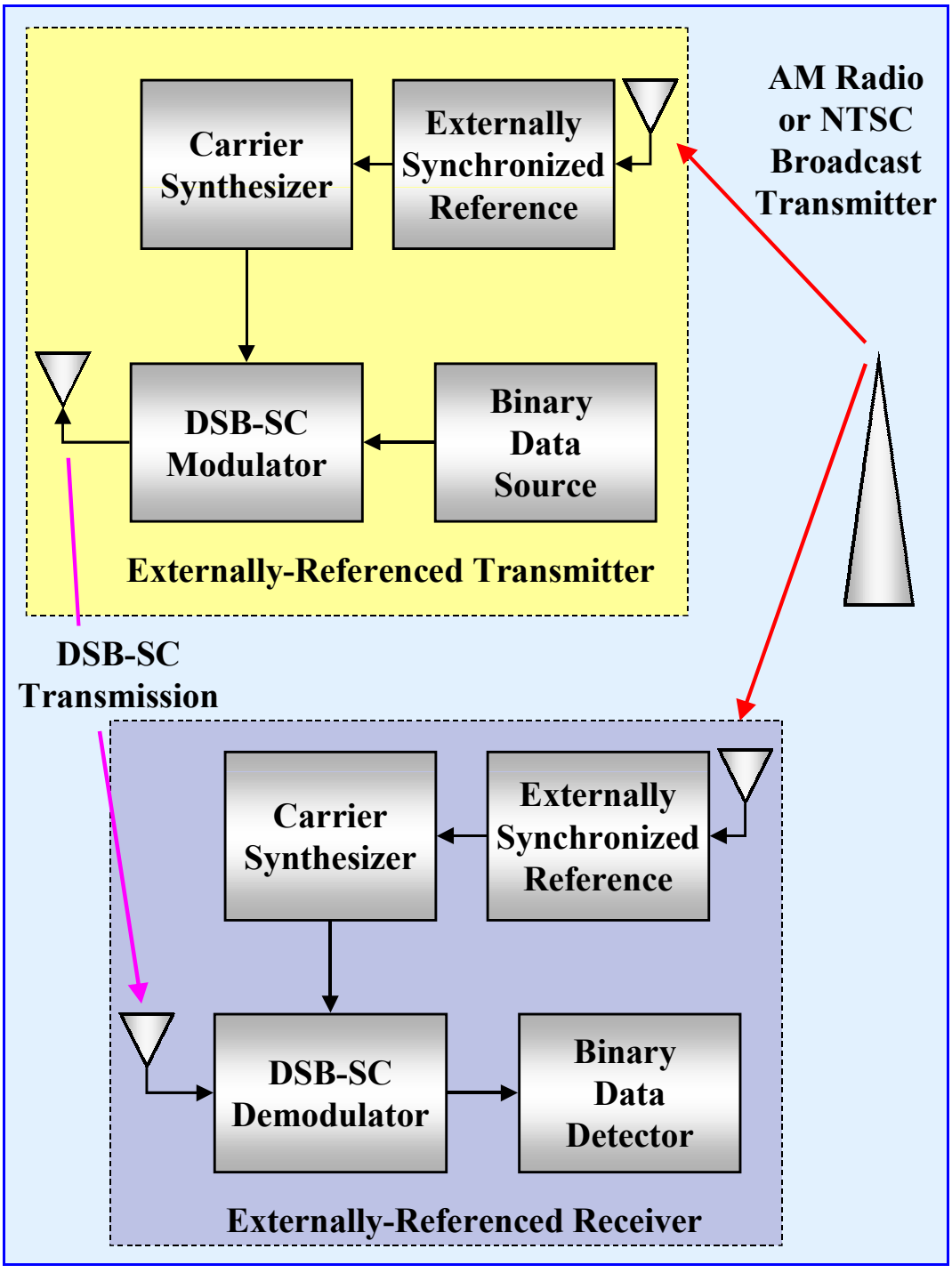

Figure 1–1. Wireless Modems Synchronized to an AM Broadcast

wireless modems use the AM station as an intermediate frequency reference for binary phase shift keying (BPSK) or differential phase shift keying (DPSK) modulation at an arbitrary broadcast frequency. Externally-referenced transceivers have a continuous source of synchronization so long as the AM broadcast is present and is not experiencing over-modulation. Questions arise regarding the affects of noise and AM modulation on transceiver reference accuracy.

1.2.2 Considered Questions

Synchronizing a wireless system to a DSB-RC broadcast raises questions regarding the resulting system design. Clearly, a system configured as shown in Figure 1–1 will lose synchronization in the absence of the reference broadcast. Answers to other design questions are not so obvious. There are four research questions under consideration within this study:

1. Is it possible to predict the mean phase error at the receiver?
2. Is it possible to predict the phase jitter (error standard deviation) σ_ϕ at the receiver?
3. Is it possible to predict the BPSK bit error probability?
4. Is it possible to predict the required AM carrier SNR at the transceiver?

CHAPTER 2 RELATED RESEARCH

A literature search found several research areas involving related forms of system synchronization. Key words used in the search included:

- “common frequency reference” or “common timing reference”
- “coherent detection”
- “carrier recovery”
- “BER improvement”
- “link margin”
- “pilot carrier”
- “demodulation”
- “synchronization” or “symbol synchronization” or “bit synchronization”
- “PLL” or “phase-locked loop” or “phase lock loop”
- “external” or “out of band” or “common channel”
- "external synchronization reference" or "external synchronization"
- “bistatic” or “tristatic”
- “opportunity” or “opportunistic”
- “DPSK” or “differential phase shift keying”
- “phase offset” or “phase error” or “phase jitter”
- “frequency offset” or “frequency error” or “frequency stabilization”

2.1 Related Patents and Experimentation

The search found expired US Patent No. 4,117,005 in which Louis Martinez proposes the concept explored by this paper. Martinez's patent discloses the use of an AM radio broadcast as a source of frequency stabilization for a narrow-band frequency division multiplexed telemetry system [11]. It predicts reduced transmission bandwidth requirements and makes claims of improved data reception. The patent reveals no analysis of the effects of noise and AM modulation upon system synchronization accuracy. The patent offers no evidential research or measurements to support its claims of improved reception performance.

In [13], Martinez describes experiments conducted for the Electric Power Research Institute (EPRI) exploring the wireless exchange of power management control commands and telemetry. During these experiments, Martinez developed a telemetry system based upon Patent No. 4,117,005 in which an AM radio broadcast was used as synchronization for a population of narrow-band transceivers. Telemetry transmitters sent kilowatt-hour readings from power usage meters to a centrally located receiver. His publication mentions error rates of less than 1%, but does not quantify the nature of the errors, how they were measured, or why they occurred. Martinez documented his work in a report provided to EPRI.

Martinez discussed his experiments during telephone interviews on April 8 and April 18, 2000 [12]. Martinez described externally-referenced, wireless modems that were stable to within 10^{-9} Hz at the carrier frequencies employed during his experiments. The experimental systems maintained synchronization except when large trucks passed

within 300 feet of the system. Multipath signal distortion created by the passing trucks caused momentary losses of system synchronization.

Some of Martinez's experiments employed Fast Fourier Transforms (FFTs) as narrow-band filters and an AM broadcast reference configured into a closely spaced frequency division multiplexed (FDM) system. The lack of powerful digital signal processors during the late 1970's and early 1980's constrained his system to four, closely spaced FDM channels. His experiments ended when he sold his company.

When contacted directly, Martinez could not provide experimental data regarding the bit error rate performance or signal-to-noise ratio (SNR) sensitivity. He was unable to supply a copy of the EPRI project report cited in [13]. Literature searches found no record of EPRI publishing Martinez's reports. EPRI could not provide copies of the Martinez project report when contacted directly by the Southwest Research Institute Library.

Available publications of Martinez's work contain no analysis or experimental data that describe the performance or design constraints of externally-referenced, wireless modems. His publications describe conceptual or functional systems, but do not quantify the resulting system behavior beyond those observations already mentioned. Consequently, Martinez's work provides no theoretical analysis upon which to base system designs or predict the behavior of a given design.

2.2 External Synchronization in Spread-Spectrum Radio

Spread-spectrum radio systems share spectrum through a method called code division multiple access (CDMA). Code division multiple access methods spread an

information bearing signal over a much wider bandwidth by functionally combining each transmission with the output of a pseudo-random number (PN) generator [14]. Each transmitter's PN generator operates upon a specially designed "chipping" code. Chipping codes are mutually orthogonal. Consequently, only transceivers operating with the same chipping code may despread the transmission and receive the communication. All other transceivers perceive transmissions orthogonal to their own as low-level noise.

Spread-spectrum systems must also achieve PN generator clock synchronization as a prerequisite to communication. Lacking clock synchronization, the signal spreading and despreading process will not correlate properly between intended transceivers. Achieving CDMA clock synchronization has been a topic of considerable research. The following sections describe efforts to use external references as a source of a CDMA clock.

2.2.1 Amateur Radio Experimentation

Amateur radio operators contend with many transmitters attempting to share a relatively small portion of the radio frequency spectrum. Interference and lack of access to the medium are frequent problems, especially as the number of operators grows and as competition for spectrum increases.

Amateur radio organizations received FCC Special Temporary Authority during 1981 to carry out experiments in code division multiple access techniques with the intent of implementing a more efficient method for sharing the spectrum [15]. Amateur radio operators received permanent authority to operate wireless spread-spectrum systems when FCC Report and Order in GEN Docket 81-414, "Amendment of Parts 2 and 97 of

the Commission's Rules and Regulations," authorized spread-spectrum techniques in the Amateur Radio Service on June 1, 1986 [16, 17].

Much of the amateur radio experimentation that followed the FCC rulings focused upon maintaining spreading code synchronization. A community of code division multiple access transceivers must maintain PN generator clock synchronization as a prerequisite for spreading and despreading information-bearing broadcasts. Synchronization experiments focused on the problem of finding a common clock reference. William Sabin first suggested the use of indigenous radio broadcasts when he proposed the use of the NIST WWV radio broadcast as a source of mutual synchronization for spread-spectrum communication [18]. Other experimenters expanded upon Sabin's suggestion by exploring several forms of external synchronization.

André Kesteloot was the most actively published of the external synchronization experimenters. His early experiments in slow frequency hopping used an NTSC vertical blanking synchronization pulse extracted from a television receiver as the PN generator clock. His transceivers obtained a common clock by tuning their NTSC receiver subsystems to the same television broadcast. Kesteloot's externally-referenced, frequency-hopping system maintained synchronization for periods of 90 minutes or more [19].

Kesteloot's later experiments turned to the problem of synchronizing direct sequence spread-spectrum (DSSS) systems [20]. NTSC vertical blanking clocks were too slow to provide adequate spreading within a DSSS system. Kesteloot's DSSS

experiments created a 3.579544 MHz (±10 Hz) PN generator clock from the NTSC chrominance subcarrier [21]. His later experiments included the construction of a system incorporating a 1.5 MHz PN generator clock derived from an AM radio broadcast carrier [22].

Kesteloot's articles provide insight into the construction of externally-referenced, spread-spectrum systems. His articles provide circuit schematics, alignment procedures, and hints on achieving good system function. He describes system performance in general terms and mentions design constraints. For example, Kesteloot warns that multiplying an AM broadcast reference at 1.5 MHz to frequencies of 400 MHz or higher creates excessive phase jitter within the PN generator clock. He also states that his AM broadcast-referenced systems required a manual phase adjustment to compensate for the relative location of the transmitter, receiver, and AM broadcast antenna. His comments relate closely to Questions 1 and 2 in Section 1.2.2. His articles provide no analysis describing system design constraints. He does not make theoretical estimates or experimental measurements for clock timing jitter or mean phase error. Consequently, they provide no analysis that would lead to answers to the questions explored by this research.

Kesteloot's work differs from this research in several key areas. His DSSS research derives a PN generator clock for use in spreading and despreading a voice- or data-modulated signal. Note that the proposed research here uses the residual carrier to synchronize a phase-locked loop for the purposes of frequency stabilization and coherent demodulation. Kesteloot did not use the AM broadcast carrier for either purpose.

Instead, he relies on frequency reference oscillators internal to the transceivers and noncoherent detection of the despread signal at the receiver.

2.2.2 Code Division Multiple Access Cellular Systems

Spread-spectrum cellular telephone networks regularly use external synchronization to maintain CDMA clock timing. Early cellular networks distributed atomic clock-based timing to cellular base stations over digital landlines. Distributing clock references over landlines is a costly and complex process, especially in rural areas where digital landline technology is scarce.

Modern CDMA cellular station derive clock timing by viewing the GPS constellation [23, 24]. GPS clock timing for military applications is accurate to within 20ns of Coordinated Universal Time (UTC) [25]. United States Department of Defense restrictions, called "Selective Availability," limited the GPS accuracy for commercial use to 100ns. Recent changes in United States policy now make the full precision of GPS available to commercial applications [26].

Current practice applies external synchronization within the CDMA cellular networks to PN generator clock timing. None of the available research employs external synchronization for carrier generation or frequency stabilization.

2.3 Pilot Tone Synchronization to Combat Fading

Mobile wireless modems experience signal fading and Doppler shifts sufficient to disrupt single sideband-suppressed carrier (SSB-SC) and double sideband-suppressed carrier (DSB-SC) data communications [27, 28, 29]. Increasing the received signal

power does not mitigate rapid Rayleigh fading. Without some form of fading compensation, mobile wireless modems suffer from irreducible error, especially as the carrier frequency and the velocity of movement increase.

Researchers found that pilot tones introduced at frequencies within the communications channel spectrum could be used to counteract rapid fading and Doppler shift. Pilot tones injected by the transmitter within the channel spectrum experienced impairments similar to those experienced by the modulated signal [30]. By first assuming that good correlation exists between the pilot tone and the modulation impairments, specially designed receivers recover the impaired pilot tones and use the tones as a compensation reference for automatic gain and frequency controls, thereby counteracting the effects of fading and Doppler shift.

Correlation between the pilot tone and modulated signal impairments depends upon the placement of the tone or tones within the channel spectrum. Tones that appear near the center of channel exhibit higher degrees of impairment correlation. However, pilot tones may not appear within any portion of modulation spectrum. Otherwise, an injected pilot tone interferes with the modulated signal.

Several different schemes developed regarding tone placement and the avoidance of tone interference. Early developments placed a single pilot tone at the upper or lower boundary of a tapered channel spectrum [31]. Injecting tones at the edge of the channel spectrum minimized the bandwidth consumed by the pilot tone. Implementation of an "above band" or "below band" pilot and a shaped modulation spectrum was relatively straightforward to implement. However, the lowest impairment correlation between the

modulation and the tone occurs at the spectrum periphery. Later research combined two pilot tones placed at the upper and lower boundary as a means of improving system performance [32].

Pilot tone systems achieve their best anti-fading performance when a pilot tone appears at or near the center frequency of the channel. However, modulation techniques often have frequency components throughout the central portion of the spectrum. Improper placement of a pilot tone interferes with the modulated signal and reduces signal detection performance.

Researchers developed several designs for creating "holes" (a range of frequencies where no modulation energy appears) in the channel spectrum. "Transparent tone in-band" (TTIB) designs placed a pilot tone within a strategically created spectrum "hole." A. Bateman and J. P. McGeehan studied TTIB systems that split an SSB-SC spectrum into upper and lower bands [33, 30]. Translation of the upper band to a subcarrier frequency and carefully matched filters opened a hole for a pilot tone near the center of the spectrum. However, placement of tone at a frequency other than the carrier frequency is less than ideal for DSB-SC modulation.

A pilot tone placed at the DSB-SC carrier frequency can serve as an anti-fading pilot tone and as a carrier reference for coherent demodulation. Staff at the Jet Propulsion Labs and General Electric Corporation jointly created a TTIB scheme whereby Manchester encoding created a spectral null at the carrier frequency [34]. A pilot tone injected at the carrier frequency served the dual role of automatic gain control and coherent demodulation reference. Yokoyama proposed an "orthogonal TTIB" scheme

consisting of a BPSK modulated signal combined with an orthogonal pilot tone located at the carrier frequency. In the orthogonal TTIB scheme, the receiver recovers the orthogonal pilot tone for use in anti-fading compensation and coherent detection [35].

TTIB pilot tone systems differ from this study in two ways. First, the presence of a pilot tone by itself does not aid in frequency stabilization. The referenced TTIB techniques rely on an internal oscillator as a source of pilot tone. This oscillator may be the same reference used for modulation in Manchester-encoded and orthogonal TTIB systems. TTIB reference oscillators are subject to the same design limitations and frequency drift inherent to conventional DSB-SC modulation systems. Second, external synchronization as studied herein does not rely on a pilot tone. The addition of a pilot tone within an externally-synchronized modem poses an interesting topic for further research.

2.4 External Synchronization in Radar Systems

Like coherent modems, radar systems must maintain frequency and phase synchronization between the transmitter and receiver for effective processing of reflected signals. Conventional radar systems place the transmitter and receiver in close proximity to one another or even combine them into a single transceiver. Maintaining synchronization within a combined transceiver is a trivial problem. However, not all radar systems follow the conventional radar topology.

2.4.1 Bistatic Radar

Bistatic radar systems differ from other types of radar in that the bistatic configuration separates the radar transmitter from the receiver by a substantial distance. A bistatic transmitter illuminates targets within the detection area. The transmitter modulates its broadcast in a manner facilitating parameter estimation at the receiver [36]. Bistatic receivers process reflected signals, estimate target location, velocity, and other signal parameters using a complex set of functions.

Transceiver frequency and phase synchronization is necessary for proper processing of the modulated radar signal [37]. Research papers [38, 39] discuss five methods for bistatic transceiver synchronization:

1. The receiver tracks the transmitter's line-of-sight broadcast using a PLL [40].
2. The receiver tracks nearby ground clutter or other multipath reflections of the transmitter broadcast.
3. A separate communication channel relays synchronization signals from the transmitter to the receiver.
4. Both transmitter and receiver employ ultra-stable atomic clocks with periodic recalibration.
5. Both transmitter and receiver track an external clock source (e.g., Navstar-GPS, Loran C) [39, 36, 7].

There are several parallels between wireless modem and bistatic radar research. Synchronization Method 1 appears in the operation of conventional wireless modems in which a line-of-sight receiver derives synchronization from the transmitter's broadcast.

The transmitted signal conveys both information and a synchronization reference. Both transmitter and receiver contain moderately stable local oscillators. The receiver uses its internal oscillator, the received signal, and a PLL to track the transmitter's oscillator variations.

Bistatic radar Synchronization Method 3 resembles methods employed within digital microwave systems and other digital information distribution systems (e.g., North American digital signal hierarchy [DS-X], European CEPT, SONET, and SDH). Microwave transceivers frequently derive synchronization from a central atomic clock distributed to all transceiver sites over separate communication channels. In the case of wireless modem design, Method 3 would require a dedicated synchronization from a common source to each of the wireless transceivers.

Bistatic radar Synchronization Method 5 most closely resembles the proposed research in externally-referenced wireless modems. Method 5 and this research employ moderately stable local oscillators within the transceiver pair. Both transmitter and receiver track a highly stable synchronization signal using their local oscillator and a PLL. In both cases, the receiver ignores frequency and phase information resident within the transmitter's broadcast.

This research in externally-referenced wireless modems differs from bistatic radar research in the following ways:

1. The DSB-RC station modulation does not convey information to the modems as is the case in bistatic radar "illuminators of opportunity" [41].

2. The modems convey information at another frequency outside the DSB-RC frequency band.
3. The proposed modem configuration exchanges BPSK or DPSK modulation using the DSB-RC broadcast as a frequency stabilization and phase coherent carrier reference.
4. Conventional DSB-RC, AM radios extract information from the modulated signal using envelope detection. An AM radio does not concern itself with carrier synchronization.

2.4.2 Passive Radar

In their passive radar system, Griffiths and Long employ a Phase Alternating Line (PAL) television broadcast as an "illuminator of opportunity" [41]. Radar receivers synchronize to the line-of-sight television (TV) broadcast and correlate target parameters using the modulation inherent to the PAL broadcast. A similar system called "Silent Sentry" uses multiple TV and AM radio broadcasts to track aircraft [42]. Large amounts of signal processing give accurate results using three or more transmitters of opportunity. There are no radar transmitters in either of these bistatic radar designs other than the opportunistic transmissions of available DSB-RC or vestigial sideband-residual carrier (VSB-RC) broadcast stations.

Research in externally-referenced wireless modems has parallels to opportunistic bistatic and multistatic radar research in that the research relies on available DSB-RC or VSB-RC broadcasts for synchronization. However, the proposed wireless modem synchronization technique derives no information other than synchronization from the

AM broadcasts. In contrast, passive radar systems extract information from the line-of-sight and reflected broadcast signals.

2.5 Externally-Referenced Timing

External synchronization is common practice among time division multiplexed (TDM) communication systems. For example, the North American DS-X, European CEPT, ISDN, SONET, and SDH systems distribute network and frame synchronization derived from a dedicated atomic clock to switching and multiplexing elements via a separate communications channel [4, 43].

It is also possible to derive network synchronization across multiple network elements from a GPS transmission [8]. Many communication networks use GPS as a coordinated timing reference. For example, radio paging systems use GPS timing to arbitrate a shared broadcast channel. Time division multiple access (TDMA) cellular systems use GPS to define frame and slot timing. Many of these systems rely on GPS to produce pulse-per-second clocks that synchronize the rest of the TDMA system [25].

Past research explored residual carrier broadcasts as a source of TDMA timing. Wei Zhu experimented with a German wireless communication system that derives synchronization from an AM time reference [44]. The time reference transmitted a 100ms ("0") or 200ms. ("1") pulse each second on a precise carrier centered at 77.5 kHz. Vehicular transceivers used the pulse timing and broadcast carrier zero-crossings as delimiters of TDMA frames and time slots within a given frame. Zhu's research studied the effects of timing error and timing jitter. His system did not use the 77.5 kHz carrier

for PLL synchronization. He did not study the use of the AM broadcast as a modulation reference or as a source of frequency stabilization.

This research focuses on carrier synchronization of wireless transceivers. The proposed scheme provides the added benefit of frequency stabilization when multiple transceivers are operating on adjoining FDM channels. This research does not explore the use of AM radio transmissions as a source of network or frame synchronization. Additional research opportunities may exist for adapting the work in [44] to conventional AM broadcasts, thereby creating a system that derives carrier, frame, and slot synchronization within a wireless TDMA system.

2.6 Optical Frequency Stabilization

In [45], the authors describe a scheme for maintaining relative and absolute frequency stabilization within an optical frequency division multiplexed (OFDM) system. Their scheme requires all OFDM signals to pass through an optical hub. Contained within the hub is a precise optical reference oscillator and a frequency comparator. Optical signals are compared with the optical reference one at a time. The hub sends error signals back to the transmitters over a separate control channel. The scheme maintains relative to frequency stabilization, thereby keeping channel spacing constant. It also maintains an absolute frequency reference for distinguishing individual OFDM channels.

Based upon a comprehensive search of published literature and interviews with Martinez, no published research currently exists that analyzes or simulates the use of residual carrier broadcasts as a source of carrier synchronization for wireless applications.

The remaining sections explore the operation of an externally-referenced, carrier synchronized system.

2.7 Research Motivation

This study describes new and interesting opportunities for research in wireless modem synchronization. There are sufficient differences to distinguish this research from prior research in external synchronization. The research produces new information regarding the effect of noise and modulation upon carrier synchronization and frequency stabilization when a DSB-RC broadcast serves as a reference.

2.8 Overview and Contributions of the Research

The following sections describe a wireless data communication system that derives its carrier synchronization from an AM broadcast radio station, NTSC television broadcast station, or other residual carrier broadcast source. The system consists of a transmitter and receiver that transfer digital information over a separate RF channel using DSB-SC, BPSK modulation. Conventional wireless transceivers estimate carrier synchronization using signal components embedded within the information-bearing signal. In contrast, the proposed system synchronizes both the transmitter and receiver to the carrier wave transmitted by the DSB-RC broadcast station. The proposed transmitter-receiver pair derives its modulation and demodulation references from PLLs that track the DSB-RC broadcast.

The research will show that the proposed system (when operating from fixed locations) will maintain frequency stability with a constant phase offset between the

transmitter and receiver. The transceiver maintains carrier frequency accuracy as a function of the limits set by the FCC for the DSB-RC signal from which the transceiver derives its carrier reference. Figure 2–1 illustrates the arrangement of the transmitter, receiver, and AM broadcast station or other DSB-RC signal. This study refers to the system arrangement in Figure 2–1 as a "triad" system.

Computer simulations will show that the triad system operates with acceptably low levels of phase jitter under certain design constraints. Moreover, these simulations will show that triad system performance is predictable across a broad array of triad system configurations.

2.9 Anticipated Benefits from External Synchronization

This research anticipates direct benefits from the application of external synchronization references within wireless modem systems. Later in this document the concluding remarks will elaborate on benefits discussed briefly in the following paragraphs.

One of the more difficult problems encountered in carrier synchronization is that of economically achieving local oscillator stability. Local oscillator stability is a requirement in both the transmitter and receiver. Unless the transmitter and receiver maintain their transmission within the band-pass of the receiver, no detection can occur and automatic frequency control circuits are rendered useless. This is especially true as the operating frequency increases. At 1 MHz a frequency stability of 1 part in 10^6 is equal to 1 Hz. At 1,000 MHz the same stability is equal to 1,000 Hz. Narrow bandwidth communication systems (< 1,000 Hz), such as might be produced by low power data

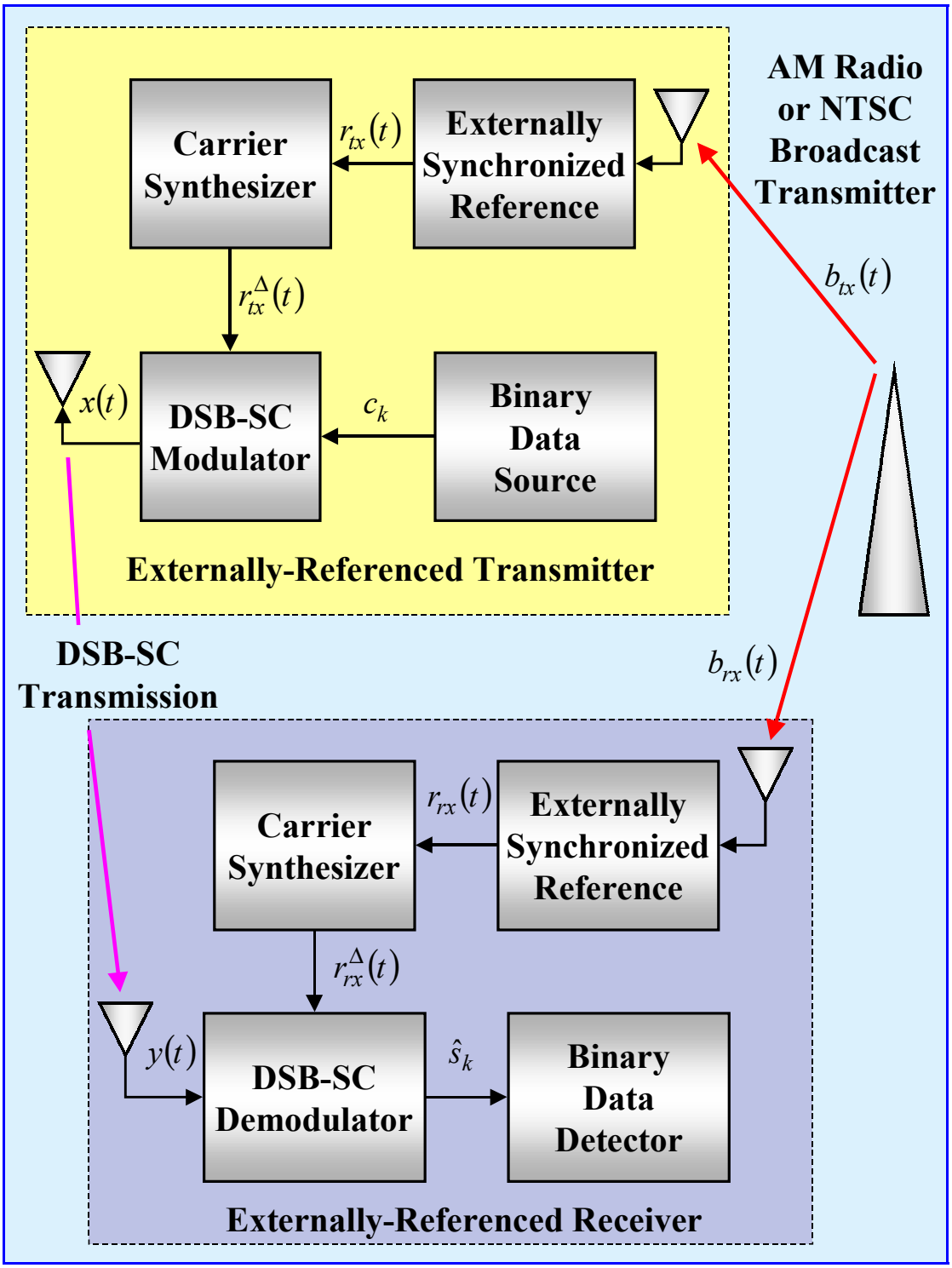

Figure 2–1. A Triad System - An Externally-Referenced Transceiver.

links, operating at high frequencies must use expensive local oscillators (e.g., a temperature controlled reference) to ensure relative accuracy between transmitter and receiver. Such stability is not normally cost effective for low data rates; consequently, wider bandwidth is normally traded for lower design cost. The wider bandwidth is often more susceptible to noise resulting in a lower link margin.

By providing a common synchronization reference, it is possible to reduce channel bandwidth to an amount related to the actual data rate of the transmission. Reduced channel bandwidth will improve the link margin, reduce interference to other users in the spectrum, and make spectrum management more efficient.

Reductions in guard band requirements will be most noticeable in narrow-band, frequency division multiplexed applications. The proposed technique maintains reliable relative and absolute frequency stability within an FDM system, thereby allowing the FDM channels to operate with more compact frequency spacing. A large number of transmitters may operate in adjacent frequency-division multiplexed channels without fear of asynchronously drifting into an adjacent channel. The triad design ensures that there is little relative frequency drift between the channels. The design also ensures that an FDM system does not drift significantly from its absolute frequency assignment.

The proposed technique may make it practical to employ coherent modulation in more wireless applications. Figure 2–2 shows that there is a significant improvement in received signal BER using coherent modulation versus noncoherent modulation. A 1 dB improvement can translate into a 26% reduction in transmitted power for the same link performance (BER) or a 26% reduction in the received bandwidth for improved data

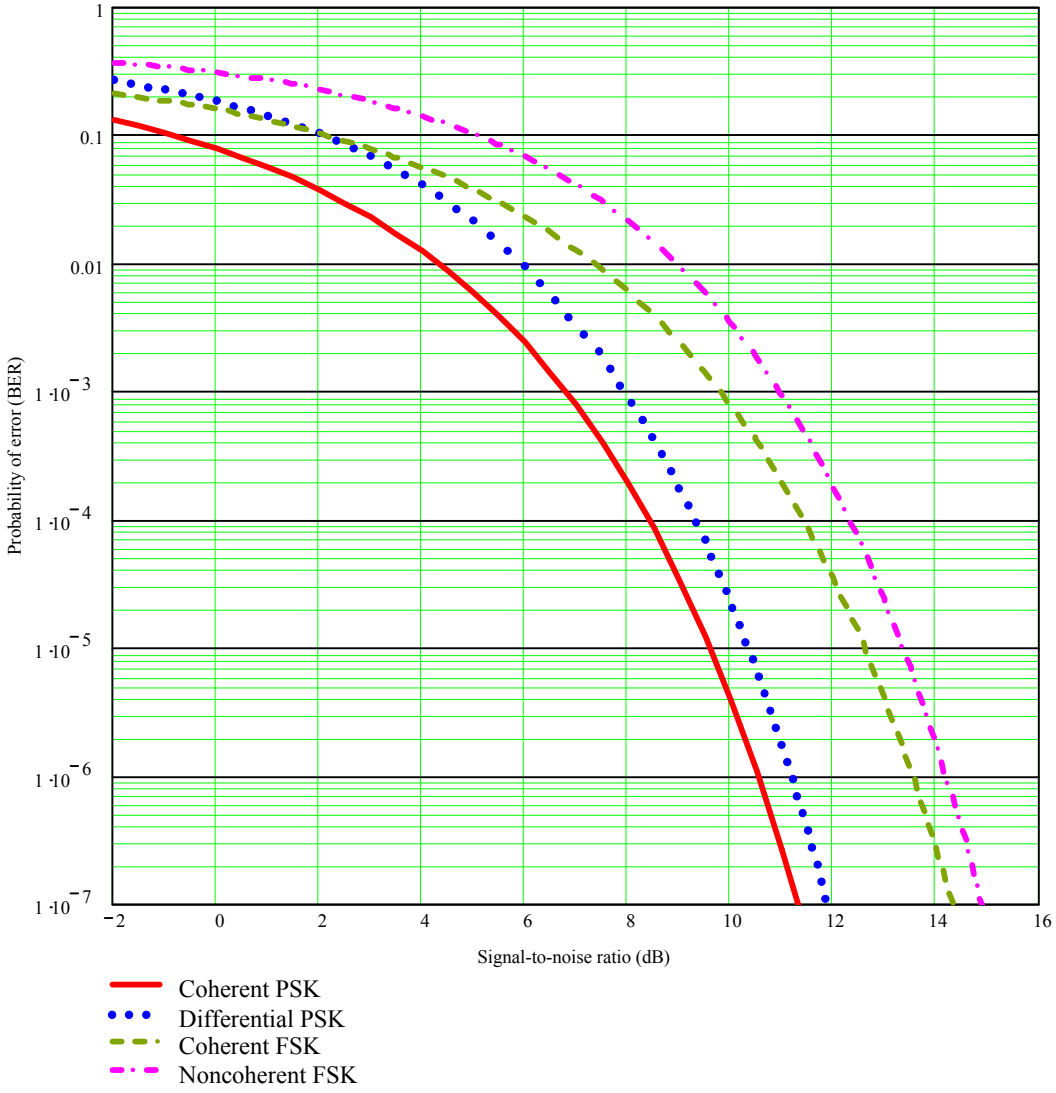

Figure 2–2. Bit Error Rate versus Modulation Type [46]

throughput. In the case of traditional internal references, the penalty for the improved performance is increased synchronization complexity and cost. For some applications, especially narrow-band applications, an external reference circuit may be less complex and could use lower cost components than a comparable design using high stability local oscillators.

The research employs narrow-band filters to extract the AM carrier for use in synchronization. It will be shown that the AM broadcast may be received at low signal-to-noise ratio and still maintain good synchronization performance.

Phase-locked loops and Costas loops commonly used in M-ary digital transmissions suffer from a phenomenon referred to as "false lock" (a condition in which tracking devices synchronize to frequencies in the modulation sidebands). The number of false lock frequencies increases as a direct relationship to the number of unique digital symbols M employed by the system [47]. Increasing M increases the number of false lock possibilities and the probability that false lock will occur.

External synchronization to AM broadcast carrier avoids the M-ary false lock condition in two ways. First, the proposed technique does not extract synchronization from the M-ary digital transmission, thereby avoiding any possibility of false lock on the digital transmission sidebands. Second, the proposed technique applies narrow-band filters to the AM broadcast signal virtually eliminating the possibility of false lock at an AM sideband frequency.

An external reference should improve frequency and phase synchronization between the transmitter and receiver as compared to conventional automatic frequency

control and phase tracking. Since the carrier establishes the frequency of the link, both the transmitter and receiver will be continuously tuned to the correct frequency and a constant phase offset. No initial synchronization, referred to as the "modem training time," will be necessary. A signal can be received immediately at the correct center frequency with the correct demodulation carrier. No signal degradation will occur due to the time lag of synchronization circuits. The synchronization channel is independent of the information channel. No reduction of synchronization accuracy should occur when the information-bearing signal is received at a low SNR.

Conceptually, narrow-band wireless modems could benefit from synchronization to a residual carrier broadcast. However, questions remain regarding an externally-referenced system design. In Chapter 3 , this research analyzes the set of system design questions raised in Section 1.2.2.

CHAPTER 3 THEORY OF OPERATION

The purpose of this research is to improve the bandwidth efficiency and accuracy of wireless communication through improvements in transceiver synchronization. It is important to understand the relationship between synchronization, modulation, demodulation, and coherent information transfer.

3.1 Modulation

Modulation is a method for matching a given information transfer to an available transmission medium (e.g., radio frequency antenna, coaxial cable, fiber optic cable). "Baseband" digital signals (e.g., unipolar, bipolar) transfer data at rates from a few bits per second to billions of bits per second. Many transmission media optimally transfer signals within a range of pass band frequencies but are not effective at the baseband frequencies comprising the digital signal. Modulation encodes baseband digital signals onto a "carrier" frequency centered within the media's transmission pass band.

Different transmitter designs use different signal encoders, called "modulators." All modulators rely on a reference oscillator as a source for carrier signal. Despite their differences, all transmitter modulators encode the data signal onto the carrier, thereby placing the data transfer within the medium's pass band.

3.2 Demodulation

There are many demodulation methods, but they all fall within two general types: coherent and noncoherent demodulation. The primary differences between the methods

lie within the receiver where demodulation is performed. Receivers contain "demodulators" that reverse the modulation process by translating the information signal back to its original form.

Demodulation is a process that translates an information-bearing signal from the pass band of a communication channel to a set of baseband frequencies. The demodulation process normally occurs immediately before the symbol detection process. Detection translates the information-bearing digital symbols back into the original information format, such as a set of binary digits (bits).

Coherent demodulators, such as phase shift keying (PSK) and coherent frequency shift keying (FSK), use a carrier reference oscillator to extract the information signal from the modulated carrier. A coherent receiver's reference oscillator approximates the frequency and phase of the transmitter oscillator. Performance of the coherent demodulation depends heavily upon the accuracy of the approximation. Consequently, designers expend considerable effort and introduce system complexity to ensure oscillator synchronization between coherent transmitters and receivers. Coherent demodulation offers the best transmission performance in exchange for its increased design complexity.

Noncoherent demodulators (e.g., noncoherent frequency shift keying [NFSK]) extract the information signal without precise knowledge of the transmitter's reference frequency. Consequently, there is little or no investment in oscillator synchronization. In fact, the receiver may not use a local oscillator. Elimination of the local frequency

reference greatly simplifies the design of noncoherent receivers. However, the reduction in design complexity has a corresponding reduction in transmission performance.

Differential phase shift keying demodulators use a local oscillator to maintain frequency coherency but do not track the transmission phase. DPSK demodulators fall in a class between coherent and noncoherent demodulators aptly called "partially coherent demodulators."

It can be shown that at the same signal-to-noise margins, coherent and to a slightly lesser degree, partially coherent demodulation, provide superior transmission performance when compared to noncoherent demodulation [48, 27]. Figure 2–2 illustrates the theoretical BER for two coherent demodulation schemes (BPSK and binary FSK [BFSK]), one partially coherent scheme (binary DPSK), and one noncoherent demodulation scheme (noncoherent BFSK) across a range of signal-to-noise margins. The curves assume perfect carrier synchronization for coherent demodulation. Using the 10 dB grid line as an example, there is a 500% improvement in BER between coherent and noncoherent PSK. Another measure of performance is to gauge the relative signal-to-noise margin for a given BER. For example, there is a difference of approximately 1 dB in margin required between coherent and noncoherent FSK at a 10^{-4} BER. Preceding arguments for coherent demodulation not withstanding, there are times when coherent modulation is not practical.

As mentioned earlier, coherent performance relies upon proper oscillator synchronization. Figure 2–2 describes the upper bounds of coherent modulation performance by assuming perfect synchronization within the transceiver. Actual

performance is worse than shown in Figure 2–2 when the receiver does not maintain perfect synchronization. Traditionally, coherent modulation involves an elaborate, internal synchronization process. There are limits to the ability of the process to track changes in carrier frequency.

For example, there are applications satisfied by narrow modulation bandwidths at high frequencies. The noise power within a transmission channel is proportional to channel modulation bandwidth [49]. Narrow bandwidth links exhibit reduced in-band noise, which may translate to lower BER. Some applications can sacrifice data latency for reduced bandwidth and improved BER. Under today's technology, transmission and reception of very narrow bandwidth signals (< 10 Hz) above a few MHz is possible but not practical for most applications. The high cost of very stable frequency reference sources is prohibitive for all but the most exotic applications. The lack of an accurate, low cost carrier reference places serious constraints on commercial, low data rate applications.

Distribution of an accurate reference from a common source is a possible solution. Modems and wireless devices could receive the same reference, thereby maintaining accurate carrier synchronization. Until recently, there has been no practical means to distribute such a reference.

New seemingly unrelated developments are enabling technologies for coherent modulation operating from a common external reference. Although not a DSB-RC source as addressed by this research, GPS provides a nearly ubiquitous source of carrier reference. Recent research and product announcements give evidence to the potential of

GPS as a carrier reference [50, 51, 52, 53, 54]. This windfall reference infrastructure promises improvements in performance and reductions in equipment cost. Figure 2–2 suggests the upper bounds of these improvements. This research quantifies the benefits of an alternative out-of-band (externally-referenced) coherent demodulation approach and substantiates its use in new applications.

Modulated information arrives at the receiver as spectral energy appearing at frequencies asymmetric (known as "single-sideband [SSB] modulation") or symmetric (known as "double-sideband [DSB] modulation") to an assigned frequency, called the "carrier frequency." If energy appears at the carrier frequency, then the signal is said to be a "residual carrier (RC) system." If no energy appears at the carrier frequency, then the system operates with a "suppressed carrier (SC)." Taken in combination, modulated information may be found in DSB-RC, VSB-RC, SSB-RC, DSB-SC, or SSB-SC forms. This research studies both DSB-RC and DSB-SC demodulation. Consequently, the discussion will not discuss the use of out-of-band synchronization for SSB modulation. Instead, this study leaves out-of-band synchronization of SSB communication as a topic for further research. All of the techniques used in this study involved either DSB-RC or DSB-SC modulation. For the purposes of this discussion, any future reference modulation will implicitly mean double-sideband modulation.

Furthermore, the study investigated the transmission of digital information encoded as a series of phase reversals modulating the carrier signal, which describes both of the modulation schemes referred to earlier as BPSK and binary DPSK.

3.2.1 Coherent Demodulation

BPSK conveys a set of binary digits $\{b\}=\{b_0,b_1,\cdots,b_k,\cdots\}$ encoded as antipodal phase shifts modulated on a DSB-SC signal. Each bit b_k occupies the channel for a fixed bit interval T_b, which, for convenience, is equal to an integer number of carrier cycles m_c.

$$f_c = \frac{m_c}{T_b} \tag{3.1}$$

The modulated carrier is of the form

$$x(t) = c_k\sqrt{2}A\cos(2\pi f_c t), \text{ where } c_k = (-1)^{(1-b_k)}. \tag{3.2}$$

Symbol $c_k = \pm 1$ represents the k-th bit of $\{b\}$ conveyed by the modulated carrier phase, i.e., phase shifts of 0 and π radians represent a binary "1" and "0," respectively. The modulated signal arrives at the receiver after some path delay Δt and disturbed by noise $n(t)$. This analysis assumes that $n(t)$ is adequately described as additive white Gaussian noise (AWGN). The received signal $y(t)$ is

$$y(t) = c_k\sqrt{2}A\cos[2\pi f_c t + \theta(t)] + n(t), \text{ where} \tag{3.3}$$

$$\theta(t) = 2\pi(f_c\Delta t + \Delta f_c t). \tag{3.4}$$

Phase variable $\theta(t)$ accounts for the channel delay Δt and any deviation Δf_c in the transmitter's reference oscillator.

Optimum BPSK demodulation requires phase coherent reception of the modulated signal, i.e., the receiver's demodulation reference must match the received signal's frequency and phase. Figure 3–1 illustrates the operation of a coherent, DSB-SC

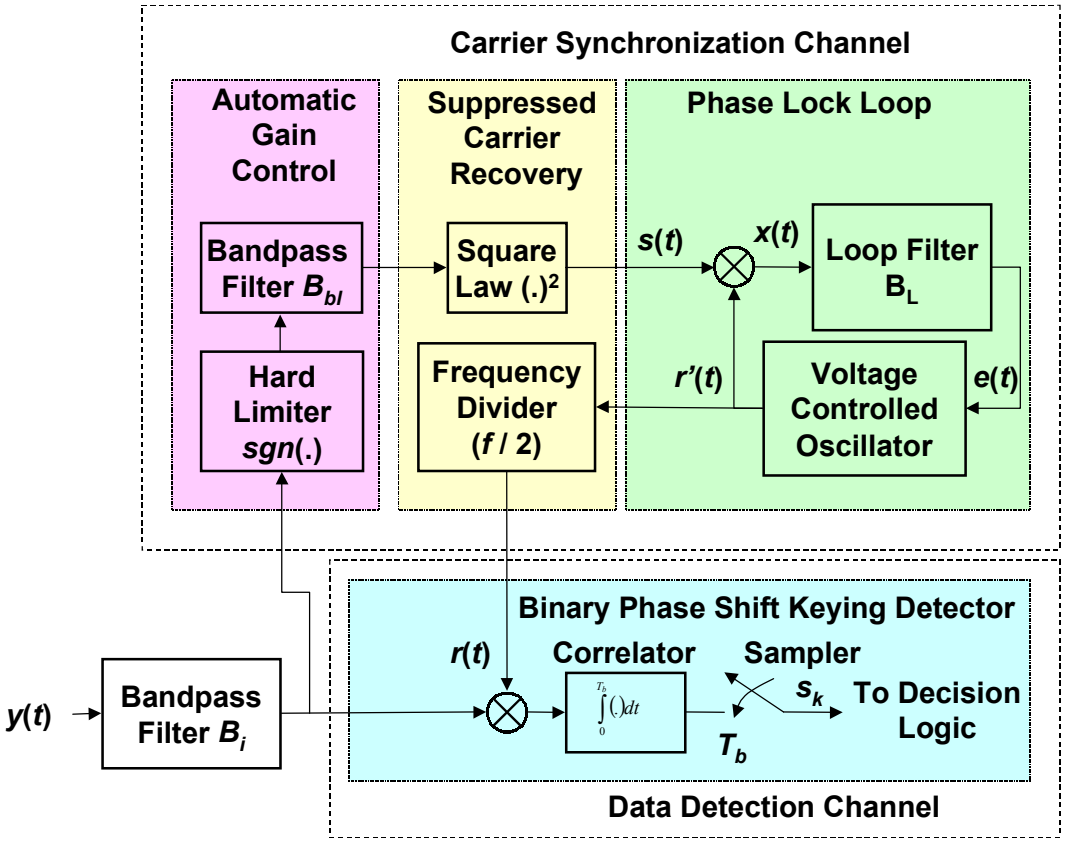

Figure 3–1. BPSK DSB-SC Receiver

demodulator. The upper portion of the demodulator is the carrier synchronization channel, which contains the receiver's local oscillator. It is the responsibility of the synchronization channel to adjust the oscillator frequency and phase to match that of the received signal. It produces a carrier estimate

$$r(t) = \sqrt{2}\cos[2\pi f_c t + \hat{\theta}(t)] \tag{3.5}$$

For the moment, assume that there is perfect carrier synchronization in the receiver's PLL, the communication channel adds no noise to the transmitted signal, and the received signal presents a BPSK-modulated carrier representing the set $\{b\}$ to a BPSK detector. The output of the BPSK detector s_k is

$$s_k = \int_{kT_b}^{(k+1)T_b} c_k \sqrt{2} A \cos[2\pi f_c t + \theta(t)] \sqrt{2} \cos\left[2\pi f_c t + \hat{\theta}(t)\right] dt \tag{3.6}$$

The detector output reduces to

$$s_k = c_k A T_b, \tag{3.7}$$

provided $\theta(t) = \hat{\theta}(t)$ over the interval $[kT_b, (k+1)T_b]$.

It is common practice to refer to the bit energy $E_b = AT_b$.

The receiver synchronization channel attempts to track the received signal phase and produces a phase estimate $\hat{\theta}(t)$. If the transmitter's carrier reference and the receiver's PLL are working properly and are in synchronization, then both $\theta(t)$ and $\hat{\theta}(t)$ vary slowly with time, $\left|\theta(t) - \hat{\theta}(t)\right| < \frac{\pi}{2}$, and are essentially constant over a given bit interval. Any difference in phase between the received signal carrier and the local

reference is phase error $\phi = \theta - \hat{\theta}$ and is assumed constant over the bit interval T_b. Continuing to ignore noise for the moment, non-zero phase error alters the BPSK detector output in the following manner.

$$s_k = \int_{kT_b}^{(k+1)T_b} c_k \sqrt{2} A \cos(2\pi f_c t + \theta) \sqrt{2} \cos(2\pi f_c t + \theta + \phi) dt$$

$$s_k = c_k A T_b \cos(\phi)$$

$$s_k = c_k E_b \cos(\phi) \tag{3.8}$$

Passing the BPSK signal through an RF channel usually adds extraneous signals, called "noise." This analysis assumes that these unwanted signals combine into a form called "additive white Gaussian noise" with a spectral power density $S_n(f) = \frac{N_O}{2}$. Variable N_O is the single-sided power spectral density of AWGN and is constant across all frequencies of interest. The conditional probability of a BPSK bit detection error given a fixed phase error ϕ is [48, 56, 57]

$$P_b(\rho_i \mid \phi) = erfc\left\{\sqrt{2\rho_i \cos(\phi)}\right\} \tag{3.9}$$

where the variable $\rho_i = \frac{E_b}{N_O}$ is commonly called the signal-to-noise ratio at the detector input and *erfc*(.) is the complementary error function. Clearly, a non-zero phase error in Equation (3.9) reduces the signal-to-noise ratio. Phase error increases the probability that the BPSK detector will make an erroneous bit estimate s_k.

3.2.2 Differentially Coherent Demodulation

There are cases in which maintaining fully coherent synchronization between the transceiver pair is impractical. For example, phase inversions are possible in some RF channels due to changes in channel conditions or changes in antenna orientation. Moreover, suppressed carrier recovery circuits found in Figure 3–1 add phase ambiguity in suppressed carrier systems [48]. These ambiguities can be overcome by using special coding sequences interspersed with normal transmission. Coding sequences add complexity and reduce throughput. Many applications resort to noncoherent reception when power and bandwidth constraints permit. Another popular option is to use a differentially coherent scheme referred to as DPSK.

Differential phase shift keying relaxes the receiver synchronization constraint by permitting a non-zero phase error. The phase error must be constant, or at least slowly varying, such that its magnitude does not change significantly during any two consecutive bit intervals $[(k\text{-}1)T_b,\ (k+1)T_b]$. DPSK transmitters modulate each bit b_k using the prior bit's phase representation as a reference according to the formula [48, 58]

$$c_k = c_{k-1}(-1)^{(1-b_k)}. \tag{3.10}$$

DPSK DSB-SC transmitters send the modulated carrier in the form

$$x(t) = c_k A\cos(2\pi f_c t). \tag{3.11}$$

Figure 3–2 describes the corresponding DPSK architecture.

DPSK receivers are insensitive to constant phase error, which simplifies the coherent synchronization process. The simplification comes at a cost of approximately 1 dB of additional signal-to-noise ratio for the same bit error probability as predicted earlier

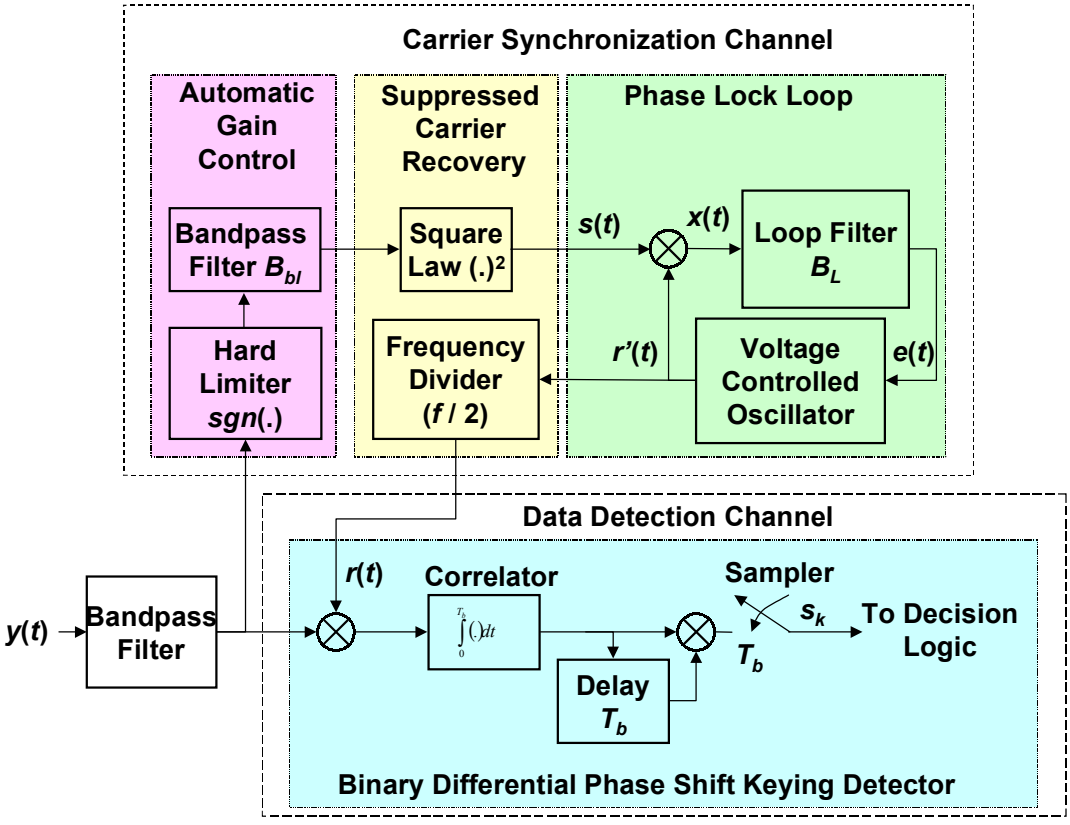

Figure 3–2. Binary DPSK DSB-SC Receiver

in Figure 2–2. Provided the synchronization channel maintains frequency coherency with a constant phase error, then the binary DPSK receiver's probability of error is [57]

$$P_B = \frac{1}{2}\exp(-\rho)\,. \tag{3.12}$$

It is important that the PLL in Figure 3–2 maintain frequency coherency with a nearly constant phase error. Otherwise, the DPSK detector estimate s_k will exhibit a bias and a corresponding increase in the probability of error.

3.3 Phase-Locked Loop

The fully coherent and differentially coherent demodulators shown in Figure 3–1 and Figure 3–2 rely on a PLL as a source of coherency with the transmitter's reference oscillator. Phase-locked loops are closed-loop feedback circuits consisting of a phase detector (signal multiplier), low-pass filter $h_L(t)$ located in the feedback loop, and a voltage-controlled oscillator (VCO) [59]. In Figure 3–1 and Figure 3–2, the signals appearing at key points in the PLL feedback loop are [60]:

$$s(t) = \sqrt{2}A\sin[2\pi f_c t + \theta(t)] \tag{3.13}$$

$$e(t) = h_L(t) * x(t) \tag{3.14}$$

where * is the time-domain convolution operator.

$$r(t) = K\cos[2\pi f_c t + \hat{\theta}(t)] \tag{3.15}$$

which is the PLL carrier estimate.

$$x(t) = AK\sin\left(\theta(t) - \hat{\theta}(t)\right) + \text{higher frequency terms.} \tag{3.16}$$

Loop filter $h_L(t)$ is low-pass and discards the higher frequency terms in the phase detector output $x(t)$. Thus, it is possible to rewrite the error signal $e(t)$ from Equation (3.16).

$$e(t) = AK \sin\left(\theta(t) - \hat{\theta}(t) \right) \tag{3.17}$$

The signal power of Equation (3.2) as seen at the PLL input is

$$S_i = A^2 . \tag{3.18}$$

Loop filter $h_L(t)$ defines the PLL's ability to track phase changes and reject input noise. Phase-locked loops may use first-, second-, or higher-order feedback filters depending upon the application requirements. Many receivers use second-order feedback loops [48]. Second-order loops are unconditionally stable, regardless of the input, and can compensate for Doppler shift effects.

It has not been possible to develop closed-form expressions for second-order PLL behavior. Instead, second-order PLL analysis generally relies upon closed-form expressions for first-order PLL behavior as approximations of second-order loop performance [57, 48].

With these factors in mind, this research uses a second-order feedback loop with the following filter transfer function [60].

$$F_L(s) = \frac{1 + sT_2}{sT_1} \tag{3.19}$$

where the filter time constants are

$$T_1 = \frac{KA}{\omega_n^2} \tag{3.20}$$

$$T_2 = \frac{2\zeta}{\omega_n}. \tag{3.21}$$

Variables K, ω_n, and ζ are the composite closed-loop gain, loop filter natural frequency (in radians per second), and loop filter damping factor, respectively. Variable A is the received signal amplitude at the phase detector input.

The closed-loop transfer function for a second-order PLL is

$$H(s) = \frac{1 + KAF(s)}{s + KAF(s)}. \tag{3.22}$$

Substituting for F(s) yields the second-order closed-loop transfer function in terms of the natural frequency and damping factor.

$$H(s) = \frac{\omega_n(\omega_n + 2s\zeta)}{s^2 + 2\omega_n s + \omega_n{}^2} \tag{3.23}$$

In [60], Heinrich Meyer and Gerd Aschied show that the optimum damping factor for a second-order PLL is ζ = 1.2. Holding the damping factor fixed at ζ = 1.2 and adjusting the natural frequency ω_n vary the behavior of the PLL so long as the loop gain K and input amplitude A are held constant. Increasing the natural frequency increases the feedback loop bandwidth B_L and makes the PLL more responsive to input phase variations.

$$B_L = \omega_n \frac{(4\zeta^2 + 1)}{8\zeta} \tag{3.24}$$

Decreasing the natural frequency reduces PLL sensitivity to input noise. There is no general optimum for the natural frequency. A designer's selected value often represents a compromise between tracking sensitivity and noise rejection. Therefore, the natural

frequency acts as a design parameter used to customize a PLL to a specific transceiver application.

If the PLL is tracking the carrier with small phase error, then the linearized PLL model approximation applies, i.e., $\sin(\phi) \approx \theta - \hat{\theta}$. It is common practice to assume that the random variable $\theta - \hat{\theta}$ has zero mean and to define the PLL output phase jitter (also known as the phase error standard deviation) to be

$$\sigma_\phi = \sqrt{E\left[\left(\theta - \hat{\theta}\right)^2\right]}, \tag{3.25}$$

where $E[\cdot]$ is the expectation function.

PLL output phase jitter for the linearized model is [48]

$$\sigma_\phi = \sqrt{\frac{2N_O B_L}{S_i}}, \tag{3.26}$$

where B_L is the PLL loop bandwidth.

If the phase error is too large for the linearized model, i.e., $\sin(\phi) \neq \theta - \hat{\theta}$, or the PLL is not in phase lock, then the phase error probability density function (pdf) for a first-order PLL is described by [57, 61].

$$p(\phi|\rho_i) = \frac{\exp[\rho_i \cos(\phi)]}{2\pi I_0(\rho_i)} \text{ for } -\pi \leq \phi \leq \pi \,. \tag{3.27}$$

Function $I_0(\rho_i)$ is the zeroth-order modified Bessel function of the first kind, evaluated for the PLL loop signal-to-noise ratio.

$$\rho_L = \frac{S_i}{2N_O B_L}. \tag{3.28}$$

Phase jitter in the non-linearized, first-order PLL approximation is the root-mean-square (RMS) phase error.

$$\sigma_\phi = \sqrt{\int_{-\pi}^{\pi} \phi^2 \frac{\exp[\rho_i \cos(\phi)]}{2\pi I_0(\rho_i)} d\phi} \tag{3.29}$$

It is possible to compute mean BPSK probability of error by combining Equation (3.27) with Equation (3.9) and integrating across the range of possible phase errors [62, 48, 5].

$$P_B(\rho_i \mid \sigma_\phi) = \int_{-\pi}^{\pi} erfc\left[\sqrt{2\rho_i \cos(\phi)}\right] \frac{\exp\left[\frac{1}{\sigma_\phi^2}\cos(\phi)\right]}{2\pi I_0\left(\frac{1}{\sigma_\phi^2}\right)} d\phi \tag{3.30}$$

As illustrated in Figure 3–3, phase jitter above 0.1 radians has an undesirable impact upon coherent receiver detection performance.

3.4 Automatic Gain Control

Equations (3.20) and (3.21) define the second-order PLL behavior in terms of the damping factor, natural frequency, loop gain, and input amplitude parameters. The first three of these parameters are a part of the PLL design and can be easily controlled. The input amplitude A is a function of the transmission channel and, as such, varies according to channel attenuation and the effects of noise. Maintaining input amplitude A at or near a predetermined design value is essential to the proper operation of the phase-locked loop. Therefore, reliable PLL operation across a range of channel losses requires an automatic gain control (AGC) prior to the PLL input.

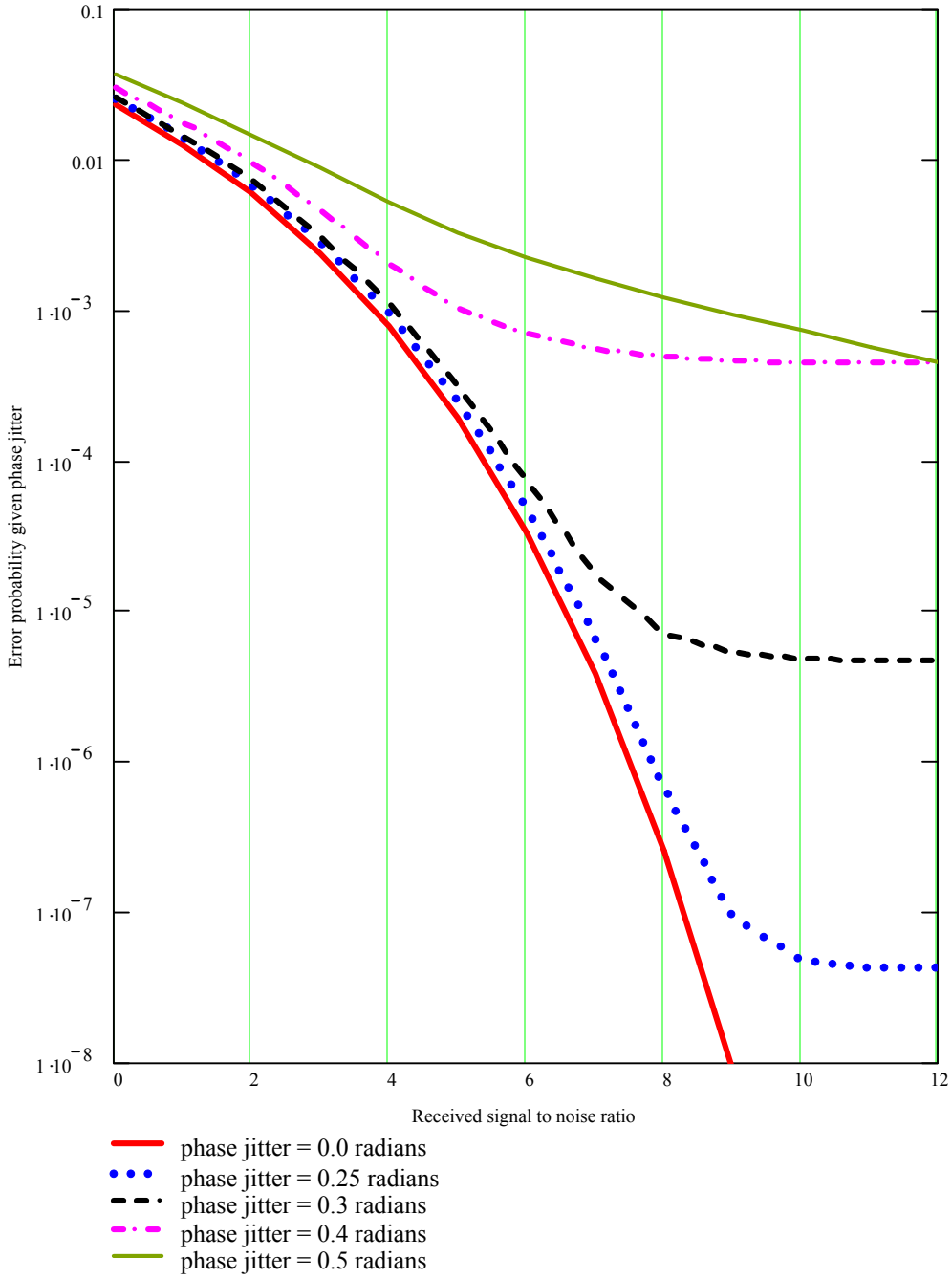

Figure 3–3. BPSK Bit Error Probability for Selected Phase Jitter Values

One popular design for an AGC is a "band-pass limiter" comprised of a hard limiter followed by a band-pass filter centered at the carrier frequency and with bandwidth B_{bl}. Figure 3–4 illustrates a band-pass limiter-PLL (BLPL) combination for a residual carrier system.

To illustrate the band-pass limiter behavior, assume that all filters shown in Figure 3–4 have unity gain within their pass bands. Let the received signal $y(t)$ be a DSB-RC modulated carrier accompanied by AWGN as described by [49]

$$y(t) = \sqrt{2}A[1 + am(t)]\cos(2\pi f_c t + \theta) + n(t) \tag{3.31}$$

where a is the modulation index and $m(t)$ is the information-bearing signal. Narrow pass band input filter $h_i(t)$ with pass bandwidth B_i removes the modulation sidebands so that the filter output

$$y_i(t) = \sqrt{2}A\cos(2\pi f_c t + \theta) + n_i(t), \tag{3.32}$$

which consists only of the carrier signal plus narrow-band Gaussian noise $n_i(t)$. Narrow-band Gaussian noise is the real part of the complex band-pass signal [4]

$$n_i(t) = \mathrm{Re}\left\{\sqrt{n_c^2 + n_s^2}\,\exp\left[j\left(2\pi f_c t + \theta\right) + j\arg\left(n_c, n_s\right)\right]\right\}. \tag{3.33}$$

Function $\arg(n_c, n_s)$ is the unambiguous phase angle of the complex bivariate noise. Equation (3.33) assumes that the filter input noise $n(t)$ is stationary, i.e., time invariant. It separates $n_i(t)$ into low-pass equivalent components. Random variables n_c and n_s have identical Gaussian distributions, are orthogonal and are statistically independent. Gaussian noise random variable n_c is in phase with the transmitted signal carrier.

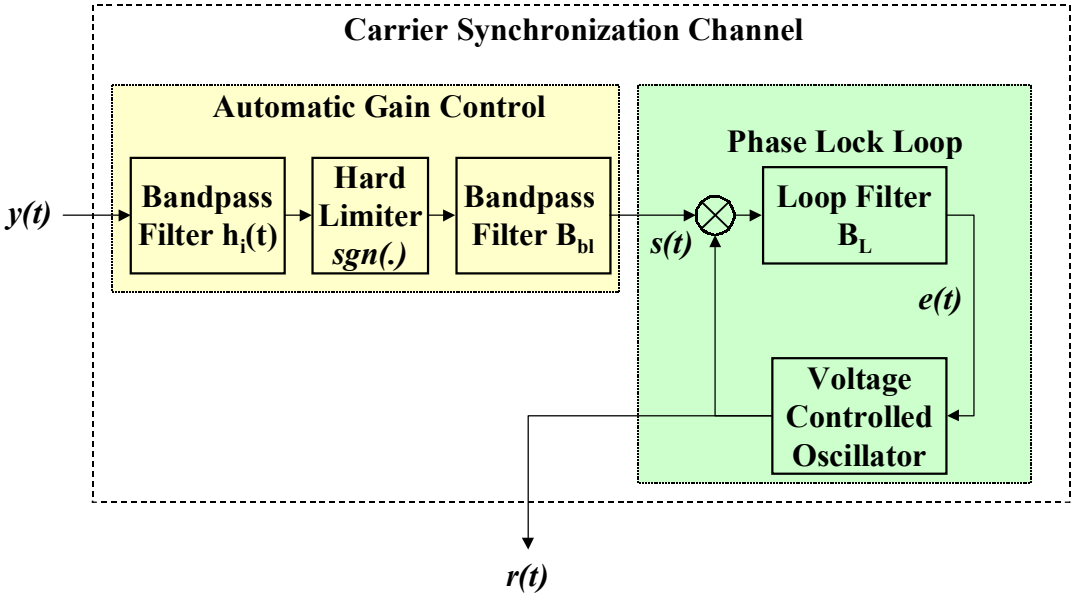

Figure 3–4. Band-pass limiter-PLL combination.

Random variable n_s is the quadrature noise component [55, 4]. Thus, the filter output $y_i(t)$ is the real part of a complex band-pass signal as described by

$$y_i(t) = \mathrm{Re}\left\{\sqrt{2}\sqrt{(A+n_c)^2+n_s^2}\,\exp\left[j\left(2\pi f_c t+\theta+\gamma\right)\right]\right\} \tag{3.34}$$

where $\gamma = \tan^{-1}\left(\frac{n_s}{A+n_c}\right)$. Further simplification of the preceding equation yields

$$y_i(t) = \sqrt{2}\sqrt{(A+n_c)^2+n_s^2}\,\cos\left(2\pi f_c t+\theta+\gamma\right), \tag{3.35}$$

given an input as described by Equation (3.31).

Output from the hard limiter consists of a rectangular waveform with noise-induced phase variations γ. Springett and Simon derived the Fourier series of the limiter output in [65].

$$y_{hl}(t) = \frac{4}{\pi}\sum_{m=0}^{\infty}\left(\frac{1}{2m+1}\right)\cos\left[(2m+1)(2\pi f_c t+\theta+\gamma)\right] \tag{3.36}$$

Band-pass filter $h_{bl}(t)$ selects the fundamental term ($m=0$) of $y_{hl}(t)$ producing a gain-compensated output $y_{bl}(t)$,

$$y_{bl}(t) = \frac{4}{\pi}\cos\left[2\pi f_c t+\theta+\gamma\right]. \tag{3.37}$$

It can be shown that the band-pass limiter output $y_{bl}(t)$ is a function of input signal-to-noise ratio ρ_i by reorganizing the output into the following form [65].

$$y_{bl}(t) = \sqrt{2}\mu(\rho_i)\cos\left(2\pi f_c t+\theta\right)+n_{bl}(t) \tag{3.38}$$

where the band-pass limiter mean output amplitude is

$$\mu(\rho_i) = \left(2\frac{\rho_i}{\pi}\right)^{\frac{1}{2}} e^{\frac{-\rho_i}{2}}\left[I_0\left(\frac{\rho_i}{2}\right)+I_1\left(\frac{\rho_i}{2}\right)\right] \tag{3.39}$$

and input signal-to-noise ratio is [48]

$$\rho_i = \frac{S_i}{2N_O B_i}. \tag{3.40}$$

The band-pass limiter output SNR is [65]

$$\rho_{bl} = \frac{\mu_{bl}(\rho_i)^2}{\frac{\pi^2}{8} - \mu_{bl}(\rho_i)^2}. \tag{3.41}$$

The ratio of the output SNR to input SNR varies within a narrow range of values.

$$\frac{\pi}{4} \le \frac{\rho_{bl}}{\rho_i} \le 1, \text{ when } 0 < \rho_i < \infty \tag{3.42}$$

Band-pass limiters provide a constant PLL input amplitude while altering the output SNR to input SNR ratio by only 1.05 dB over the full range of input SNR. This is the desired AGC behavior needed for optimum PLL operation.

A PLL phase detector multiplies the band-pass limiter output as described by Equation (3.37) and the VCO carrier estimate

$$r(t) = \sqrt{2}\cos[2\pi f_c t + \hat{\theta}] \tag{3.43}$$

to produce

$$x(t) = y_{bl}(t)r(t) = \frac{2\sqrt{2}}{\pi}\left\{\sin\left[\left(\theta - \hat{\theta}\right) + \gamma\right]\right\} + \sin\left[4\pi f_c t + \left(\theta + \hat{\theta}\right) + \gamma\right]. \tag{3.44}$$

Loop filter $h_L(t)$ rejects the high frequency term of the phase detector output leaving the phase error signal

$$e(t) = \frac{2\sqrt{2}}{\pi}\sin(\phi) \text{ where } \phi = \theta - \hat{\theta} + \gamma. \tag{3.45}$$

Note that earlier assumptions regarding constant phase error during a given bit interval and stationary Gaussian noise yield to a time-independent phase error ϕ. A further simplification is to assume that the PLL is coherent with the carrier. Coherence between the received signal and the receiver oscillator implies that

$$\theta - \hat{\theta} = 0 \tag{3.46}$$

for a given bit interval. Random phase error *e* reduces to

$$e = \frac{2\sqrt{2}}{\pi}\sin(\gamma) = \frac{2\sqrt{2}}{\pi}\frac{n_s}{\sqrt{(A+n_c)^2 + n_s^2}}. \tag{3.47}$$

It is common practice to assume n_s and n_c have zero mean and equal variance [55, 49]. Under the preceding assumptions, random VCO input variable *e* becomes a function of two independent Gaussian random variables with joint pdf

$$p_{n_c,n_s}(n_c,n_s) = p_{n_c}(n_c)\,p_{n_s}(n_s) = \frac{1}{2\pi\sigma^2}\exp\left(-\frac{\left(n_c^2+n_s^2\right)}{2\sigma^2}\right) \tag{3.48}$$

However, *e* is not, in the strict sense, a Gaussian random variable. Springett and Simon performed a set of transformations in which they show that the low-pass phase detector output has a pdf described in [65] as

$$p_{e|\rho_i}(e|\rho_i) = \frac{\exp(-\rho_i)\left(1+\sqrt{(\pi\rho_i)}\sqrt{1-\left(\frac{e\pi}{2\sqrt{2}}\right)^2}\exp\left\{\rho_i\left[1-\left(\frac{e\pi}{2\sqrt{2}}\right)^2\right]\right\}\sqrt{erf\left\{\rho_i\left[1-\left(\frac{e\pi}{2\sqrt{2}}\right)^2\right]\right\}}\right)}{2\sqrt{2}\sqrt{1-\left(\frac{e\pi}{2\sqrt{2}}\right)^2}} \tag{3.49}$$

within the interval $-2\sqrt{2}/\pi < e < 2\sqrt{2}/\pi$. See Figure 3–5 for a graphical representation of the phase detector output pdf.

A comparison of Figure 3–5 with known distributions finds that *e* exhibits a symmetric Beta pdf [66]. If the band-pass filter bandwidth B_i is small compared to the input process bandwidth *B*, then the pdf of *e* approximates that of Gaussian noise for large SNR ρ_i [57, 65].

Phase error signal *e* in Equation (3.47) takes a different form for low ρ_i.

$$\lim_{\rho_i \to 0} e = \frac{2\sqrt{2}}{\pi} \sin(\gamma) \tag{3.50}$$

$$\lim_{\rho_i \to 0} e = \frac{2\sqrt{2}}{\pi} \frac{n_s}{\sqrt{n_c{}^2 + n_s^2}}$$

with corresponding pdf

$$\lim_{\rho_i \to 0} p_{e|\rho_i}(e|\rho_i) = \frac{1}{2\sqrt{2}\sqrt{\left(1 - \left(\frac{e\pi}{2\sqrt{2}}\right)^2\right)}}. \tag{3.51}$$

Equation (3.51) is a "sinusoidal" pdf of the form $Y = k\sin(x)$ when random variable x is a uniform $[\pi, -\pi]$ random variable [67]. There is a rational explanation for the claim that the pdf of *e* is sinusoidal.

Lacking a significant carrier signal, the phase detector acts only on bivariate Gaussian noise. Transforming Equation (3.48) from Cartesian to polar coordinates yields [49]

$$p_{r,\gamma}(r,\gamma) = p_r(r) p_\gamma(\gamma) \tag{3.52}$$

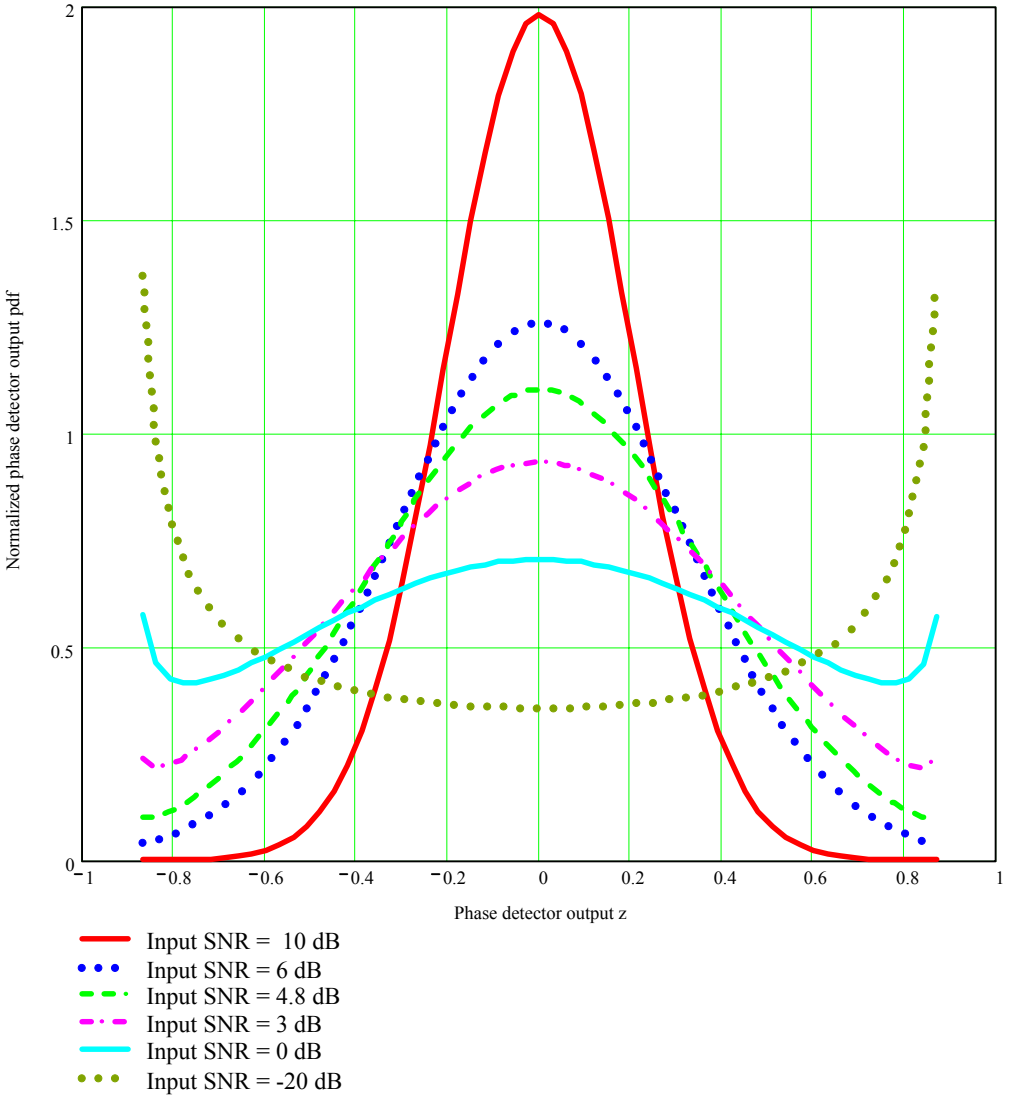

Figure 3–5. Band-pass Limiter-PLL Output Probability Density Function [65]

$$p_{r,\gamma}(r,\gamma) = \frac{r}{\sigma^2}\exp\left(\frac{-r^2}{2\sigma^2}\right)\left(\frac{1}{2\pi}\right) \tag{3.53}$$

when $r = \sqrt{n_c^2 + n_s^2} \geq 0$ and $-\pi \leq \gamma = \tan^{-1}\frac{n_s}{n_c} \leq \pi$. Note that r and γ are statistically independent because n_c and n_s are independent [49]. Probability density function $p_r(r)$ is a Rayleigh distribution of the noise magnitude. Thus, the noise phase angle γ has a uniform $[\pi,-\pi]$ distribution.

$$p_\gamma(\gamma) = \frac{1}{2\pi} \text{ on the interval } -\pi \leq \gamma = \tan^{-1}\frac{n_s}{n_c} \leq \pi. \tag{3.54}$$

Therefore, phase error $\phi = \gamma$ at low SNR is the pdf of a uniformly distributed random variable and $e = \frac{2\sqrt{2}}{\pi}\sin(\phi)$ has a corresponding sinusoidal pdf.

3.5 Internally-Referenced, Suppressed Carrier Synchronization

Internally-referenced BPSK or DPSK systems transmit a DSB-SC signal that must be tracked and detected by the receiver. Suppressed carrier transmissions have no spectral energy at the carrier frequency. Consequently, there is no continuous signal at the carrier frequency for PLL tracking. Several methods exist for carrier recovery from suppressed carrier signals. Two popular techniques for BPSK and DPSK systems are squaring loops and Costas loops.

3.5.1 Costas Loop

A typical Costas loop implementation begins with two orthogonal carrier estimates provided by a voltage-controlled oscillator. Each VCO output enters one of a

matched pair of phase detectors where the VCO estimate is multiplied with the received signal $y_i(t)$. Both phase detector outputs pass through a matched pair of low-pass filters. A third phase detector compares the orthogonal low-pass outputs. A loop filter processes the result and produces VCO control signal *e* [64, 63].

3.5.2 Squaring Loop

Figure 3–1 and Figure 3–2 recover a suppressed carrier from a DSB-SC transmission by adding a square law device prior to the PLL. A squaring device produces a spectral component at twice the carrier frequency. A frequency divider reduces the PLL output to an estimate of the received signal carrier frequency and phase, which is used as the coherent demodulation reference. Industrial practice refers to the squaring circuit and PLL combination as a "squaring loop." Squaring loops are a common feature in BPSK and DPSK receivers.

A PLL as shown in Figure 3–1 tracks the squaring device output component at frequency $2f_c$. A carrier estimate

$$r'(t) = \sqrt{2}\cos\left(4\pi f_c t + 2\hat{\theta} + 2\gamma\right) \tag{3.55}$$

passes from the PLL output through a divide-by-two frequency divider, thereby producing carrier estimate

$$r(t) = \sqrt{2}\cos\left(2\pi f_c t + \hat{\theta} + \gamma\right). \tag{3.56}$$

Multiplying $r(t)$ and a received DSB-SC signal as described by Equation (3.3) demodulates the BPSK-modulated signal. Performance of a squaring loop is a function of the input SNR.

A squaring device increases the noise-induced phase jitter within the synchronization channel. Equation (3.55) shows that the squaring device multiplies the PLL output frequency f_c, phase estimate $\hat{\theta}$, and phase error γ by a factor of 2. Recall that γ is a random variable with zero mean and variance σ_ϕ. Consequently, PLL output phase variance σ_ϕ increases by a factor of 4 [48]. The divide-by-2 circuit nullifies the frequency- and angle-doubling effects of the squaring circuit so that the squaring effect has no direct bearing on the demodulator phase accuracy. However, the squaring circuit increases the phase variance in the PLL feedback loop, thereby contributing to PLL output phase jitter. Theoretically, a DSB-SC system using a squaring loop will require 6 dB of additional SNR in order to maintain phase lock when compared to a residual carrier system.

At medium to low SNR, signal-noise and noise-noise cross-product terms produced by the squaring device become significant and create an effect called "loop squaring loss." The "squaring noise" interferes with the PLL behavior and increases the output phase jitter. For low to medium SNR, the squaring loss is [48, 61]

$$G_{SL} = 1 + \frac{1}{2\rho_i}, \tag{3.57}$$

where the squaring circuit processes an input signal with bandwidth B_i and an input SNR of

$$\rho_i = \frac{S_i}{2N_O B_i} \tag{3.58}$$

The phase jitter model for a first-order, linear squaring loop at the PLL output is [61]

$$2\sigma_\phi = \sqrt{4\left(\frac{2B_L N_O}{S_i}\right)\left(1+\frac{1}{2\rho_i}\right)} \tag{3.59}$$

The phase jitter for a squaring loop as seen by a BPSK or DPSK detector is [48]

$$\sigma_\phi = \sqrt{\left(\frac{2B_L N_O}{S_i}\right)\left(1+\frac{1}{2\rho_i}\right)}. \tag{3.60}$$

In [61] and [63], Gardner and Lindsey point out that the statistical behavior of the Costas loop is identical to the squaring loop. Therefore, phase jitter as a function of input SNR should be the same for a squaring loop or Costas loop. The preceding analysis is applicable to squaring loops and Costas loops, provided the filters in each are equivalent and both use ideal phase detectors.

Costas loops are more difficult to simulate in computer models. As a matter of convenience, this research will focus instead on the behavior of a squaring loop for suppressed carrier recovery with the understanding that the results are applicable to systems employing a Costas loop.

Combining the squaring loop and the band-pass limiter as shown in Figure 3–1 and Figure 3–2 makes exact analysis difficult. The pdf of the band-pass limiter output approaches a Gaussian pdf for large SNR and is non-Gaussian elsewhere. Available squaring loop derivations assume that the output of the squaring device is a Gaussian process, but this assumption is an idealized representation [61]. Thus, the equations describing the PLL loop behavior in conjunction with nonlinear devices are

approximations that serve as useful guides to the actual behavior of a band-pass limiter-squaring loop (BLSL) combination.

It is possible to approximate the range of the PLL output phase jitter by combining the asymptotic range of the band-pass limiter gain in Equation (3.42) and the squaring loop phase jitter in Equation (3.60).

$$\sqrt{\left(\frac{2B_L N_O}{S_i}\right)\left(1+\frac{1}{2\rho_i}\right)} \le \sigma_\phi \le \sqrt{\frac{4}{\pi}\left(\frac{2B_L N_O}{S_i}\right)\left(1+\frac{1}{2\rho_i}\right)}, \tag{3.61}$$

when

$$0 < \rho_i = \frac{S_i}{2N_O B_i} < \infty . \tag{3.62}$$

Equation (3.61) relies on a linearized, first-order PLL phase jitter model as described by Equation (3.26), i.e., it assumes a small phase error. It will not necessarily hold for small SNR and large phase variations. In sections to follow, this study will employ computer models of BLPLs and BLSLs to gain additional insight into the behavior of PLL-based synchronization devices.

Notice in Equation (3.61) that the PLL output phase jitter varies across a range determined by the PLL feedback loop bandwidth B_L and the input bandwidth B_i. The former value is a PLL design parameter selected as a compromise between noise immunity and tracking sensitivity. The modulation type and data rate set the input bandwidth B_i. As such, B_i is not within the control of the PLL designer. Thus, the PLL detects the carrier signal by processing an input bandwidth equal to the modulation bandwidth B_i, which, from the PLL's standpoint, is the "PLL detection bandwidth."

As the modulation bandwidth B_i increases, so does the PLL detection bandwidth with corresponding reductions in signal-to-noise ratio. Reducing modulation bandwidth translates into a reduction in the PLL detection bandwidth with corresponding improvement in receiver synchronization performance.

3.6 Detection Bandwidth

Unlike residual carrier systems, suppressed carrier systems must derive their synchronization reference from modulation sideband information. Modulation sidebands contain other signals that may not be beneficial to the synchronization. Consequently, suppressed carrier recovery performance depends, in part, on the modulation bandwidth, also called the "detection bandwidth," of the communications channel.

3.6.1 Link Margin/Bandwidth Tradeoff

A received signal SNR is a function of the noise power bandwidth. If the signal bandwidth is reduced, then the noise power is reduced. The relationship is not necessarily direct, since the noise power distribution over a given band may vary significantly. In addition, the nature of the noise power (bursty, white, quasi-coherent, etc.) affects the relationship. Assuming that the noise power is "white," i.e., evenly distributed over a frequency band, a reduction in bandwidth by one half will reduce the noise power by one-half (3 dB). For free-space propagation of a radio signal in the far field, a decrease in noise power of 6 dB will increase reception range by a factor of 2 [70]. If the signal detection bandwidth at the receiver is reduced by a factor of 4 (6 dB), there is the prospect of doubling the range at which the signal can be received with the

same bit error rate. Of course, reducing signal bandwidth reduces data throughput, but throughput is not the primary concern of narrow-band applications.

3.6.2 Detection Bandwidth and Operating Frequency

As mentioned, the noise power distribution and noise type in a wireless communications channel frequency range may vary considerably. The relationship between received signal-to-noise ratio and reduced detection bandwidth will be heavily influenced by the noise situation in the frequency range of interest. At low frequencies (< 30 MHz), the noise in a channel is usually limited by atmospheric noise, which can be quite variable in nature [70]. At frequencies from about 100 kHz to 3 MHz, the atmospheric noise is very bursty, since it is primarily due to motor noise, power line fluctuations, and other manmade signals, as well as lighting strikes worldwide. There is a dip in the daytime atmospheric noise between 1 to 3 MHz due to reduction in noise from atmospheric reflections (various ionospheric layers). However, the nighttime noise is normally much higher. From 3 to 30MHz the noise level gradually reduces on average but is very dependent on time of day and time of year. This dependency is so great that a variation in noise levels of 30 to 60 dB from night to day is a common occurrence. In this sort of signal environment any reduction in noise level is usually welcome, even at the expense of information bandwidth.

Residual carrier systems employ a narrower PLL detection bandwidth for synchronization as compared with an equivalent suppressed carrier system. This research explores the benefits and limitations of relying upon residual carrier synchronization in lieu of suppressed carrier recovery for the purpose of DSB-SC demodulation.

3.7 Residual Carrier Synchronization

Residual carrier transmissions may take several forms, including a DSB-RC or VSB-RC. In all cases, the residual carrier transmissions have significant energy at the carrier frequency. The presence of energy at the carrier frequency and the use of a band-pass limiter-PLL (BLPL) combination distinguish the DSB-RC receiver from a DSB-SC receiver and its BLSL synchronization subsystem.

There are two major differences between a BLPL and its BLSL counterpart. First, the BLPL does not employ a squaring circuit for residual carrier recovery. Eliminating the squaring circuit also eliminates the effects of the squaring loss, the doubling of the PLL output frequency, and reduces the PLL phase jitter. Second, the DSB-RC sidebands hold no necessary information for carrier tracking by the BLPL. A BLPL input filter may have a much narrower pass band, thereby eliminating part or all of the sideband information and the associated sideband noise. Eliminating the sidebands also eliminates the possibility of false synchronization lock in M-ary PSK systems. Reducing the noise equivalent bandwidth at the BLPL input improves the PLL performance, as will be shown in the following sections. The following analysis considers how these differences may equate to improved performance in a DSB-RC-referenced BLPL.

Removing the squaring circuit from Figure 3–1 and Figure 3–2 eliminates the effects of squaring loss. Equation (3.61) simplifies to

$$\sqrt{\left(\frac{2B_L N_O}{S_i}\right)} \le \sigma_\phi \le \sqrt{\frac{4}{\pi}\left(\frac{2B_L N_O}{S_i}\right)}. \tag{3.63}$$

Equation (3.63) indicates that a linear, first-order BLPL model will have an output phase jitter upper bound that is within -1.05 dB of a first-order PLL under equivalent input signal conditions. Expressions such as Equation (3.63) have not been tractable for second-order BLPL designs [61]. Consequently, Equation (3.63) can serve only as a guide to second-order BLPL behavior.

This study investigates the behavior of a second-order BLPL tracking a DSB-RC reference and compares its behavior with that of a second-order BLSL tracking a DSB-SC reference. It will also draw comparisons of second-order BLSL and BLPL behavior with the predictions of Equation (3.63).

3.8 Externally-Referenced, Residual Carrier Synchronization

Figure 1–1 proposes an externally-referenced transceiver pair arranged in a triad configuration. A triad relies on a broadcast from a stationary DSB-RC station as a synchronization source for a stationary DSB-SC transmitter and a stationary DSB-SC receiver. The positions of the DSB-RC broadcast station, DSB-SC transmitter, and DSB-SC receiver may be at any arbitrary distance relative to one another within the limits of allowable free-space path loss. The DSB-RC station must maintain an accurate carrier frequency, i.e., the DSB-RC transmitter may not drift significantly from its designated carrier frequency.

The DSB-RC station could be one constructed deliberately for the purpose of synchronizing two or more triad transceivers or the transceivers might opportunistically use an indigenous broadcast from an AM radio, NTSC television station, or other DSB-RC signal. In the first case, it may be economically feasible to construct an accurate

broadcast transmitter dedicated to the synchronization of a large number of transceivers (e.g., wireless LANs, oil field telemetry) and spread the cost of the dedicated residual carrier transmitter across a population of transceivers. Dedicated transmitters need only broadcast an unmodulated carrier. The second case uses an existing residual carrier transmitter broadcasting as an accurate carrier reference in the vicinity of a triad transceiver. The arrangement shown in Figure 2–1 applies whether the reference is an indigenous source of synchronization or a broadcast dedicated to the purpose of synchronization.

In Figure 2–1, a triad transmitter receives the DSB-RC reference signal

$$b_{tx}(t) = G_{tx}B[1 + am(t)]\cos(2\pi f_{RC}t + \delta_{tx}) + n_{tx}(t) \tag{3.64}$$

where a is the modulation index; $m(t)$ is the baseband, AM modulation signal; $n_{tx}(t)$ is AWGN at the triad transmitter; G_{tx} is the AM broadcast path loss; and δ_{tx} is phase offset created by the propagation of a DSB-RC signal from an AM broadcast station to the triad transmitter. In like manner, the same DSB-RC reference signal arrives at a triad receiver as

$$b_{rx}(t) = G_{rx}B[1 + am(t)]\cos(2\pi f_{RC}t + \delta_{rx}) + n_{rx}(t)\,. \tag{3.65}$$

A BLPL within the triad transmitter shown in Figure 3–6 produces the reference estimate

$$r_{tx}(t) = \sqrt{2}\cos(2\pi f_{RC}t + \delta_{tx} + \gamma_{tx}) \tag{3.66}$$

where γ_{tx} is the random phase error introduced by the AWGN term $n_{tx}(t)$. Within the

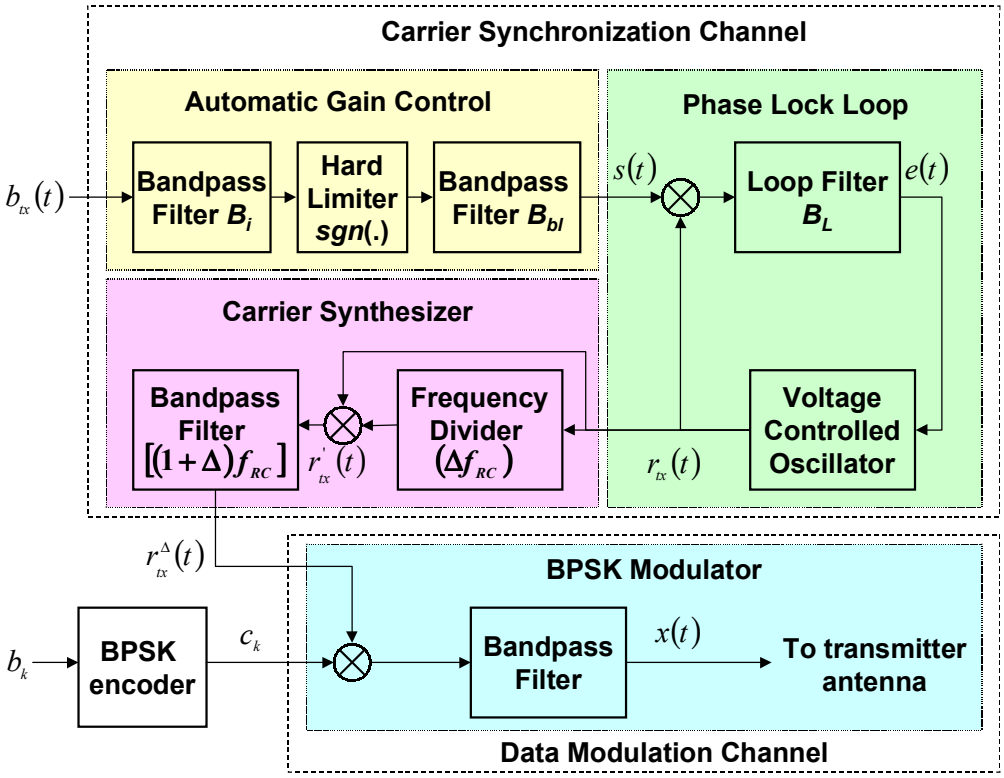

Figure 3–6. Externally-referenced BLPL with BPSK modulator.

transmitter's carrier synthesizer, a frequency divider circuit divides the frequency and phase of r_{tx} by $\frac{1}{\Delta}$. A multiplier combines the divider output with r_{tx} to form

$$r_{tx}^{'}(t) = \sqrt{2}\cos(2\pi f_{RC}t + \delta_{tx} + \gamma_{tx})2\cos\left[(2\pi\Delta f_{RC}t + \Delta\delta_{tx} + \Delta\gamma_{tx})\right] \tag{3.67}$$

Expanding the preceding equation yields two distinct spectral components.

$$r_{tx}^{'}(t) = \sqrt{2}\cos\left[2\pi(1+\Delta)f_{RC}t + (1+\Delta)(\delta_{tx} + \gamma_{tx})\right] + \sqrt{2}\cos\left[2\pi(1-\Delta)f_{RC}t + (1-\Delta)(\delta_{tx} + \gamma_{tx})\right] \tag{3.68}$$

Either term of the preceding equation may serve as a triad carrier reference. A band-pass filter with center frequency $f_c = (1 \pm \Delta)f_{RC}$ selects one of the terms. Its output is the transmitter's carrier reference signal used by the data modulator in Figure 3–6.

$$r_{tx}^{\Delta}(t) = \sqrt{2}\cos\left[2\pi f_c t + (1 \pm \Delta)(\delta_{tx} + \gamma_{tx})\right] \tag{3.69}$$

In like manner, a triad receiver shown in Figure 3–7 produces a demodulation sinusoid

$$r_{rx}^{\Delta}(t) = \sqrt{2}\cos\left[2\pi f_c t + (1 \pm \Delta)(\delta_{rx} + \gamma_{rx})\right]. \tag{3.70}$$

Note that the process of synthesizing the carrier reference from the DSB-RC broadcast multiplies the path delay phase error δ and the noise-induced phase error γ by $(1+\Delta)$. In effect, the frequency synthesizer amplifies phase error inherent within Equations (3.66) and (3.70). Amplification of phase error will be an important consideration in triad system performance as will be shown later in this research.

A modulator within the triad transmitter combines reference sinusoid $r_{tx}^{\Delta}(t)$ with the data to be transmitted and sends a DSB-SC signal in the form as

$$x(t) = c_k\sqrt{2}A\cos\left[2\pi f_c t + (1 \pm \Delta)(\delta_{tx} + \gamma_{tx})\right] \tag{3.71}$$

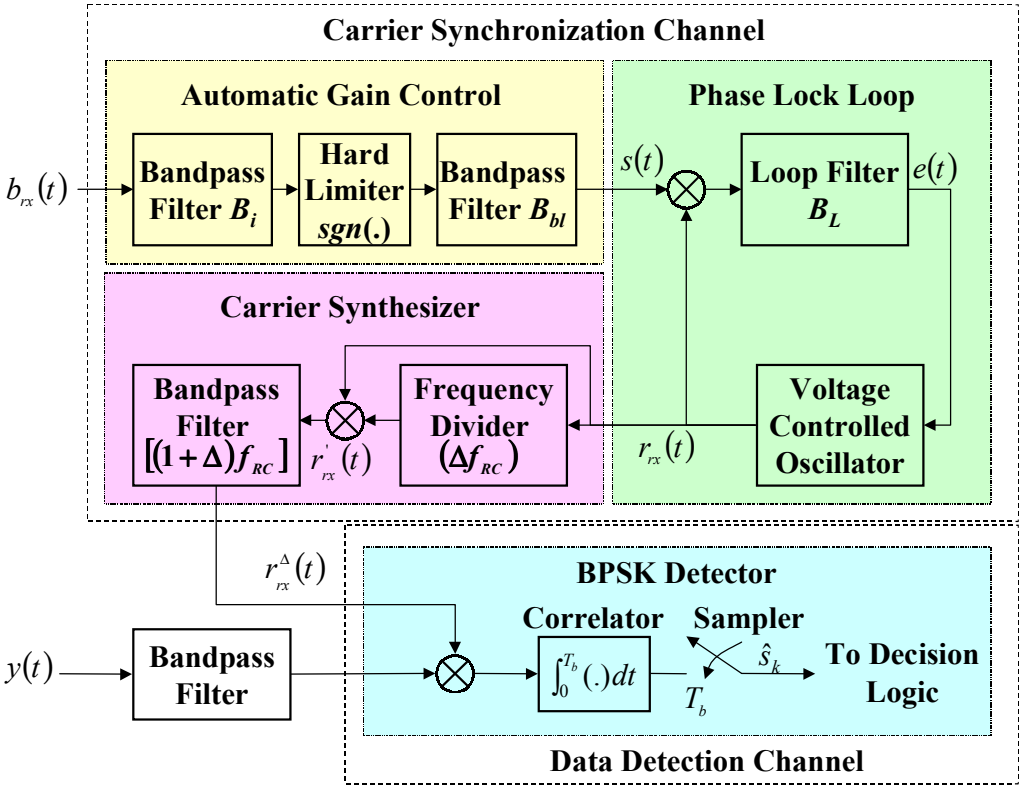

Figure 3–7. Externally-referenced BLPL with BPSK demodulator

where c_k is a BPSK-encoded binary sequence. The communications path adds path loss G_p, AWGN $n_p(t)$, and a phase offset δ_p corresponding to the path delay between the triad transceiver pair. Let the signal arriving at the receiver input be

$$y(t) = c_k \sqrt{2} A G_p \cos\left[2\pi f_c t + (1 \pm \Delta)\delta_{tx} + \delta_p + (1 \pm \Delta)\gamma_{tx}\right] + n_p(t). \qquad (3.72)$$

A given triad receiver multiplies the received signal y(t) with its demodulation reference $r_{rx}^{\Delta}(t)$ and passes the product through an integrate-and-dump correlator. The output of the receiver correlator is

$$\hat{s}_k = c_k A T_b G_p \cos\left[(1 \pm \Delta)(\delta_{rx} - \delta_{tx}) - \delta_p + (1 \pm \Delta)(\gamma_{rx} - \gamma_{tx})\right] + \int_{kT_b}^{(k+1)T_b} n_p(t) r_{rx}^{\Delta}(t) dt \qquad (3.73)$$

The first term of $\hat{s}_k$ has the same form as the detected data estimate in Equation (3.8). The rightmost term of $\hat{s}_k$ is demodulated and correlated noise added by the DSB-SC channel. It is a common (and undesirable) by-product of the DSB-SC transmission.

Note that the BLPLs within the triad transmitter and receiver do not depend upon the BPSK-modulated, DSB-SC transmission for synchronization. Therefore, the noise term in Equation (3.73) does not contribute to phase error ϕ. It is possible to ignore the transmission channel noise in any analysis regarding triad synchronization. By ignoring the noise term in Equation (3.73), it is possible to simplify $\hat{s}_k$ to

$$\hat{s}_k = c_k A T_b G_p \cos(\beta_{\Delta} + \gamma_{\Delta}) \qquad (3.74)$$

where

$$\beta_{\Delta} = (1 \pm \Delta)(\delta_{rx} - \delta_{tx}) - \delta_p \qquad (3.75)$$

is a fixed phase offset attributable to triad path delays and

$$\gamma_{\Delta} = (1 \pm \Delta)(\gamma_{rx} - \gamma_{tx}) \tag{3.76}$$

is the random triad phase error.

Equation (3.75) is a function of the relative positions of the DSB-RC broadcast transmitter and the triad transceiver pair. Phase offset β_{Δ} is constant so long as the components of the triad are stationary.

The second moment of the phase error in Equation (3.74) is

$$\overline{\theta_{\Delta}^2} = E\left\{(\beta_{\Delta} + \gamma_{\Delta})^2\right\}. \tag{3.77}$$

Random variables γ_{rx} and γ_{tx} have zero mean and are statistically independent. This leads to the conclusion that a triad system has mean phase error at the receiver

$$\overline{\theta_{\Delta}} = \beta_{\Delta} \tag{3.78}$$

Taking the second moment of the phase error yields

$$\overline{\theta_{\Delta}^2} = \beta_{\Delta}^2 + (1 \pm \Delta)^2 (\sigma_{rx}^2 + \sigma_{tx}^2). \tag{3.79}$$

The triad receiver phase error has a mean of β_{Δ} and a variance of $(1 \pm \Delta)^2 (\sigma_{rx}^2 + \sigma_{tx}^2)$.

Mean phase error β_{Δ} is dependent upon the relative placement of the residual carrier reference transmitter, the triad transmitter, and the triad receiver. It may take values between $-\pi$ and π. When $|\beta_{\Delta}| > 0.1$ radians, the triad system will experience nonreducible probability of error as shown in Figure 3–3. An absolute mean phase error $|\beta_{\Delta}| > 0.4$ will render the triad system ineffective.

It is essential that measures be taken to compensate for the mean phase error within the triad system design. Measurement of the mean phase error at the triad receiver

and adjustment of the PLL to introduce a compensating tracking offset could be used in stationary triad systems. It may be possible to create mean phase error compensation methods. Development of automated mean phase error compensation is a matter left for future research.

For the purposes of this research, it assumed hence forward that adjustments made to the triad receiver PLL nullify the mean phase offset, i.e., $\beta_{\Delta} \equiv 0$. Upon examination of Equation (3.79), it is clear that a triad receiver correlator detector will encounter phase jitter

$$\sigma_{\Delta} = (1 \pm \Delta)\sqrt{\sigma_{rx}^2 + \sigma_{tx}^2} \ . \tag{3.80}$$

Note that frequency offset Δ contributes directly to the triad phase jitter. Keeping Δ as small as possible is a synchronization performance constraint inherent to triad system design.

CHAPTER 4 TECHNICAL APPROACH

The following sections describe the methods used during the planning, execution, and documentation of this research.

4.1 Modeling Tools, Laboratory Equipment, and Facilities

The author used tools, laboratory equipment, library, and facilities provided by Southwest Research Institute (SwRI) during the study and compilation of this report. The SwRI Library staff provided valuable literature research assistance and acquired most of the reference materials. The research employed Mathsoft Mathcad Professional for analysis and simple computer models. National Instruments LabVIEW was the tool of preference for complex computer models, especially those involving the PLL behavior.

4.2 Methods

The following sections discuss a four-phase project approach used to perform the research. Phase 1 developed the project concept, literature research, and the establishment of a synchronization performance metric. Phase 2 modeled current DSB-SC synchronization technology, which created a baseline for drawing comparisons during Phase 3. Phase 3 modeled the operational behavior of externally-referenced modulation designs. A comparison of model results taken during Phase 2 and Phase 3 looked for any architectural advantages that one synchronization method might exhibit over the other. Phase 4 created a computer model to be used in predictions of triad system performance.

4.2.1 Project Planning, Research, and Concept Development

Phase 1 investigated promising modulation techniques (e.g., PSK, QAM, FSK) and selecting a subset for detailed study. Selected techniques exhibited such desirable traits as good signal-to-noise performance or bandwidth efficiency. Literature reviews, computer models, and laboratory tests quantified candidate performance in the presence of phase error and noise.

A literature review compiled applicable data from prior research. New investigation employed prior research whenever possible to avoid duplicated effort and to increase research value. For example, much of the theoretical information used during internal and external model development came from the literature search. Theoretical derivations for BLSL, BLPL, and BPSK behavior were compiled from published research. Literature searches provided baseline reference materials describing the operational behavior and limitations of BPSK and DPSK modulation. In addition, a search identified expired U.S. Patent No. 4,117,405, in which the concept of using AM, DSB-RC broadcasts as a synchronization reference for telemetry transmission was formally proposed.

Investigation established coherent modulation and external reference selection criteria early in the project. Selection of modulation criteria focused on techniques likely to benefit RF transmission (e.g., noise immunity, data throughput, and bandwidth efficiency).

BPSK and DPSK modulation proved to be the best candidates for this study. Prior research provided an extensive resource for predicting behavior and developing tractable computer models.

Selection of an external reference gave preference to sources usable within marketable applications. Profiles of candidate frequency references provided comparisons of desirable attributes such as accuracy, geographic coverage, and simplicity. Comparisons pointed to AM, DSB-RC broadcasts as an external reference due to its relative simplicity, ease of construction, ready availability in most locations, and because its use represents a unique approach to external synchronization.

Using selection criteria and prior research as a guide, further analysis sought performance metrics suitable for comparisons of internally-referenced versus externally-referenced coherent RF transmission. Analysis found PLL output phase jitter [as defined in Equation (3.25)] versus band-pass limiter input signal-to-noise ratio [as described by Equation (3.40)] to be an appropriate technology comparison metric [62, 65, 48, 60, 61, 68]. Phase jitter versus SNR quantified the relative performance of internally-referenced versus externally-referenced modulation in terms readily understood by practitioners in the field of coherent synchronization.

4.2.2 Internally-Referenced BLSL Model

Phase 2 of this research created a computer model of the BLSL shown in Figure 3–1. The BLSL computer model consists of a number of LabVIEW subroutines, called "virtual instruments (VIs) [69]." LabVIEW VIs recreate the behavior of a second-order PLL, squaring circuit, and band-pass limiter with variables for filter and feedback

parameters. Signal generation VIs compute the desired SNR, synthesize a BPSK-modulated carrier with data rate of 145 bits per second, and apply the resulting DSB-SC signal with AWGN to the input of the BLSL. Virtual instruments located at the BLSL output measure the phase jitter, compute the output power spectral density, and display model results in numeric indicators and graphs.

This research selected a data rate of 145 bits per second as a compromise forced by three design constraints. First, there was the desire to compare the BLSL and BLPL behavior operating at the same PLL input frequency. A typical North American AM broadcast frequency was selected at 1.16 MHz for use in BLPL experiments. A squaring circuit within BLSL doubles the tracking frequency as seen by the DSB-SC receiver PLL. Therefore, a DSB-SC carrier frequency of 0.58MHz provided a PLL input frequency of 1.16 MHz. Finally, there was the desire to compare BLPL and BLSL behavior for low data rates applicable to narrowband communications. Having arrived at a common carrier frequency, memory constraints within available computing resources limited the maximum number of carrier cycles to 4,000 cycles per bit. A data rate of 145 bits per second represented the lowest data rate achievable at a broadcast frequency of 0.58 MHz under available computer resource constraints.

Figure 4–1 gives an example of typical internally-referenced, BLSL experiment using the "Internal BLSL Model" VI taken from one model iteration. Model operators specify the configuration of the internally-referenced BLSL by entering appropriate values in the "channel parameters" and "hard limiter filter" controls. A phase jitter σ_ϕ measurement during any given model iteration is a random variable. As such,

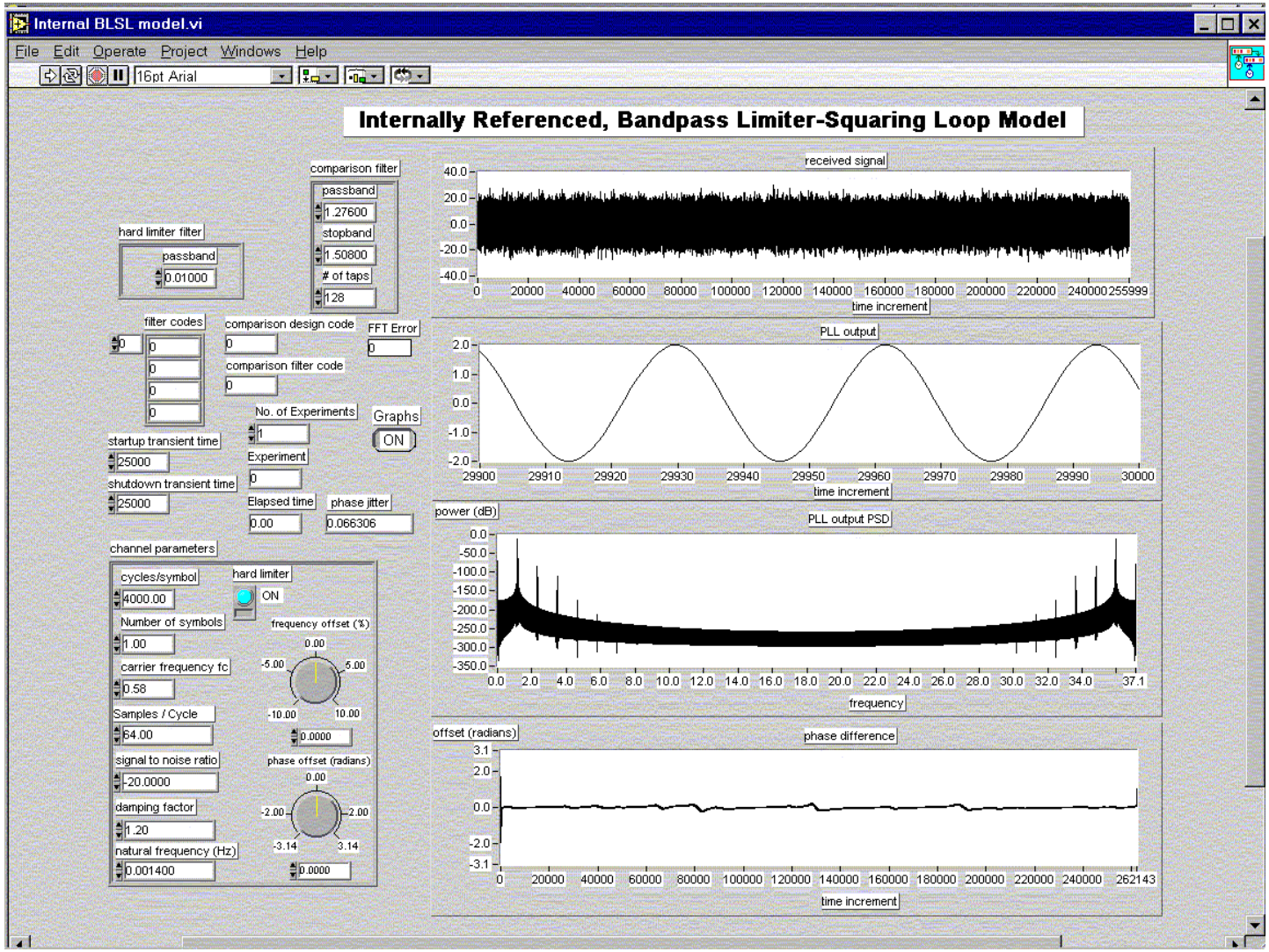

Figure 4–1. Internal BLSL Model Virtual Instrument

experiments conducted using Internal BLSL Model VI must average phase jitter measurements taken from a sufficiently large number of iterations so as to be statistically reliable. A "No. of Experiments" control permits the operator to specify an arbitrary number of iterations for a given model configuration. Averages taken from a set of model iterations appear in a numeric indicator labeled "phase jitter."

A complete study of a given BLSL configuration involves repeatedly executing the model over a range of SNR values. "Internal BLSL Iterant Test" VI repeatedly executes the Internal BLSL Model VI for the operator-specified BLSL configuration and a set of SNRs as specified in the "channel quality" control. (See Figure 4–2.) Results from the experiment appear in the graph labeled "Phase jitter vs. signal-to-noise ratio."

Note that the values shown across the x-axis of the graph are transmission channel signal-to-noise process ratios ρ_p and do not, without adjustment, reflect the effects of the hard limiter input filter.

$$\rho_p = \frac{S_i}{N_O f_s} \tag{4.1}$$

where f_s is the model discrete sampling rate. Solving for the noise process spectral density yields

$$N_O = \frac{S_i}{\rho_p f_s} \tag{4.2}$$

Substituting N_O into Equation (3.40) converts the transmission channel process SNR ρ_p shown in the "channel quality" control and on the graph's x-axis into the corresponding BLSL input SNR ρ_i for a given input filter noise equivalent bandwidth B_i.

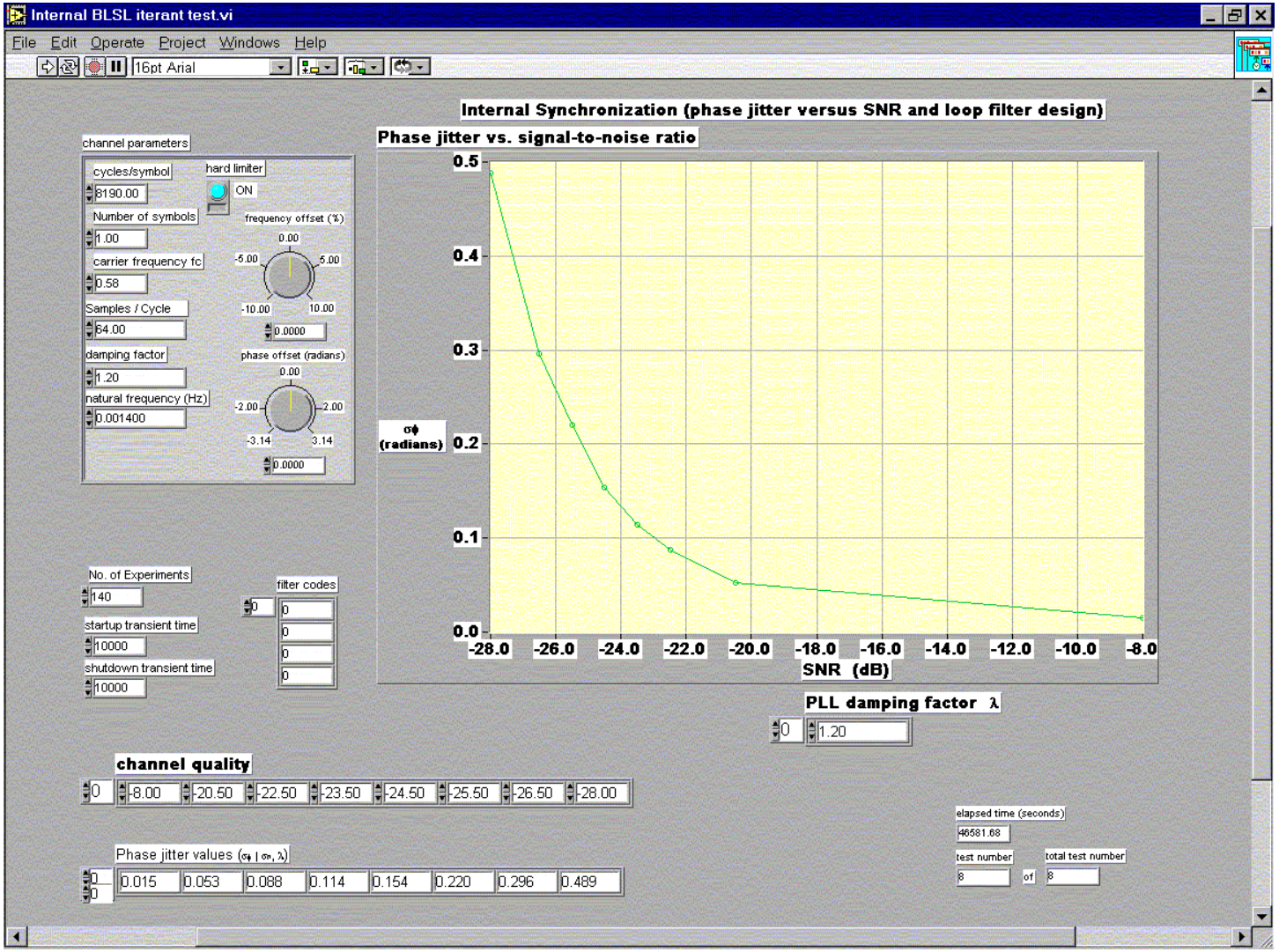

Figure 4–2. Internal BLSL Iterant Test Virtual Instrument

$$\rho_i = \frac{\rho_p f_s}{2B_i} \tag{4.3}$$

Applying Equation (4.3) to the ρ_p values given in the "channel quality" control adjusts for the effects of the hard limiter input filter and gives a set of ρ_i as seen at the BLSL input.

All BLSL and BLPL models found in this research use a variable-Q input filter VI called " Variable *Q* Filter Design ". In Figure 4–3, Variable *Q* Filter Design VI computes the noise equivalent bandwidth B_i for a given filter design. It displays B_i in the "single-sided noise equivalent bandwidth" indicator.

4.2.3 Externally-Referenced BLPL Model

An externally-referenced BLPL model is a computerized realization of Figure 3–7. The BLPL model differs from its BLSL counterpart in that it does not contain a squaring circuit for carrier recovery, and it is designed to process a DSB-RC signal.

It is not surprising that the BLPL model (See Figure 4–4), called "External BLPL Model VI," is similar to the BLSL model as shown in Figure 4–1. Like its BLSL counterpart, the BLPL model also consists of a number of LabVIEW VIs that recreate the behavior of a second-order PLL and band-pass limiter with variables for input filter and feedback loop parameters. Signal generation VIs compute the desired SNR and apply a DSB-RC signal with AWGN to the input of the BLPL. Virtual instruments located at the BLPL output measure the phase jitter, compute the output power spectral density, and display model results in numeric indicators and graphs as shown in the figure.

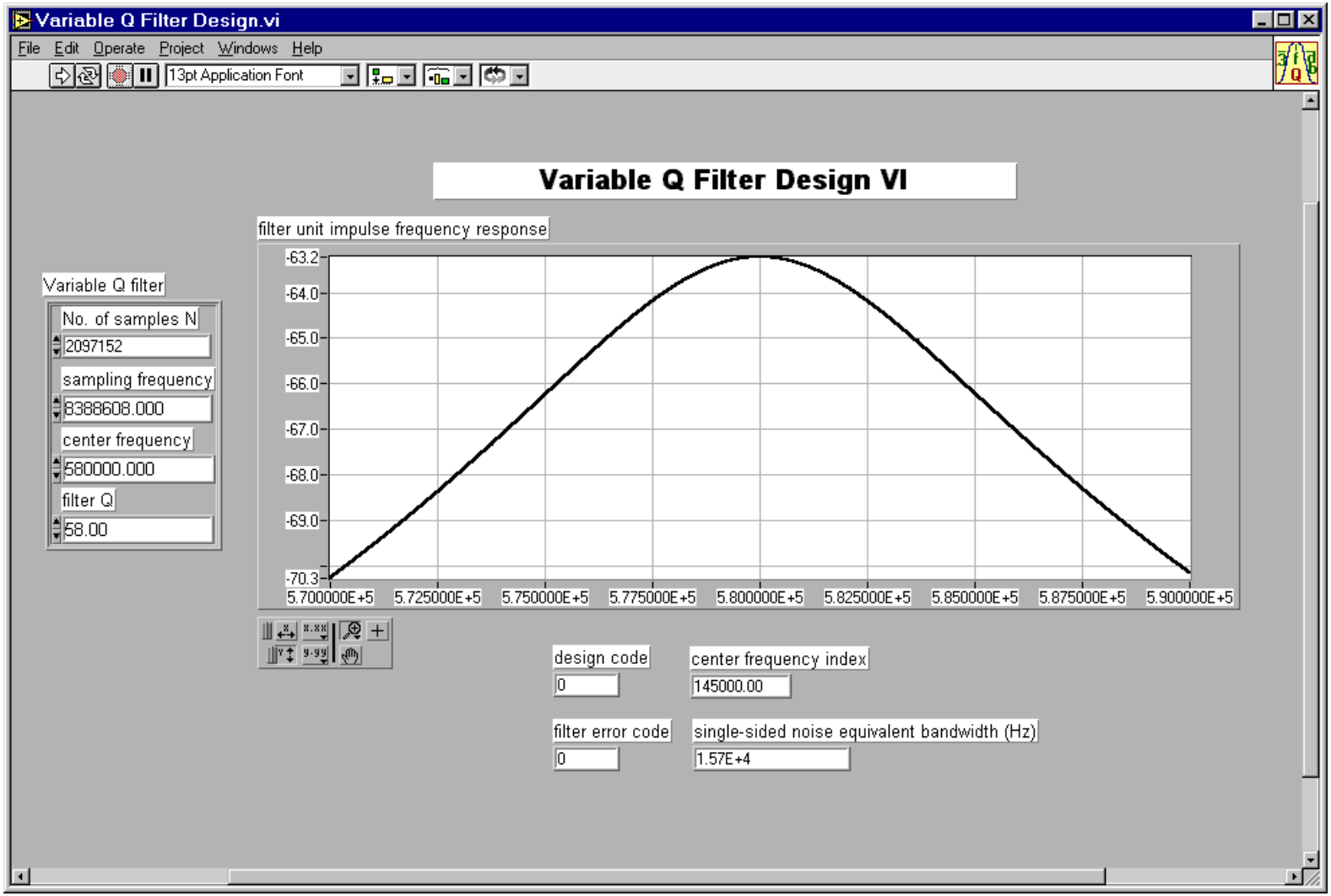

Figure 4–3. Variable *Q* Filter Design Virtual Instrument

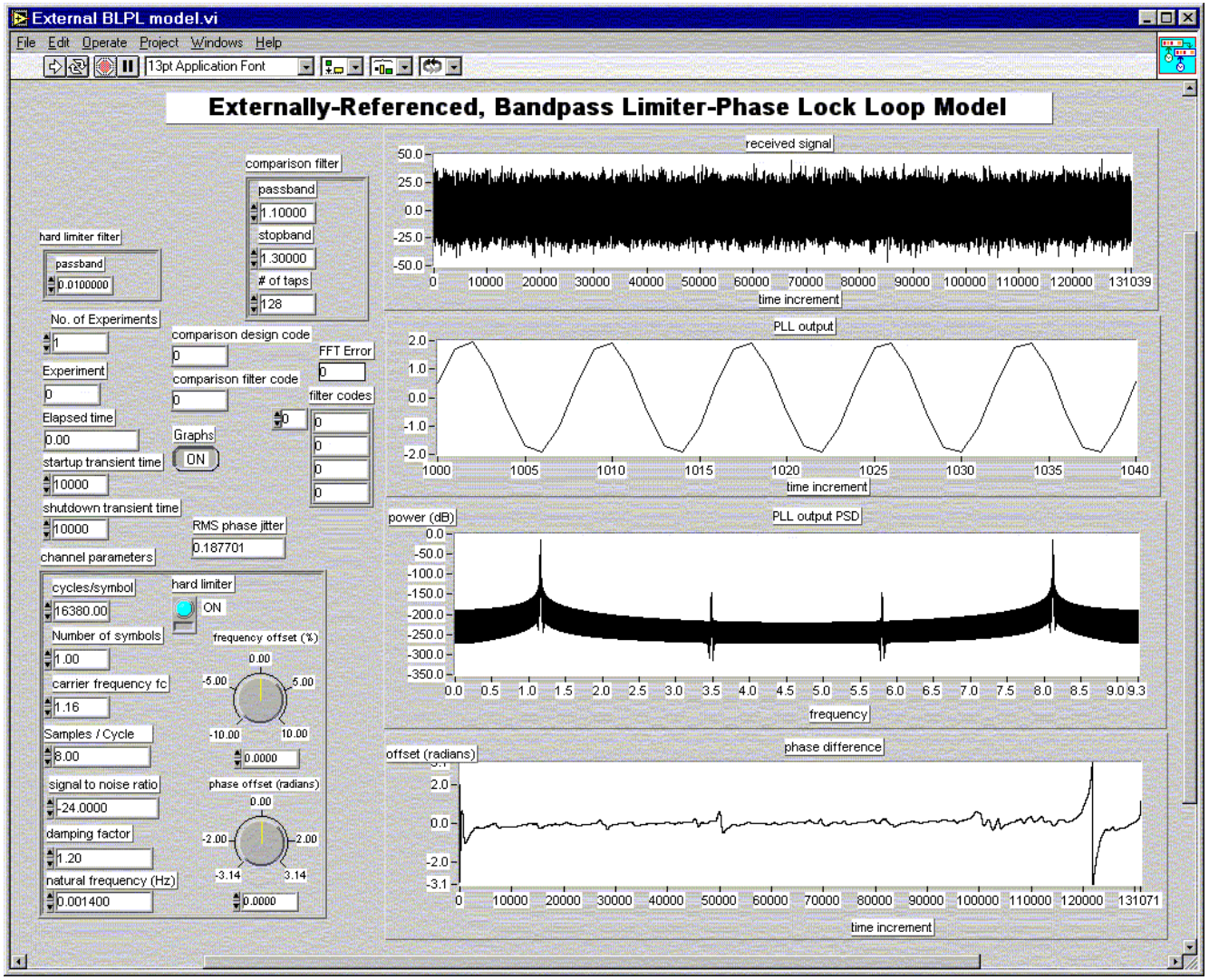

Figure 4–4. External BLPL Model Virtual Instrument

There are distinct differences in the way External BLPL Model VI and Internal BLSL Model VI treat the SNR of the synchronization reference. Differences in the models lie in the differences between DSB-SC and DSB-RC modulation.

A double sideband-suppressed carrier signal as described by Equation (3.3) conveys information by means of phase reversals. Its amplitude is constant so long as the transmission channel is not experiencing fading. If the noise process is stationary, then the received SNR is constant for a given path loss and noise spectral density.

Double sideband-residual carrier signals as described by Equations (3.64) and (3.65) convey information as a randomly varying carrier amplitude, which is functionally related to the sounds comprising the broadcast message. Received SNR ρ_i is a random, time-varying quantity with unknown distribution. A random ρ_i with unknown distribution presents a difficult problem for the creation of a statistically reliable BLPL computer model.

Provided the distribution of the broadcast message was known, statistically reliable results would require experiments spanning minutes of the message. Available computer memory and the maximum allowable array sizes permitted within certain LabVIEW VIs constrain the length of a given BLPL experiment to less than 16,384 carrier cycles. In addition, execution times for simulations spanning minutes of AM broadcast would require days to complete using readily available computer processors. With the resources available for this research, it is not practicable to model more than 14 milliseconds of an AM broadcast within any given experiment. A careful analysis of the known characteristics of audio communications and BLPL design

requirements lead to a means of simulating BLPL behavior without requiring a recreation of a random audio message.

Consider first that only the AM carrier is of interest as an external synchronization reference. Ideally, a BLPL referenced to an AM broadcast would select the carrier frequency and filter out all sideband modulation. In fact, the External BLPL VI uses a narrow-band filter at the BLPL input in an effort to block as much of the sideband modulation and noise as possible. However, FCC regulations permit an AM broadcast to vary from its assigned frequency within a range of $\pm 20\,\text{Hz}$ [9, 10]. Limitations in the External BLPL VI filter design further limit BLPL input filter quality Q to $Q \leq 30{,}000$ for a model operating at the chosen carrier frequency of 1.16 MHz. Filter design constraints limit input selectivity to $\pm 55\,\text{Hz}$. Practically speaking, modulation below 100 Hz will cause variations in ρ_i as seen at the input to the BLPL.

An AM broadcast is a function of the speech and voice content of the audio message. In addition, broadcast regulation places restrictions upon the message content. Federal Communication Commission regulations restrict AM modulation bandwidth to 10,000 Hz [72]. Modulation of the carrier may not exceed 100% at any time [73]. Within these regulatory boundaries, natural phenomena further confine the behavior of AM modulation.

Studies by the Acoustical Society of America show that certain behavior appears consistently within speech and music [74]. The human ear has a maximum frequency range from $20\,\text{Hz}$ to $20{,}000\,\text{Hz}$. Accordingly, there is no energy outside this range. Furthermore, human speech has 85% of its energy distributed below $1000\,\text{Hz}$. Studies by

Bell Telephone Laboratories show that a small amount of the speech power falls below 300 Hz. As a result, standard telephone circuits have a band-pass from 200 Hz to 3400 Hz.

Speech and music amplitudes (volumes) vary around some mean value [74]. Taking the ratio of the peak amplitude to the mean amplitude at a given frequency, a ratio referred to as the "peak factor," provides a measure of this variance taken across the message spectrum. Studies show that AM broadcast peak factors are statistically less than 8 dB below 200 Hz. Peak factors as high as 17 dB occur above 2000 Hz. From these studies, it is possible to conclude that a small amount of the total modulation power appears below 100 Hz, there is no modulation below 20 Hz, and variation of the envelope below 200 Hz is relatively small.

To make the model practicable, the design of the External BLPL VI assumes that ρ_i varies slowly and is essentially constant during the span of a single experiment. Experiments taken across a broad range of ρ_i provide information regarding BLPL behavior under a given path loss and modulation depth. These simplifying assumptions take advantage of the known behavior of speech and the human ear. They permit the creation of a viable model within available computer resources.

Avenues do exist for performing simulations like those described in this research over long simulation intervals and within practical computer resources. Oppenheim and Schafer describe two methods in [75] for processing signals over a large number of samples and within limited computer memory. The "overlap-and-add" method and the "overlap-and-save" method perform linear convolution of a finite filter impulse response

and very long or infinite length input signal. With significant modification to the models, either of these methods could be applied to the simulating BLSL and BLPL behavior over long signal intervals. Overlap-and-add and overlap-and save methods lend themselves directly to the several filters used in the simulation provided care is taken in truncating the impulse responses to avoid signal phase distortion [76, 77]. A modified version of the PLL model could process segments provided that the intermediate states of the PLL were preserved across segment boundaries with good fidelity. Segmenting the simulation in this manner would allow processing of longer simulation intervals within finite memory resources.

There remains the problem of the computer processing time. BLPL and BLSL models described in this research take several hours to process 14 milliseconds of input signal when using AMD Athlon or Intel Pentium processors. It is possible to reduce processing time by reorganizing the sub-VIs comprising these models into process threads. Each thread would process a signal segment concurrently with other threads within a multiprocessor workstation or within multiple workstations operating in a distributed computing environment.

Available resources provided for the construction and execution of models achieve the goals set for this research by repeatedly processing 14 millisecond segments of input signal to obtain statistically sound results. Time and funding for multiprocessor workstations were not available for reorganizing the models into a segmented, multiple thread form. These model enhancements are left as a topic for further research in external synchronization simulation.

A complete study of a given BLPL configuration involves repeatedly executing the model for selected SNR values. "External BLPL Iterant Test" VI repeatedly executes the External BLPL Model VI for the operator-specified configuration and a set of SNRs as specified in the "channel quality" control, as shown in Figure 4–5. Results from the experiment set appear in the graph labeled "Phase jitter vs. signal-to-noise ratio." As with the Internal BLSL Iterant Test VI, values shown in the “channel quality” control and along the graph’s x-axis are process SNR ρ_p values. A model operator must convert the values in the "channel quality" control into the corresponding set of BLPL input SNR ρ_i by using Equation (4.3).

4.2.4 Triad System Performance Model

It is a goal of this research to produce a computer model that describes the performance of a triad system across a range of system configurations. A triad system model must execute quickly and produce results within a few seconds or, at most, a few minutes. In comparison, the "internal BLSL model" and "external BLPL model" execute for hours or even days before producing statistically reliable results.

It is possible to create a straightforward triad system model by first assuming the existence of a linear relationship between the phase jitter at any given SNR and the BLPL input filter noise equivalent bandwidth. Model results described later in Section 5.2.2 validate the linearity assumption across a broad range of BLPL input filter designs.

The Mathcad document (MCD), called "Triad System Model" (See Appendix A), creates an interpolated phase jitter function $\sigma_{\text{int}erp}(\cdot)$. The interpolation function *interp*

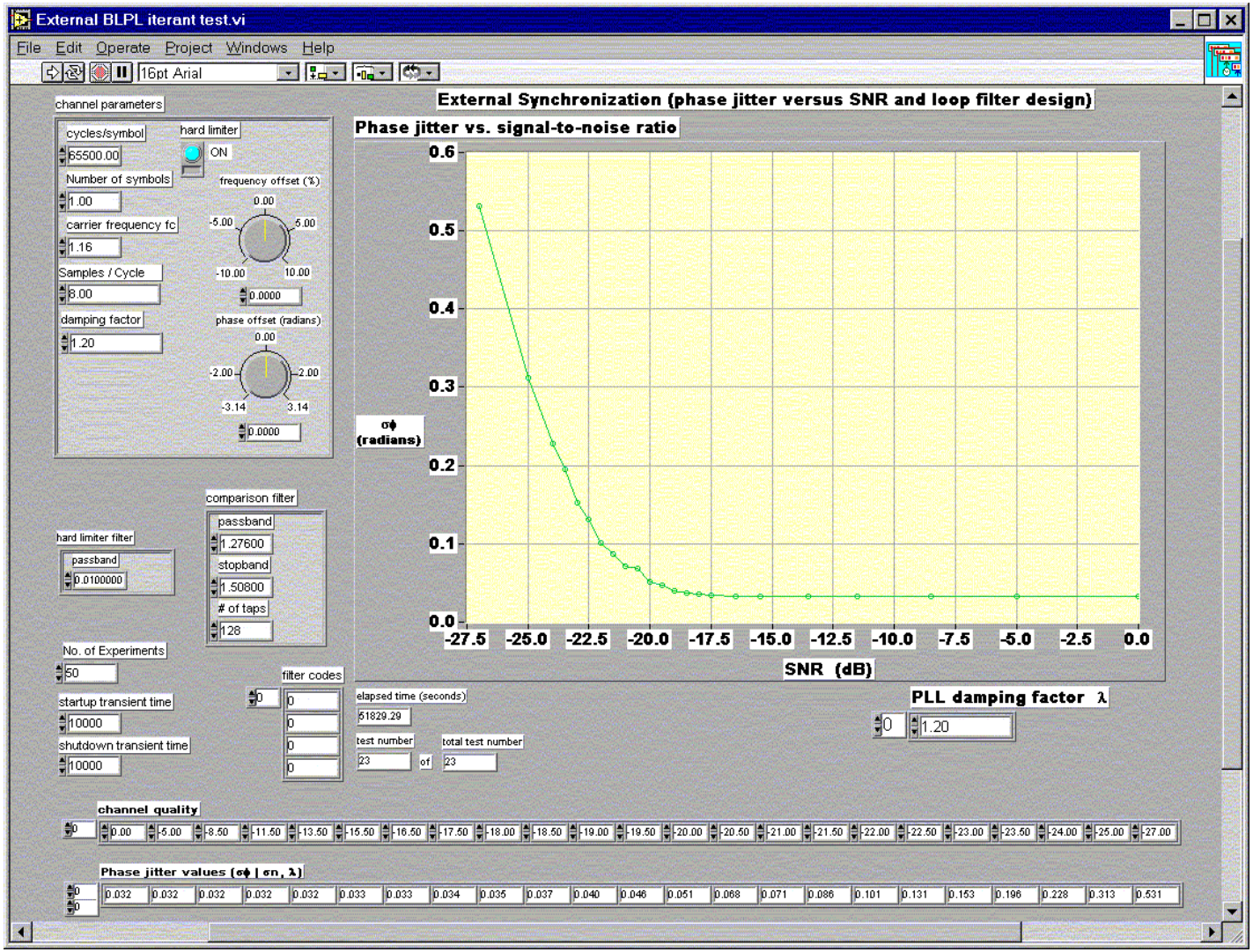

Figure 4–5. External BLPL Iterant Test Virtual Instrument

uses a basis set of phase jitter and channel SNR results $\{\rho_{Base}, \sigma_{Base}\}$ created by executing the External BLPL Iterated Test VI for a given BLPL input filter noise equivalent bandwidth. Triad System Model uses $\sigma_{\text{int}erp}(\cdot)$ and the basis set to estimate the BLPL phase jitter for arbitrarily chosen input filter design and input SNR.

Execution of the triad model follows four steps. First, External BLPL Iterated Test VI computes a basis set of phase jitter and channel SNR values $\{\rho_{Base}, \sigma_{Base}\}$ to be used in the interpolation. Second, Variable *Q* Filter Design VI computes the noise equivalent bandwidth B_{Base} used in the experiments that produced $\{\rho_{Base}, \sigma_{Base}\}$. Third, a model operator stores the DSB-RC carrier amplitude, phase jitter set, channel SNR set, and the input filter noise equivalent bandwidth in the variables labeled A, ρ_{Base}, σ_{Base}, and B_{Base}, respectively. These "Base" variables are sufficient to define the interpolation to be performed by the function $\sigma_{\text{int}erp}(\cdot)$. Finally, the operator defines desired model behavior by specifying the following model parameters:

- desired input filter quality (Q),
- desired input filter noise equivalent bandwidth (B_i),
- DSB-RC reference signal SNR at the triad transmitter (ρ_{tx}),
- DSB-RC reference signal SNR at the triad receiver (ρ_{rx}),
- BPSK-modulated DSB-SC SNR at the triad receiver (ρ_{path}), and
- DSB-SC carrier frequency offset (Δ).

Triad System Model produces three estimates as shown in Appendix A. In Appendix A, the figure labeled "BLPL estimated phase jitter performance" predicts the

specified BLPL phase jitter performance across a range of input SNRs. Function $\sigma_{triad}(\cdot)$computes the total phase jitter as seen by the triad receiver BPSK detector. Function $P_b(\rho_{path},\sigma_{triad})$ computes the expected receiver bit error rate for the given triad configuration.

Chapter 4 describes three computer models: the Internally-Referenced BLSL Model, the Externally-Referenced BLPL Model, and the Triad System Model. Taken together, the models provide a framework for a set of interrelated experiments. Internally-Referenced BLSL Model establishes a phase jitter performance baseline to be used in BLSL and BLPL performance comparisons. External BLPL Model predicts a set of phase jitter results for a BLPL under conditions similar to those used to baseline the BLSL. Triad System Model extrapolates External BLPL Model results and makes predictions of triad system performance within definable system configurations. Chapter 5 applies the models in a series of experiments from which comparisons and conclusions are drawn.

CHAPTER 5 RESULTS

This research develops three working models used in the study of externally-referenced, coherent modulation. The following sections describe the experimental results derived from these research models. The sections use a set of related examples as a framework for comparing the BLSL versus BLPL behavior.

The goals of the models are to provide better understanding of the behavior of coherent transceivers, to predict the behavior of the transceivers in a triad configuration, and to demonstrate the operation of a triad system. The BLSL model offers insight into the performance of an internally-referenced, coherent transceiver operating on a DSB-SC data transmission. The BLPL model describes the behavior of an externally-referenced, coherent transceiver synchronized to a DSB-RC broadcast. The triad system model translates and extrapolates the BLPL model results to provide predictions of triad performance.

5.1 Internally-Referenced BLSL Model Predictions

The internal BLSL model in Figure 4–2 predicts the behavior of an internally-referenced BLSL for an operator-specified configuration and a set of input process SNRs. For example, consider a BLSL operating within a receiver. The BLSL operating parameters as defined in Figure 3–1 are as follows:

Example 1. BLSL with $B_i = 10\,\text{kHz}$

- received carrier frequency $f_c = 580\,\text{kHz}$
- received signal peak amplitude $A = 1\,\text{volt}$

- single-sided, input band-pass filter bandwidth of 10 kHz, i.e., filter quality $Q = 58$
- single-sided, noise equivalent bandwidth of the input filter $B_i = 15.7\,\text{kHz}$
- PLL damping factor $\zeta = 1.2$
- PLL feedback loop natural frequency $\varpi_n = 0.0014$ radians per second
- PLL loop bandwidth $B_L = 1.57 \cdot 10^{-4}\,\text{Hz}$
- PLL output carrier estimate $2\hat{f}_c = 1{,}160\,\text{kHz}$

Using the preceding BLSL design parameters as a basis, Figure 5–1 compares second-order BLSL model results developed during this study with the predictions of linear, first-order BLSL phase jitter bounds defined by Equation (3.61) and with the linear, first-order PLL behavior defined by Equation (3.28). The simulation results show that the second-order BLSL will produce less phase jitter than the first-order, linear PLL model across the functional range of both devices, i.e., SNRs producing $\sigma_\phi \le 0.4$ radians. Equation (3.28) serves as a useful upper bound for second-order PLL behavior as suggested by [48].

The same simulation results show that Equation (3.61) predicts phase jitter far greater than are likely to be produced by a second-order BLSL. Clearly, Equation (3.61) only provides reasonable predictions of second-order BLSL behavior at large SNRs [48].

5.2 Externally-Referenced BLPL Model Predictions

There is a need to compare the performance of a BLSL versus a BLPL under similar operating conditions. The external BLPL model in Figure 4–5 provides the

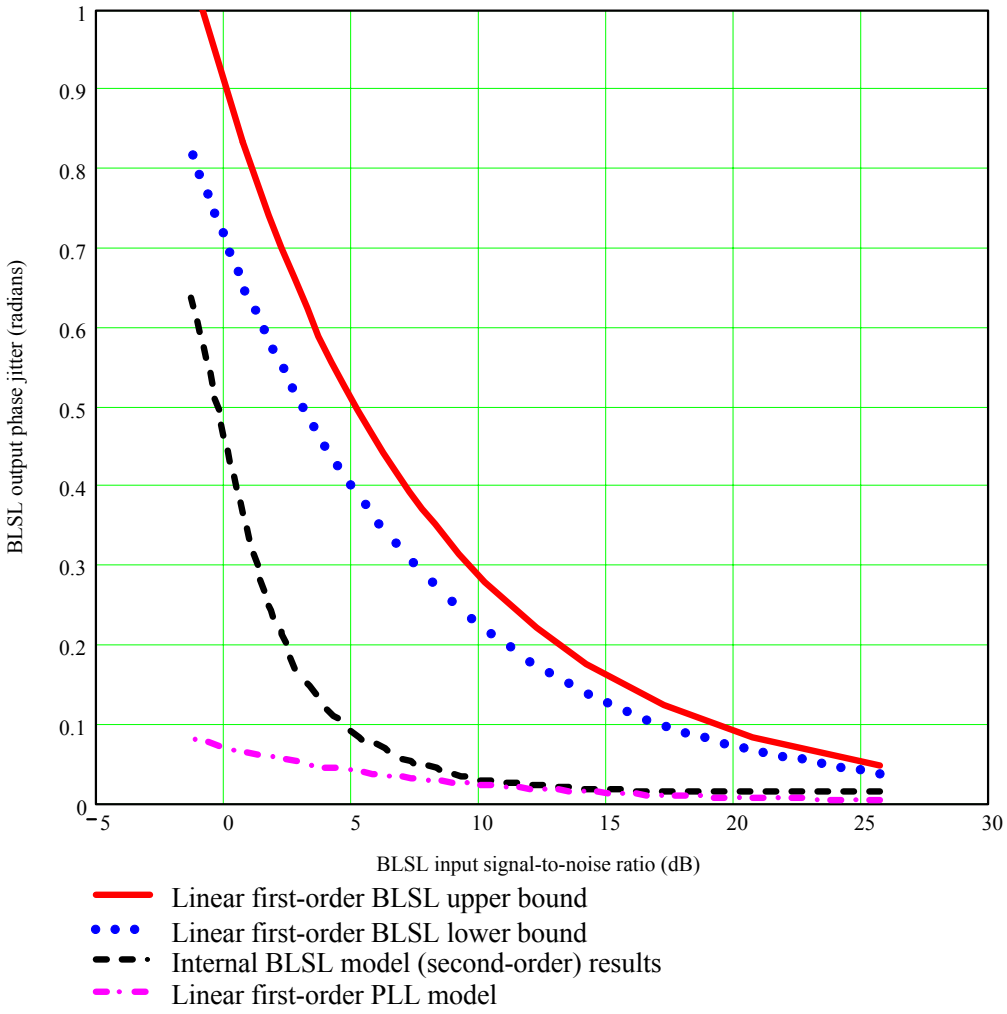

Figure 5–1. BLSL Theoretical Behavior Vs. Simulated Behavior (B_i = 15.7 kHz)

means to study BLPL behavior and draw comparisons with results from the internal BLSL model in Figure 4–2. However, it is difficult to study the effects of squaring loss in second-order systems unless the BLSL and BLPL under study have the same input process bandwidth.

The following example deliberately chooses a DSB-RC system with a 10 kHz-input bandwidth so that its behavior can be directly compared with Example 1. Consider a BLPL having the same output frequency and operating under conditions equivalent to the BLSL described in Example 1. The BLPL operating conditions are as follows:

Example 2. BLPL with $Q = 116$

- received carrier frequency $f_c = 1{,}160\,\text{kHz}$
- received signal peak amplitude $A = 1$ volts
- single-sided, input filter band-pass bandwidth of 10 kHz, i.e., filter quality $Q = 116$
- single-sided, noise equivalent bandwidth of the input filter $B_i = 15.7\,\text{kHz}$
- PLL damping factor $\zeta = 1.2$
- PLL feedback loop natural frequency $\varpi_n = 0.0014$ radians per second
- PLL loop bandwidth $B_L = 1.57 \cdot 10^{-4}\,\text{Hz}$
- PLL output carrier estimate $\hat{f}_c = 1{,}160\,\text{kHz}$

Figure 5–2 illustrates a triad prototype similar to the one described by Example 2 constructed by Tom Warnagiris [70]. The example is typical of a triad system referenced to the KENS broadcast signal and operating within the San Antonio, Texas, broadcast area as illustrated in Figure 5–3. Example 2 has the same 10 kHz modulation bandwidth

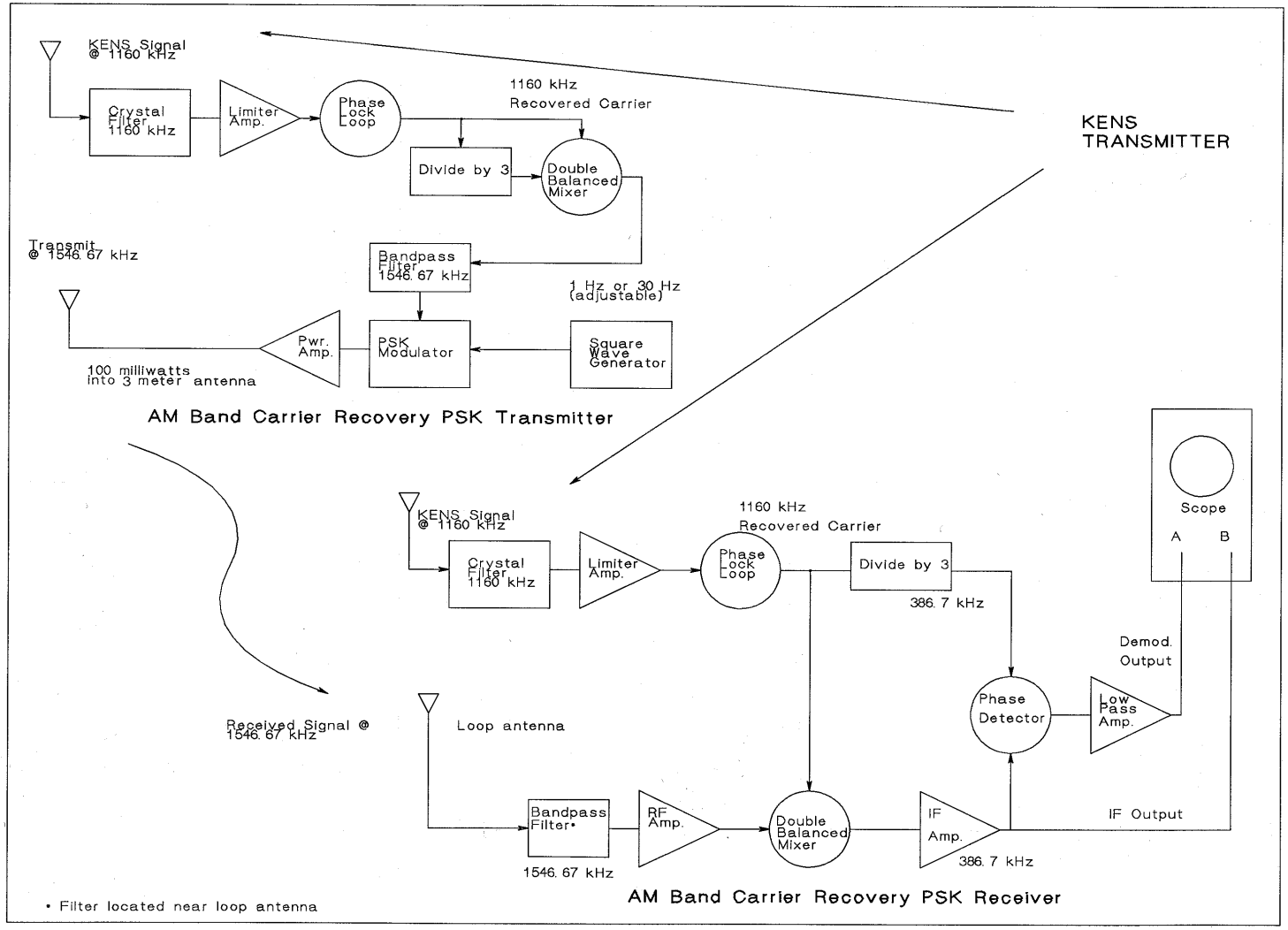

Figure 5–2. A Triad System Using an AM Broadcast as a Reference [70]

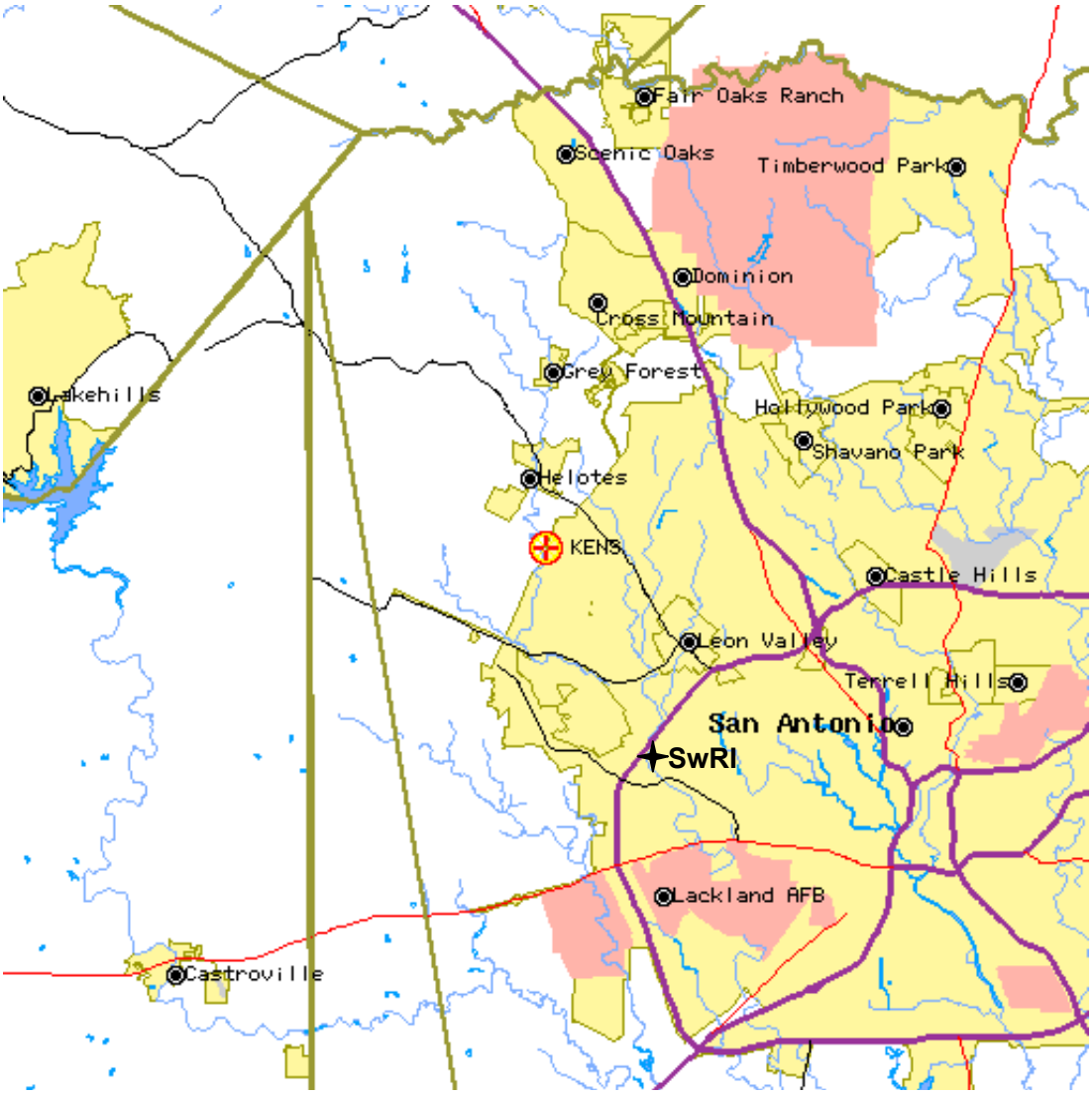

Figure 5–3. Map Showing the Location of KENS AM Radio Station [71, 78]

as used in Example 1, i.e., the DSB-SC example. The BLSL output frequency in Example 1 is two times its input frequency. The BLPL output frequency in Example 2 is the same as its input frequency, which is due to the lack of a squaring circuit. A fair comparison of BLPL and BLSL methods requires that the BLPL input frequency and the input filter quality be two times the input frequency and filter quality of the equivalent BLSL. Thus, the BLSL and BLPL systems in Example 1 and Example 2 have the same input bandwidths and the same output frequencies.

Simulation results for Example 2 (See Figure 5–4) show that BLPL has significantly less phase jitter than described by the upper bound of Equation (3.63) over the useful range of its operation, i.e., $\sigma_\phi \leq 0.4$ radians. Like the BLSL case, Equation (3.63) represents an upper bound approximation of second-order BLPL phase jitter.

5.2.1 Squaring Device Effects

A comparison of the 0.4 radian crossings of the BLSL in Figure 5–1 and of the BLPL in Figure 5–4 occur at 0.4 dB and -1.1 dB, respectively. The models predict that an externally-referenced BLPL has approximately 1.5 dB advantage over the equivalent internally-referenced BLSL. The difference is attributable to the presence of the squaring circuit in the BLSL.

The BLSL squaring circuit adds phase jitter to the results presented in Example 1 in two ways (See Section 3.5). The squaring circuit doubles the phase error and quadruples the phase variance, thereby reducing BLSL phase jitter performance by 6 dB [48]. The 0.4 radian crossing in Figure 5–1 occurs at approximately 0.4 dB. Equation (3.57) predicts an additional BLSL performance degradation of 1.5 dB due to squaring

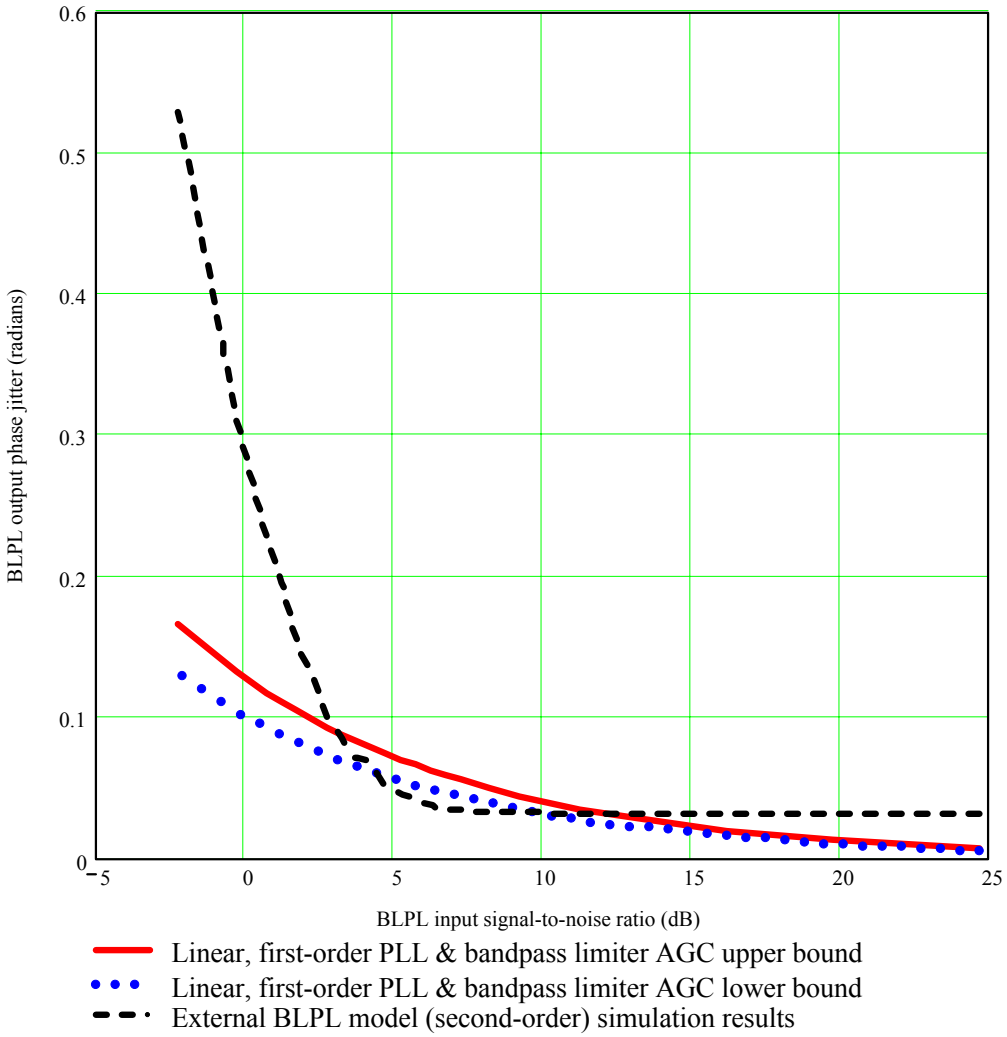

Figure 5–4. BLPL Theoretical Bounds Versus Modeled Results (B_i = 15.7 kHz)

loss at an input SNR of 0.4 dB. Therefore, the absence of a squaring circuit in the BLPL should give the BLPL a 7.5 dB performance advantage over the BLSL.

Model results generally support theoretical predictions by showing a significant BLPL performance advantage. However, the modeled BLPL performance improvement is 6.0 dB less than that predicted by the theory described in Section 3.5 and Equation (3.57). Recall that the theoretical analysis in Section 3.5 is based upon first-order PLL theory and serves only as an upper bound for second-order PLL behavior. A second-order PLL exhibits superior tracking and noise immunity when compared to a first-order PLL. Unfortunately, closed-form expressions for second-order BLSL behavior have proven to be intractable [57, 48, 61].

The 6.0 dB discrepancy between theoretical predictions and model results may be due to the low-pass response of the second-order PLL loop filter and the frequency doubling effects of the squaring circuit. The squaring circuit may spread the spectrum of the feedback loop noise, thereby placing more of the noise energy outside the pass band of the PLL loop filter. The hypothesis requires further study before a firm conclusion is possible. Even so, the model results show that the presence of a squaring circuit creates a significant difference (1.5 dB) in the behaviors of the second-order BLSL and BLPL circuits.

5.2.2 High-*Q* Input Filter Effects

A BLSL must process all of the DSB-SC sideband information to extract an accurate estimate of the transmit carrier. Therefore, its synchronization bandwidth

encompasses the entire DSB-SC signal bandwidth. Any noise found within the DSB-SC spectrum will reduce the SNR as seen by the BLSL.

On the other hand, a BLPL need only process the spectrum in which a DSB-RC carrier may be found to extract its carrier estimate. By design, the DSB-RC carrier is stable with a small deviation from the assigned frequency. Therefore, it is possible to filter the BLPL input to a much narrower bandwidth than that of the BLSL. Under similar conditions, a relatively narrow input bandwidth reduces the noise energy processed by the BLPL with a corresponding gain in BLPL synchronization performance.

Any attempt to gain a performance improvement by significantly reducing the BLPL input bandwidth is conditional upon the residual carrier reference maintaining a nearly constant carrier frequency. This condition can be met by building a dedicated RC reference with the required frequency stability or by using a readily available source having adequate frequency stability. For instance, FCC regulations require AM radio broadcast stations to transmit within a frequency range $f_{deviation} = \pm 20\,\text{Hz}$ of their assigned carrier frequency.

An AM radio broadcast may be a sufficiently stable DSB-RC reference. Expired US Patent No. 4,117,405 proposes just such an arrangement, in which an AM radio broadcast would be used as the synchronization reference for telemetry transmission. A goal of this research is to study the use of a DSB-RC signal, such as an AM radio broadcast signal, as an improvement to transceiver synchronization.

Figure 5–2 offers one possible implementation in which both the transmitter and the receiver derive their carrier frequency from a commercial AM radio station operating

at 1,160 kHz. Both the transmitter and the receiver use identical band-pass limiters and PLLs to recover the AM carrier. Given the accuracy of the AM carrier signal, it is feasible to precede the BLPL with a narrow band-pass filter. The upper bound on the filter quality, referred to as the filter "*Q*," depends on the accuracy of the residual carrier reference. In the case of commercial AM radio signals, the filter quality can be as high as

$$Q_{DSB-RC} \leq \frac{f_{RC}}{2 f_{deviation}} \tag{5.1}$$

where f_{RC} is the DSB-RC broadcast carrier frequency. A band-pass limiter like that depicted in Figure 5–2 tracks a carrier frequency $f_{RC} = 1.16\,\text{MHz}$. The AM carrier accuracy permits the use of an input filter quality as high as

$$Q_{DSB-RC} \leq 29{,}000 \tag{5.2}$$

for the recovery of broadcast carrier.

All BLPL and BLSL experiments conducted by this research use a variable *Q*, band-pass input filter, called "Variable *Q* Filter Design Virtual Instrument" and shown in Figure 4–3. Variable *Q* Filter Design Virtual Instrument is a computer model for a band-pass filter with a transfer function described by

$$H(s) = \frac{2\pi f_0 s}{Q s^2 + 2\pi f_0 s + (2\pi f_0)^2 Q} \tag{5.3}$$

where f_0 is the filter center frequency and *Q* is the filter quality at the center frequency [79]. The virtual instrument displays the filter's power spectral density for a given *Q* as shown in Figure 4–3. It computes the filter's noise equivalent bandwidth as [48, 69]

$$B_i = \frac{\int_{-\infty}^{\infty} |H(2\pi f)|^2 \, df}{2|H(2\pi f_c)|^2}. \tag{5.4}$$

Assuming that all input BLPL and BLSL input filters are of the form described by Equation (5.3), then the lower bound for the input filter noise equivalent bandwidth is

$$B_{29,000} = 62.9 \text{ Hz} \tag{5.5}$$

as computed by Variable *Q* Filter Design Virtual Instrument for a band-pass filter with a filter quality of 29,000.

Using the 10 kHz modulation bandwidth in Example 1 as a basis of comparison, a BLSL has an input filter quality of 116 and a noise equivalent bandwidth of

$$B_{116} = 15.7 \text{ kHz}. \tag{5.6}$$

In the case of Example 2, the use of an external AM carrier reference suggests an input bandwidth gain as high as

$$10 \log\left(\frac{116}{29{,}000}\right) = 24 \text{ dB} \tag{5.7}$$

A DSB-RC signal received by a BLPL with $Q_{DSB-RC} = 116$ must have a received SNR that is 24 dB greater than the received AM carrier received by a BLPL using a $Q_{DSB-RC} = 29{,}000$. Equation (5.7) assumes that the noise equivalent bandwidth of the input filter is directly proportional to *Q*. The assumption holds so long as the filter quality is the only parameter varying in the filter design.

A more general expression for input bandwidth gain is given by

$$G_i = 10\log\left(\frac{B_{116}}{B_{29,000}}\right) \tag{5.8}$$

where $B_{29,000}$ and B_{116} are the noise equivalent bandwidths for input filter qualities of 29,000 and 116, respectively.

Table 5-1 summarizes the externally-referenced BLPL model results simulated across a broad range of filter qualities. The simulated gains track closely with the linear gain predictions in Figure 5–5. Figure 5–5 clearly shows that reducing the input bandwidth yields a linear gain in BLPL phase jitter performance.

Reconsider the externally-referenced BLPL in Example 2 by first replacing the input filter with an input filter having a filter quality Q = 29,000. The BLPL input noise equivalent bandwidth becomes approximately 63 Hz. External BLPL model results found in Table 5-1 describe an input noise equivalent bandwidth gain of 24 dB when compared to the BLPL with $Q = 116$. The simulated results match the prediction in Equation (5.7).

Elimination of the squaring circuit and its associated squaring loss adds another 1.5 dB to the phase jitter performance of the BLPL when operating with an external reference. Table 5-1 shows that a BLPL referenced to an external, DSB-RC source and having an input filter bandwidth of $B_i = 63$ Hz has a useful tracking range ($\sigma_\phi \le 0.4$ radians) for a received reference SNR $\rho_i \ge -30.6$ dB. The 0.4 radian crossing in Figure 5–1 is at approximately 0.4 dB for the BLSL. Simulations demonstrate a 31.0 dB difference in performance between the BLSL with input filter quality of 116 and a

Table 5-1. External BLPL Model Results (f_{RC} = 1.16 MHz)

filter quality Q	noise equivalent bandwidth B_i (Hz), f_c = 1.160 MHz	0.05 radian crossing (dB)	0.1 radian crossing (dB)	0.2 radian crossing (dB)	0.3 radian crossing (dB)	0.4 radian crossing (dB)
58	31326.8	1.7	-1.0	-3.0	-4.3	-5.3
116	15685.5	-1.3	-3.3	-4.8	-5.8	-6.8
300	6076.4	-5.3	-7.1	-8.6	-9.8	-10.8
500	3653.1	-7.3	-9.1	-10.8	-12.0	-13.0
900	2024.2	-10.8	-11.6	-13.6	-14.6	-15.6
1800	1012.2	-13.8	-15.1	-16.8	-17.5	-18.8
4000	455.5	-16.3	-18.3	-20.1	-21.3	-22.5
5800	314.2	-18.8	-20.1	-21.8	-22.8	-24.1
10000	183.4	-21.3	-22.8	-24.0	-25.0	-26.1
11600	160.8	-22.3	-23.8	-24.8	-25.5	-26.6
13000	140.2	-21.8	-23.8	-25.1	-26.3	-27.8
15000	121.5	-23.8	-24.3	-26.1	-27.3	-28.1
17000	107.2	-23.8	-25.4	-26.8	-27.4	-28.6
23000	79.2	-24.3	-26.3	-27.8	-28.5	-29.6
29000	62.9	-25.3	-27.3	-28.8	-30.0	-30.6

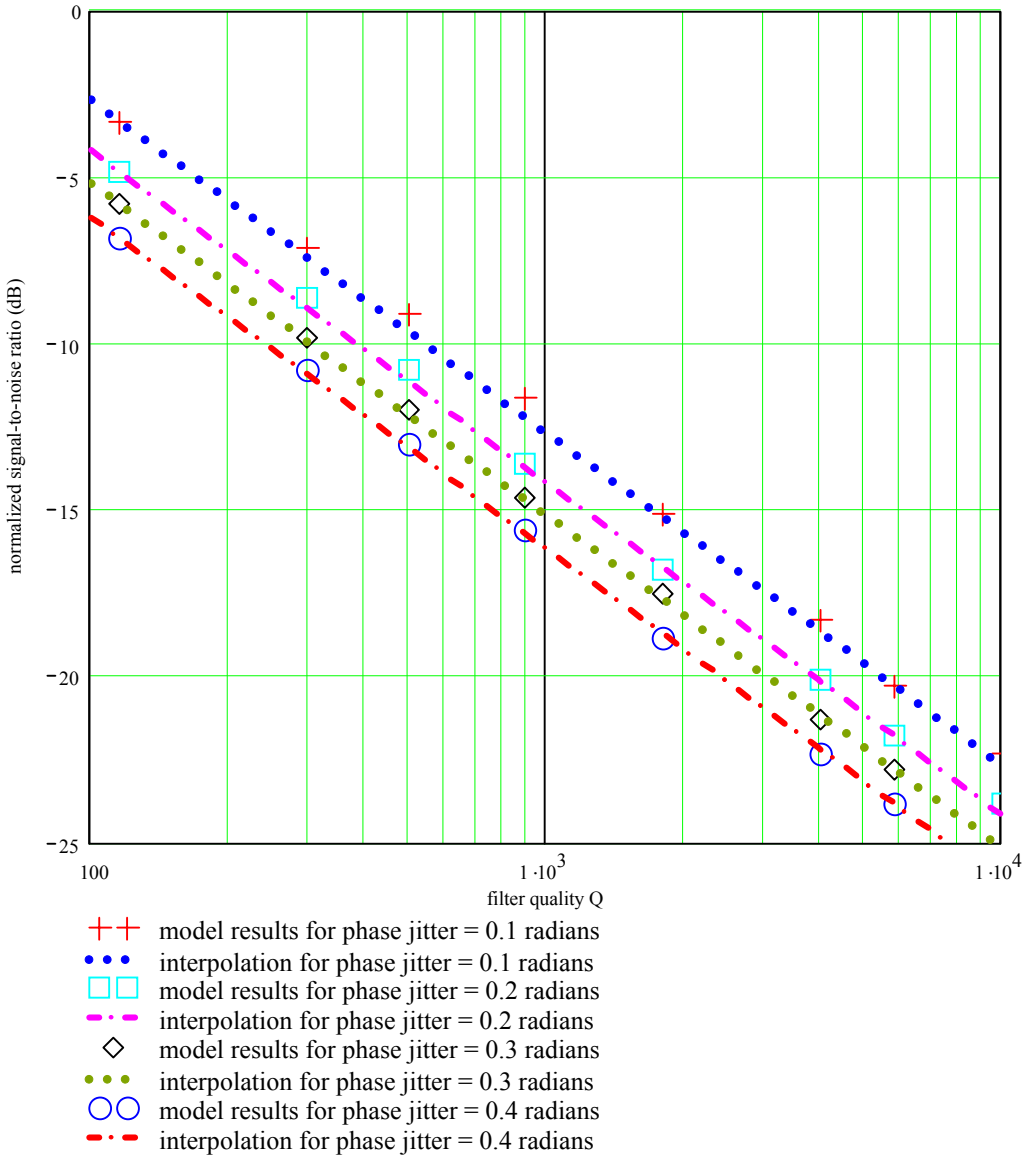

Figure 5–5. BLPL Phase Jitter Versus Linear Model (f_{RC} = 1.16 MHz)

BLPL with input filter quality of 29,000, which compares favorably with the 25.9 dB difference predicted by Figure 5–4 and Equation (5.7).

Studies of AM radio reception encountering varying levels of jamming show that adequate AM reception requires a received SNR of $\rho_i \geq 0\,\text{dB}$ [80]. Therefore, a triad transceiver should maintain synchronization beyond the normal reception area of a conventional AM broadcast. Moreover, a transceiver operating within the normal AM reception area will have at least 30.6 dB free space, synchronization link margin.

5.3 Triad System Model Predictions

Equation (5.8), Equation (3.80), and the BLPL model results from Example 2 provide the necessary framework for a model of triad system behavior. Let $\{\sigma_{Base}\}$ be the set of phase jitter values produced by the BLPL computer model in Example 2 for the corresponding set of input SNRs $\{\rho_{Base}\}$. Figure 5–4 gives the values produced by the model for Q = 116.

It is possible to estimate intermediate values of σ_ϕ for a given SNR ρ_i (given in dB) by using the model results shown in Figure 5–4 and an interpolation function

$$\hat{\sigma}_\phi(\rho_i, B_i) = interp\left[\{v_{cs}\}, \{\rho_{Base}\}, \{\sigma_{Base}\}, \rho_i + Log_{10}\left(\frac{B_{Base}}{B_i}\right)\right]. \qquad (5.9)$$

Note that the computed value of $\rho_i + Log_{10}\left(\frac{B_{Base}}{B_i}\right)$ must be within the range of $\{\rho_{Base}\}$.

Variable B_{Base} is the noise equivalent bandwidth for a filter quality of 116, ρ_i is the desired SNR, and B_i is the noise equivalent bandwidth for a band-pass filter. Function

interp is a general purpose, interpolation function as defined by Mathcad [81]. The function returns values for $\hat{\sigma}_\phi$ as points along a polynomial curve with coefficients as found within vector $\{v_{cs}\}$. This research chooses cubic spline interpolation with polynomial coefficients defined by

$$\{v_{cs}\} = cspline[\{\rho_{Base}\}, \{\sigma_{Base}\}]. \tag{5.10}$$

Mathcad function *cspline* computes a set of cubic spline coefficients for a polynomial that connects a set of points described by the basis set $\{\rho_{Base}, \sigma_{Base}\}$ [81, 82].

To interpolate intermediate values of σ_ϕ within Figure 5–4, select a B_i corresponding to a filter $Q = 116$. Recall that the input filter quality in Example 2 is $Q = 116$. Therefore,

$$B_i = B_{Base} = 15.7\,\text{kHz} \tag{5.11}$$

and

$$Log_{10}\left(\frac{B_{Base}}{B_i}\right) = 0\,\text{dB} \tag{5.12}.$$

Function $\hat{\sigma}_\phi(\cdot)$ can interpolate the BLPL phase jitter for an arbitrary input filter design. Specifying an input noise equivalent bandwidth B_i produces values of phase jitter estimates for filter designs with a corresponding filter quality.

If the triad transceiver pair use identical BLPL designs, i.e., the transmitter and receiver have the same input filter bandwidth B_i, then substituting Equation (5.9) into Equation (3.80) yields a phase jitter estimate $\hat{\sigma}_{triad}$ at the triad receiver BLPL output

$$\hat{\sigma}_{triad} = (1 \pm \Delta)\sqrt{[\hat{\sigma}_\phi(\rho_{tx}, B_i)]^2 + [\hat{\sigma}_\phi(\rho_{rx}, B_i)]^2} \tag{5.13}$$

where ρ_{tx} and ρ_{rx} are the BLPL input SNRs at the triad transmitter and the triad receiver, respectively.

Substituting the preceding estimate into Equation (3.9) provides a triad bit error rate prediction for BPSK-encoded data.

$$P_b(\rho \mid \hat{\sigma}_{triad}) = erfc\left[\sqrt{2\rho\cos(\hat{\sigma}_{triad})}\right] \tag{5.14}$$

The following example illustrates the triad system model. Consider a triad system having the following configuration.

Example 3. Triad System Model

- received DSB-RC carrier frequency $f_{RC} = 1{,}160\,\text{kHz}$
- received signal peak amplitude $A = 1$ volt
- single-sided, input filter band-pass bandwidth of 50.43 Hz, i.e., Q = 23,000
- single-sided, noise equivalent bandwidth of the input filter $B_i = 79.24\,\text{Hz}$
- PLL damping factor $\zeta = 1.2$
- PLL feedback loop natural frequency $\varpi_n = 0.0014$ radians per second
- PLL loop bandwidth $B_L = 1.57 \cdot 10^{-4}\,\text{Hz}$
- PLL output carrier estimate $\hat{f}_{RC} = 1{,}160\,\text{kHz}$
- Triad carrier frequency offset $f_c = 1.1 f_{RC}$, i.e., $\Delta = 0.1$
- DSB-RC signal-to-noise ratio measured at the triad transmitter $\rho_{tx} = -25\,\text{dB}$
- DSB-RC signal-to-noise ratio measured at the triad receiver $\rho_{rx} = -18\,\text{dB}$
- The triad DSB-SC signal-to-noise ratio at the triad receiver $\rho_p = 6\,\text{dB}$

The BLPL input bandwidth gain G_i relative to the BLPL configuration in Example 2 is 23 dB. Equation (5.13) estimates the triad receiver phase jitter $\hat{\sigma}_{\Delta}$ to be 0.084 radians. The triad system model estimates the BPSK bit error probability $P_b\left(\rho_p \mid \hat{\sigma}_{triad}\right)$to be $6.8 \cdot 10^{-5}$ errors per bit. Appendix A illustrates the Triad System Model MCD operation for the case described by Example 3.

Results derived from this research lead to several interesting conclusions. The next chapter will summarize these conclusions, discuss possible applications of the results, and suggest opportunities for further research.

CHAPTER 6 DISCUSSION AND CONCLUSIONS

Research results show that a triad system has certain advantages when compared to an internally-referenced, DSB-SC system. Computer models demonstrate that BLPL synchronization is independent from the data transfer channel, maintains continuous synchronization with a DSB-RC broadcast, and will maintain synchronization even at a very low DSB-RC SNR. Comparisons of the two synchronization approaches lead to the following detailed conclusions:

1. Second-order BLSL phase jitter performance is significantly better than the first-order BLSL predictions made by Equation (3.61).
2. Second-order BLPL phase jitter performance is significantly better than the first-order BLPL predictions made by Equation (3.63).
3. Models of second-order BLSL and second-order BLPL behavior demonstrate that the second-order BLPL has approximately 1.5 dB better phase jitter performance than the equivalent second-order BLSL.
4. Equation (3.75) shows that the triad system will track a residual carrier broadcast with a constant phase error.
5. Triad phase error is a function of the relative position of the transmitter, receiver, and the residual carrier broadcast antenna.
6. BLPL phase jitter is a linear function of the BLPL input noise equivalent bandwidth.
7. It is possible to predict BLPL performance across a range of input filter designs using a single set of External BLPL Model results as a BLPL phase jitter performance basis set.

8. Simulations show that an externally-referenced BLPL will track a DSB-RC reference operating at 1.16 MHz with an SNR $\rho_i \geq -30.6\,\text{dB}$ with a phase jitter $\sigma_\phi \leq 0.4\,\text{radians}$.
9. The preceding observation shows that a BLPL will track an AM broadcast beyond the normal AM reception area, which prior research shows is bounded by $\rho_i \geq 0\,\text{dB}$.
10. Equation (5.14) shows that a BLPL bit error probability is a predictable function of phase jitter at the triad transmitter and receiver.
11. It is possible to predict triad system performance for a range of system configurations using External BLPL model results as a phase jitter performance basis set.
12. A straightforward performance model exists for triad system phase jitter and bit error rate performance. Triad System Model extrapolates the results of the External BLPL Model, thereby providing predictions over a range of triad system configurations.

The nonlinear nature of BLPL and BLSL devices makes closed-form expressions for first-order devices difficult. Closed-form expressions for higher-order devices have proven intractable. Equations (3.61) and (3.63) serve as a useful and conservative upper bounds for phase jitter in higher-order devices. Figure 5–1 demonstrates that a second-order BLSL exhibits significantly better phase jitter performance than predicted by Equation (3.61) for first-order. Likewise, the simulation illustrated in Figure 5–4 show that a second-order BLPL has substantially better phase jitter performance than a first-order BLPL described by Equation (3.63).

A comparison of the model results show that a second-order BLPL has a 1.5 dB performance advantage over the equivalent BLSL. First-order device analysis predicts a

7.5 dB advantage in favor of the BLPL. The discrepancy points out the uncertainty of first-order PLL theory when applied to higher-order PLL design.

Triad System Model embodies several important points developed during the research. First, phase jitter is a predictable function of the transmitter BLPL phase jitter, the receiver BLPL phase jitter, and the ratio of the residual carrier and DSB-SC carrier frequencies. Phase jitter with the transmitter and receiver is a function of the received reference SNR and the BLPL input bandwidth. Furthermore, computer models show the relationship between BLPL phase jitter and input bandwidth to be linear. These points lead to a computationally straightforward design model for triad bit error probability.

Triad transceivers like the one shown in Figure 1–1 have the same SNR requirements along its data transfer path as their internally-referenced counterparts shown in Figure 3–1. Any differences between internally- and externally-referenced transceiver behavior lie in their ability to maintain accurate synchronization. A triad's synchronization channel is independent of the data transfer channel. Consequently, a triad system will maintain synchronization at times when the data transfer SNR is inadequate to support meaningful data detection and when the data transfer channel is not in use. Continuous synchronization has special benefits to wireless modem operation. These benefits will be discussed in later sections of this research.

Careful consideration should be given to the choice of a residual carrier reference. It has been shown that an externally referenced BLPL will maintain synchronization in areas where the received reference SNR is too low for normal AM reception. Even so,

consideration must be given to avoid areas where the residual carrier SNR is inadequate either due to the free space loss or to terrain such as mountains.

Care must also be taken to avoid an ambiguous selection of a residual carrier reference. Ambiguities arise when two indigenous references appear to occupy the same frequency within a common reception area. For example, the FCC may assign two AM broadcast stations to the same carrier frequency and broadcast area, but with different broadcast hours. An externally referenced system will synchronize to either station depending upon the time of day. However, the mean phase error at the triad receiver will vary depending upon the location of the station relative to the triad transceiver and the station's assigned broadcast schedule. Poor performance will result at times when the triad receiver PLL is not adjusted to compensate for time-dependent mean phase error.

Atmospheric conditions may induce overlapping broadcast coverage, thereby creating an ambiguous reference. Consider an externally referenced triad transceiver operating in an area where two broadcasts operating at the same assigned frequency overlap during certain weather conditions. The overlapping broadcast signals may differ somewhat in phase and frequency. Under overlapping broadcast conditions, members of the same triad community may synchronize to different residual carrier signals. Consequently, the triad community will be split with one group out of synchronization with the other group. Poor data reception will persist between the two groups so long as there is a difference in their frequency and phase. In severe cases, no data reception between the two triad groups will occur until the ambiguity is eliminated and the entire community synchronizes to the same residual carrier broadcast.

Any pragmatic improvement in BER performance achieved by adopting external synchronization is contingent upon internal referenced synchronization failure at times when there remains sufficient SNR to sustain adequate data detection. However, such is not the case in fact for most internally-referenced transceivers.

Most coherent transceivers employ second-order or higher-order PLLs. Simulations of second-order BLSL and BLPL behavior show that second-order PLLs maintain good synchronization at received signal SNRs well below the SNR specified by Figure 2–2 for adequate data detection. Adding external synchronization to a transceiver receiving a data-bearing signal with low SNR will not improve its BER appreciably.

As a consequence, there is no direct improvement in BER performance gained by externally-referencing a transceiver to a synchronizing broadcast if the received data signal SNR is too low. However, other important benefits do exist and will be discussed in the remaining sections.

6.1 External Synchronization Reference Technical Improvements

There are several technical improvements available to wireless communications systems. These improvements are made possible when a common reference is used for frequency stabilization and coherent demodulation.

6.1.1 Reduced Signal Acquisition Time

A residual carrier broadcast offers a constant source of synchronization. Externally-referenced modems maintain continuous synchronization, even when the modem is not transmitting or receiving information.

Because transmitters and receivers are continuously synchronized to the same reference signal, there is no need for sophisticated carrier recovery circuits to acquire the transmitted data signal. The transmitter and receiver are always in phase and frequency synchronization. Triad systems will maintain synchronization during times when severe information transfer path impairments causes the triad receiver to lose the transmitted signal. A triad receiver will immediately detect the information signal when the information signal-to-noise ratio again exceeds the receiver detection threshold. There is no need for a carrier training sequence during the reacquisition of the information transfer channel.

6.1.2 Improved Data Throughput for Shared and Half-Duplex Channels

Wireless modems often share a common RF channel by only transmitting and receiving information for limited periods of time. At other times, the modems relinquish the channel so that other modems may transfer information. Internally-referenced modems lose synchronization during these quiescent periods. Each modem must resynchronize at the beginning of each channel acquisition. Useful data transfer time is lost during the resynchronization interval, called the "modem training interval." The training interval significantly reduces the data throughput of a shared channel, especially in systems where the average data transfer interval is relatively short (e.g., wireless Ethernet modems).

Synchronization to a continuous external reference eliminates the modem training interval. Externally-referenced modems will devote a larger portion of the channel

acquisition time to data transfer, thereby improving the effective data throughput of the shared channel.

6.1.3 Improved Bandwidth Efficiency

Wireless modems share a set of FDM channels by reliably tuning to channels within an FDM band. Tuning stability within an internally-referenced modem is dependent upon the frequency stability of its BLSL. Allowances must be made in the channel guard bands for any frequency variations anticipated within the transmitter's BLSL oscillator. Reducing guard band allocations comes at increased modem cost for more stable oscillators. Conventional wireless modem design involves tradeoffs between bandwidth efficiency, oscillator stability, and modem cost.

Residual carrier broadcasts offer a source for a highly stable synchronization reference. If necessary, a triad design can include the construction of a residual carrier broadcast station with a transmitter oscillator having the required frequency stability. The cost of the broadcast station is a shared expense distributed across the population of wireless modems. This research shows that the use of an existing RC broadcast will also yield good performance. It is a ready-made reference available at no additional cost, provided that the wireless modem application operates within the vicinity of such a broadcast and that the broadcast frequency stability is sufficient for the application requirements. In either case, the externally-referenced, wireless modems require less bandwidth for guard bands. Reduction in the size of the guard bands increases the bandwidth efficiency of the triad system as compared to conventional FDM modem configuration.

6.1.4 Circuit Simplification

Unlike most carrier recovery circuits, a residual carrier reference can often be obtained through straightforward filtering and automatic gain control of existing commercial broadcasts or time reference signals. There is no need for a squaring circuit for carrier recovery as is the case in DSB-SC recovery. A PLL is necessary, but its operation is not dependent on the SNR of the data transfer signal as with conventional carrier recovery circuits. Instead, the PLL relies on the continuous broadcast of a residual carrier signal. Triad system synchronization SNR is independent of information transmission signal quality.

The use of a BLPL and an external reference lowers the cost of synchronization circuitry within many coherent transceiver applications. Internally-referenced transceivers require more complex carrier tracking, frequency acquisition, and modem training circuitry. An external reference reduces the complexity of the synchronization circuitry. The reduced synchronization cost can lower the cost per unit of the transceiver. Alternatively, the transceiver designer may reinvest the synchronization savings in more elaborate modulation and forward error correction schemes, thereby improving the data throughput and BER performance of the transceiver. For example, an externally-referenced, narrow-band modem might employ M-ary modulation techniques to increase data rate and forward error correction to achieve coding gain. The resulting modem would have a higher data rate and improved BER as compared to a simpler BPSK design. Savings in the synchronization circuitry would pay for some portion of the increased cost in the data transfer circuitry.

6.1.5 Operation over a Wide Range of Frequencies

Many existing signals can be used as a common communications frequency reference. They range from low frequency time stations such as WWVB at 60 kHz to the GPS signal at 1.575 GHz. Even signals not intended as references such as television video and AM broadcast signals may suffice, depending on the application. Potential reference signals exist at only discrete frequencies across the radio spectrum. Even so, the triad design applies the reference signal as synchronization over a broad range of data transfer frequencies. Within the practical limits of triad phase jitter described by Equation (3.80), an AM broadcast signal could synchronize the transmission and reception of signals anywhere in the electromagnetic spectrum. For example, a GPS signal may be used to synchronize a PSK link in the AM broadcast band (0.54 MHz to 1.71 MHz) or an AM broadcast signal can be used to synchronize a communications link operating in the L-band. A given application's requirements will influence the selection of an available reference or the decision to build a dedicated reference.

6.1.6 Elimination of False Lock on M-ary Sidebands

As mentioned in Section 2.9, triad systems avoid false lock conditions indigenous to carrier recovery from an M-ary DSB-SC signal. Triad synchronization relies exclusively upon the carrier spectral component of a residual carrier broadcast. It is therefore independent of the symbol configuration of the information channel. Narrow-band filters placed at the BLPL input virtually eliminate the DSB-RC or VSB-RC sidebands making false lock on AM sideband components unlikely. Triad system

designers may select symbol combinations consistent with their application requirements and without concern for M-ary sideband false lock conditions.

6.2 Potential Applications

The proposed triad configuration may not be useful for mobile applications due to the varying phase error and Doppler shift conditions. Even so, a triad design may be beneficial for many stationary wireless applications.

6.2.1 Point-to-Point Telemetry

Point-to-point telemetry lends itself to a fixed antenna orientation and, therefore, is a good candidate for a triad system design. Both the reference-receiving antennas and the information transfer antennas may be oriented for optimum response.

6.2.2 Links Requiring Time and Frequency Synchronization

Several wireless communications techniques require accurate time and frequency synchronization for optimum performance. These include Automatic Link Establishment (ALE), meteor scatter, and spread spectrum communications.

6.2.2.1 Automatic Link Establishment

Automatic link establishment is a military standard protocol (MIL-STD-188) for establishment of beyond-line-of-sight voice or data links. The links rely on signals transmitted at high frequencies (2 MHz – 32 MHz) and reflected off the ionosphere. The variable nature of the ionosphere and the variable atmospheric noise level of the HF band make it difficult to predict which frequencies will provide a viable link at any given time.

MIL-STD-188 defines an automatic search and link establishment protocol. MIL-STD-188 transmitters and receivers search for the best frequency and establish a two-way link. All transceivers must track precisely in frequency and time in order for the search protocol to be effective. By using a residual carrier reference, it should be possible to use narrower search bandwidths and shorter acknowledgment times than is possible with free running time and frequency references.

6.2.2.2 Meteor Scatter

Each day a large number of meteors enter the upper atmosphere with enough energy to ionize gas molecules. Meteor ionized molecules are sufficient for the reflection of radio waves. The typical height of an ionized meteor trail is about 100 kilometers. Meteor trails offer another mechanism for beyond-line-of-sight communication typically to a distance of 1800 kilometers. Until recently, there was no way to detect and take advantage of a usable meteor trail before it dissipated. The advent of modern, low-cost digital technology and high-speed numerical processing equipment has brought about a rapid evolution of meteor burst technology. Meteor burst communication systems are commercially available and provide viable beyond-line-of-sight communications when other media fail [83]

Meteor burst communications from one station to another station is a complicated process. The existence of a usable trail is usually determined by the reception of a probe signal transmitted by one station to another. When a station receives the probe signal, it transmits back an acknowledgment to the other station indicating that a usable trail exists and it is ready to exchange data. Once a usable trail is detected and its quality

determined, the meteor burst system transmits digitized data in a high speed burst. Typical transmission data rates vary from a few kilobits per second to over 100 kilobits per second.

Meteor scatter link acquisition handshaking uses a substantial portion of the meteor trail's useful lifetime and takes place each time a burst of data is transmitted. It may be possible to reduce signal acquisition time and increase data throughput by using coherent modulation techniques and external references.

6.2.2.3 Spread Spectrum

There are several spread spectrum communications techniques, all of which require precise time and frequency control at transmit and receive locations. The primary techniques are direct sequence (DS), frequency hopping (FH), and time hopping (TH) spread spectrum. Of these, the most popular are direct sequence and frequency hopping spread spectrum systems. DS systems spread the information signal across a band of frequencies by use of a high speed "chipping" code. The resulting signal occupies a bandwidth much wider than the bandwidth necessary to convey the signal. FH systems spread the signal over a wide band by rapidly hopping from one frequency to another in a pseudorandom pattern. Both techniques require transmitter and receiver synchronization. Synchronization may be required in both time and frequency. Use of external references should reduce the relative frequency and time drift between the transmitted and received signal to such a degree that code synchronization can be maintained at all times. A triad spread spectrum system does not require resynchronization when noise or jamming disrupts the information signal. The signal can be accurately demodulated as soon as the

information signal-to-noise ratio exceeds the level required for reliable symbol detection. However, consideration should be given to the possible jamming of the reference signal, which, if successful, would be highly disruptive to an externally-referenced, spread spectrum system.

6.3 Opportunities for Further Research

This research explores external synchronization of DSB-SC data transmission using a DSB-RC broadcast as a synchronization reference. It assumes the DSB-SC transceivers and DSB-RC transmitter are stationary. Gaussian noise is the only impairment considered in the performance analysis. There remain many open topics worthy of further research related to refinements in the models, considerations for other types of impairments, and adaptations of external synchronization to other forms of communication.

Commercial AM broadcast equipment momentarily cease transmission when driven into over-modulation. AM broadcast nonlinear behavior during over-modulation adversely affects BLPL operation. Further research would seek methods for mitigating the effects related to AM broadcast over-modulation.

A triad system configuration exhibits a fixed phase error that is dependent upon the relative position of stationary triad components. The phase error varies if the components are in motion. Further research would seek modified BLPL designs that compensate for fixed and varying phase error in triad systems.

Martinez noted momentary loss of synchronization when large trucks passed near an externally-referenced transceiver [12]. This research does not address the effects of

multipath fading upon the synchronization channel in an externally-referenced system. Further research would quantify the nature of multipath impairments in triad systems and might seek methods for improving the immunity of transceivers to multipath synchronization loss.

Triad systems maintain continuous carrier synchronization, but do not by themselves maintain bit synchronization necessary for clocking the sample-and-hold data detector. Additional research would explore efficient methods for maintaining bit synchronization within a triad system design. Optimization of bit synchronization could further improve shared channel data throughput by reducing or eliminating the bit synchronization portion of the modem training interval.

The analysis contained herein focuses on external synchronization as it relates to the modulation and demodulation of DSB-SC signals. Opportunities remain for determining the applicability and performance of external synchronization to SSB modulation and demodulation.

The External BLPL Model currently simulates triad system behavior by repeatedly processing randomly generated, 14 millisecond segments of a DSB-RC signal. Section 4.2.3 suggests possible enhancements involving segmenting much longer DSB-RC signal intervals, redesign of the model filters, and reorganization of the model into multiprocessing threads. These model enhancements are left as a topic for further research in external synchronization simulation.

Literature searches found no closed-form expression for higher-order BLSL and BLPL behavior. Consequently, this research relied on first-order expressions as an upper

bound for second-order device behavior. Development of closed-form expressions for second-order BLPL and BLSL behavior promises to be a challenging area for further research.

BIBLIOGRAPHY

Bibliography

[1] *The American Heritage Dictionary of the English Language – New College Edition*, Houghton Mifflin Company, 1976, ISBN 0-395-20360-0.

[2] Merrill Skolnik, *Radar Handbook, 2nd Edition*, McGraw Hill Publishing Co., 1990.

[3] Floyd M. Gardner and William C. Lindsey, "Guest Editorial: Special Issue on Synchronization," IEEE Transactions on Communications, VOL. COM-28, NO. 8. August 1980.

[4] Leon W. Couch II, *Modern Communication Systems – Principles and Applications*, Prentice Hall, Inc., 1994, ISBN 0-02-325286-3.

[5] J. J. Stiffler, *Theory of Synchronous Communications*, Prentice-Hall, Inc, 1971.

[6] "National Institute of Standards and Technology Radio Station WWVB," http://www.boulder.nist.gov/timefreq/stations/wwvb.htm, July 16, 2000.

[7] Zhou Wenyu and Jiao Peinan, "Signal Processing of Sky Wave OTH-B Radar," 1994 IEEE International Conference on Acoustics, Speech and Signal Processing, April 19-22, 1994, Adelaide, South Australia, IEEE, ISBN 0-7803-1775-0.

[8] Jeng-Hong Chen and William C. Lindsey, "Mutual Clock Synchronization In Global Digital Communication Networks," Vehicular Technology Conference, 1996, Mobile Technology for the Human Race, IEEE 46th, IEEE Catalog Number 96CH35894, ISBN 0-7803-3157-5.

[9] Lester Ostroy; Willmore F. Holbrow, Jr.; and Louis Martinez, "Microprocessors in Distributed Broadcast Radio Systems," 1983 International Telemetering Conference, San Diego, CA, October 24-27, 1983, pp.201-207.

[10] "FCC Rule Part 73.1545," Federal Communications Commission, Broadcast Net, http://hallikainen.com/cgi-bin/section.pl?section=73.0, September 26, 2000.

[11] Louis Martinez, "NARROW-BAND RADIO COMMUNICATION SYSTEM," United States Patent No. 4,117,405, September 26, 1978.

[12] Louis Martinez, telephone interview conducted by Gary Ragsdale, April 8 and April 18, 2000.

[13] Louis Martinez, "Energy Management by AM Broadcast Radio," National Telecommunications Conference, New Orleans, Louisiana, November 29 -- December 3, 1981, 81CH1679-0, NTC Record -- 1981, IEEE, CH1679-0/81/0000-0097.

[14] Dixon, Robert C, *Spread Spectrum Systems*, Third Edition, copyright 1994, John Wiley & Sons, Inc., pp. 192 – 200.

[15] André Kesteloot, N4ICK, and Charles L. Hutchinson, K8CH, The ARRL Spread Spectrum Sourcebook, The American Radio Relay League, Inc., ISBN 0-87259-317-7, 1997.

[16] David Newkirk, AK7M, "Happenings – Our Spread-Spectrum Systems Rules," QST, April 1986.

[17] André Kesteloot, "Spread-Spectrum: A fascinating mode – and legal for hams to use!," 73 Amateur Radio, June, 1989, pp. 12-13.

[18] William Sabin, W0IYH, "Spread-Spectrum Applications in Amateur Radio, QST, p. 16, July 1983.

[19] André Kesteloot, "Practical Spread Spectrum: A Simple Clock Synchronization Scheme," QEX, October, 1986, pp. 4-7.

[20] André Kesteloot, N4ICK, "Experimenting With Direct-Sequence Spread Spectrum," QEX, pp. 5-9, Dec 1986.

[21] André Kesteloot, N4ICK, "First Steps in Direct-Sequence Spread-Spectrum," AMRAD Newsletter, Vol. XIV, No. 1, pp. 5-9, Jan 1987.

[22] André Kesteloot, "Extracting Stable Clock Signals From AM Broadcast Carriers for Amateur Spread-Spectrum Applications," QEX, October, 1987, pp. 5-9.

[23] Peter Kuykendall and Peter Loomis, "Cellular/PCS Systems Get IN SYNC with GPS," Wireless Systems Design, February 1998.

[24] "GPS Time and Frequency Generators Synchronize Cell Sites," Wireless Systems Design September 1996.

[25] Hewlett Packard, "GPS and Precision Timing Applications," Application Note 1272, May 1996.

[26] Bob Brewin, "White House frees up civil GPS signal," CNN.com, May 2, 2000, http://www.cnn.com/2000/TECH/computing/05/02/civil.gps.idg/index.html.

[27] John G. Proakis, *Digital Communications -- 2nd Edition*, McGraw-Hill Book Company, 1989, ISBN 0-07-050937-9.

[28] A. Bateman, "A General Analysis of Bit Error Probability for Reference-Based BPSK Mobile Data Transmission," IEEE Transactions on Communications," Vol. 37. No. 4, pp. 398-402, April 1989.

[29] John H. Lodge, Michael L. Moher and Stewart N. Crozier, "A Comparison of Data Modulation Techniques for Land Mobile Satellite Channels," IEEE Transactions on Vehicular Technology, Vol. VT-36. No. 1, pp. 28-35, February 1987.

[30] A. Bateman and J. P. McGreehan, "Phase Locked transparent tone – In-band (TTIB): A New Spectrum Configuration Particularly Suited to the Transmission of Data Over SSB Mobile Radio Networks," IEEE Trans. Commun., Vol. COM-32, pp. 81-87, Jan. 1984.

[31] A. Bateman and J. P. McGeehan, "Narrow-band Coherent Data Transmission-Mobile," 37th IEEE Vehicular Technology Conference, Tampa, Florida, pp. 281-286, June 1-3, 1987.

[32] M.K. Simon, “Dual-pilot tone calibration technique,” IEEE Transactions Vehic. Technol., Vol. VT-35, pp. 63-70, May 1986.

[33] J. Bateman, Ph.D., and J. P. McGeehan, Ph.D., “Data Transmission Over UHF Fading Mobile Radio Channels,” IEEE Proceedings, Vol. 131, Pt. F, No. 4, pp. 364-374, July 1984.

[34] W. Rafferty, J. B. Anderson, G. J. Saulnier, and J. R. Holm, “Laboratory Measurements and a Theoretical Analysis of the TCT Fading Channel Radio System,” IEEE Trans. Commun., Vol. COM-35, pp. 172-180, Feb. 1987.

[35] Mitsuo Yokoyama, “BPSK System with Sounder to Combat Rayleigh Fading in Mobile Radio Communication,” IEEE Transactions on Vehicular Technology, Vol. VT-34, No. 1, February 1985.

[36] John C. Kirk, Jr., “BISTATIC SAR MOTION COMPENSATION,” IEEE International Radar Conference, Arlington, VA, May 6-9, 1985.

[37] James L. Auterman, “PHASE STABILITY REQUIREMENTS FOR A BISTATIC SAR,” Proceedings of the 1984 IEEE National Radar Conference, Atlanta, GA, March 13-14, 1984

[38] H. D. Griffiths and S. M. Carter, “Provision of moving target indication in an independent bistatic radar receiver,” The Radio and Electronic Engineer, Vol. 54, No. 7/8, pp. 336.342, July/August 1984.

[39] Gert Retzer, “Some Basic Comments on Multistatic Radar Concepts and Techniques,” Colloquium on “Ground and Airborne Multistatic Radar,” Institute of Electrical Engineers (Great Britain), London, UK, 4 December 1981.

[40] J. G. Schoenenberger, J. R. Forrest, and D. E. N. Davies, “DESIGN AND IMPLEMENTATION OF A UHF BAND BISTATIC RADAR RECEIVER,” Colloquium on “Ground and Airborne Multistatic Radar,” Institute of Electrical Engineers (Great Britain), London, UK, 4 December 1981.

[41] H. D. Griffiths and N. R. W. Long, “ Television-based bistatic radar,” IEE Proceedings, Vol. 133, Pt. F, No. 7, December 1986.

[42] Wilson P Dizard III, "COTS technology enables passive ground-based radar," Military & Aerospace Electronics, December 1998.

[43] Jacqueline Walker and Antonio Cantoni, “Jitter Analysis for Two Methods of Synchronization for External Timing Injection,” IEEE Transactions on Communications, VOL. COM-37, NO. 4, April 1989, pp. 398-402.

[44] Wei Zhu, "TDMA Frame Synchronization of Mobile Stations Using a Radio Clock Signal for Short Range Communications," Vehicular Technology Conference, 1994 IEEE 44th, 8-10 June 1994, Stockholm Sweden, IEEE Catalog Number: 94CH3438-9, ISSN 0-7803-1927-3.

[45] A. Gladisch, L. Giehmann, N. Geischen and M. Rocks, “Remote Controlled Absolute Frequency Stabilization of Locally Independent Subscriber Lasers for

Coherent Communication Systems," Research Institute of DBP, SPIE, Vol. 1837 (1992), ISSN 0-8194-1038-1/93.

[46] Bernard Sklar, "A Structured Overview of Digital Communications – Part I," IEEE Communications Magazine, 0163-6804/83/0800-0004, 1983.

[47] Kamran Kiasaleh, "On False Lock in Suppressed Carrier MPSK Tracking Loops," IEEE Transactions on Communications," VOL. 39, NO. 11, November 1991.

[48] Bernard Sklar, *Digital Communications Fundamentals and Applications*, Prentice-Hall, 1988, ISBN 0-13-211939-0.

[49] A. Bruce Carlson, *Communication Systems, An Introduction to Signals and Noise in Electrical Communication*, McGraw-Hill Book Co., 1968.

[50] David Robinson, Joseph Fontes, and Gregory Dowd, "Synchronizing Computers and Workstations Using Network and Direct Connect Time Transfer Techniques," Datum Inc., Bancomm Division, May 1995, http://www.bancomm.com/cntpapp.htm, July 26, 2000.

[51] Peter H. Dana and Bruce Penrod, "The Role of GPS in Precise Time and Frequency Dissemination," GPS World, July/August 1990, http://www.bancomm.com/cgprole.htm, July 26, 2000.

[52] Hewlett Packard, "GPS and Precision Timing Applications," Application Note 1272, May 1996.

[53] "GPS Time and Frequency Generators Synchronize Cell Sites," Wireless Systems Design September 1996.

[54] Bob Pitcock, "History of Frequency Traceability at HP-Santa Clara," Hewlett-Packard, Pub. No. 5964-6005E, 1997.

[55] Robert G. Lyons, "The Effect of a Bandpass Nonlinearity on Signal Detectability," IEEE Transactions On Communications, Vol. Com-21, No. 1, January 1973.

[56] William C. Lindsey and Marvin K. Simon, "The Effect of Loop Stress on the Performance of Phase-Coherent Communication Systems," IEEE Transactions on Communication Technology, Vol. COM-18, No. 5, October 1970.

[57] Andrew J. Viterbi, *Principles of Coherent Communications*, McGraw-Hill, Inc., TK5101.V55, 1966.

[58] R. E. Zeimer and W. H. Trantor, *Principles of Communications, 3rd Edition*, Houghton Mifflin Company, 1990, ISBN 0-395-43313-4.

[59] Someshwar C. Gupta, "Phase-Locked Loops," Proceedings of the IEEE, Vol. 63, No. 2, February 1975.

[60] Heinrich Meyr and Gerd Ascheid, *Synchronization in Digital Communications, Volume 1 -- Phase-, Frequency-Locked Loops, and Amplitude Control*, John Wiley & Sons, 1990, ISBN 0-471-50193-X (v. 1).

[61] Floyd M. Gardner, *Phaselock Techniques - Second Edition*, John Wiley & Sons, 1979, ISBN 0-471-04294-3, TK7872.P38G37.

[62] Kamilo Feher, *Digital Communications: Satellite/Earth Station Engineering*, Prentice-Hall Inc., Englewood Cliffs, NJ, 1981.

[63] William C. Lindsey, *Synchronization Systems in Communications and Control*, Prentice-Hall, Inc., 1972, ISBN 0-13-879957-1.

[64] John P. Costas, "Synchronous Communications," Proceedings of the IRE, pp. 1713-1718, December 1956.

[65] James C. Springett and Marvin K. Simon, "An Analysis of the Phase Coherent-Incoherent Output of the Bandpass Limiter," IEEE Transactions on Communication Technology, Vol. COM-19, February 1971.

[66] George Casella and Roger L. Berger, *Statistical Inference*, Duxbury Press, A division of Wadsworth, Inc., ISBN 0-534-11958-1, 1990.

[67] Hwei P. Hsu, *Shaum's Outline of Theory and Problems of Analog and Digital Communications*, McGraw-Hill, ISBN 0-07-030636-2, 1993.

[68] Thierry Pollet, Mark Van Bladel, and Marc Moeneclaey, "BER Sensitivity of OFDM Systems to Carrier Frequency Offset and Wiener Phase Noise," IEEE Transactions on Communications, Vol. 43, No. 2/3/4, February/March/April 1995.

[69] *LabVIEW Function and VI Reference Manual, Version 5.0*, National Instruments, January 1998 Edition.

[70] Gary Ragsdale and Tom Warnagiris, "Externally Synchronized Coherent Transmission Optimization," SwRI Project No. 10-9047, Southwest Research Institute, September 1999.

[71] "Tiger Mapping Service – The 'Coast to Coast' Digital Map Database," U.S. Census Bureau, http://tiger.census.gov, September 18, 2000.

[72] "FCC Rule Part 73.44," Federal Communications Commission, Broadcast Net, http://hallikainen.com/cgi-bin/section.pl?section=73.0, September 26, 2000.

[73] "FCC Rule Part 73.1570," Federal Communications Commission, Broadcast Net, http://hallikainen.com/cgi-bin/section.pl?section=73.0, September 26, 2000.

[74] E. H. B. Bartelink, *Telephone Transmission Theory*, Bartelink Enterprises Corporation, Concord, New Hampshire, 1996.

[75] Alan V. Oppenheim and Ronald W. Schafer, *Digital Signal Processing*, Prentice-Hall, Inc. ISBN 0-13-214635-5, 1975.

[76] Michel C. Jeruchim, Philip Balaban, and K. Sam Shanmugan, *Simulation of Communication Systems*, Plenum Press, ISBN 0-306-43989-1, 1992.

[77] Lonnie C. Ludeman, *Fundamentals of Digital Signal Processing*, John Wiley & Sons, ISBN 0-471-60363-5, 1986.

[78] John Kodis, "Welcome to the Broadcast Station Location Page," http://207.91.54.150/radiostation/, September 19, 2000.

[79] William H. Hayt, Jr. and Jack E. Kemmerly, "*Engineering Circuit Analysis – Fifth Edition*," McGraw-Hill, ISBN 0-07-027410-X, 1993.

[80] *Electronic Countermeasures*, Peninsula Publishing, 1978, Library of Congress Number 78-69599, pp. 14-55 through 14-56.

[81] *Mathcad 8 User's Guide*, Mathsoft, Inc., Cambridge, MA, August 1998.

[82] Richard L. Burden and J. Douglas Faires, *Numerical Analysis – Sixth Edition*, Brooks/Cole Publishing Company, ISBN 0-534-95532-0, 1997.

[83] Daniel E. Warren, D. E. Desourdis, "Meteor Burst Communications The Gap Filler" Rome Laboratory and Science Applications International Corporation, http://www.borg.com/~warrend/metburdu.html.

Related Reference Materials

[1] Zhou Zheng-Ou, Ding Yi-Yuan, Gong Yao-Huan, and Huang Shun-Ji, “A Bistatic Radar for Geological Probing,” Microwave Journal, May 1984.

[2] Mohamed K. Nezami, “Evaluate The Impact Of Phase Noise On Receiver Performance – Phase-noise analysis, Part 1 and Part 2,” Microwaves & RF, May and June 1998.

[3] P. M. Woodward, *“Probability and Information Theory, with Applications to Radar,”* Artech House Books, TK6575W6, 1964.

[4] M. J. B. Scanlan, *Modern Radar Techniques*, Collins Professional Books, TK6575M623, 1987.

[5] Jerry L. Eaves and Edward K. Reedy, *Principles of Modern Radar*, Van Nostrand Reinhold, TK6575P74, 1987.

[6] Charles E. Cook and Marvin Bernfeld, *Radar Signals -- An Introduction to Theory and Application*, Academic Press, TK6575.C65.

[7] L. C. Palmer and S. Lebowitz, "Including synchronization in time-domain channel simulations," COMSAT Technical Review, Volume 7, Number 2, Fall 1977.

[8] Richer, "A BLOCK PHASE ESTIMATOR FOR OFFSET-QPSK SIGNALING," National Telecommunications Conference, NTC Conference Record Volume 2, December 1-3, 1975, New Orleans, LA, IEEE Catalogue Number 75 CH 1015-7 CSCB.

[9] L. E. Franks and J. P. Bubrouski, "Statistical Properties of Timing Jitter in a PAM Timing Recovery Scheme," IEEE Transactions on Communications, Vol. COM-22, No. 7, July 1974.

[10] Charles R. Cahn and Donald K. Leimer, "Digital Phase Sampling for Microcomputer Implementation of Carrier Acquisition and Coherent Tracking," IEEE Transactions on Communications, Vol. COM-28, No. 8, August 1980.

[11] Mohamed K. Nezami, "Evaluate The Impact Of Phase Noise On Receiver Performance," Microwaves & RF, May 1998.

APPENDICES

APPENDIX A. TRIAD SYSTEM MODEL (EXAMPLE 3)

Triad System Model

Created by Gary Ragsdale

March 4, 2001

The Triad System Model predicts the behavior of an externally referenced BPSK transceiver pair operating in a configuration called a "triad." The triad transmitter and receiver employ identical BLPL synchronization circuits. Transceiver BLPLs track the carrier of an external DSB-RC broadcast, which could be an AM radio broadcast or NTSC television broadcast.

The Triad System Model uses values created by the external BLPL model. The values ρ_{Base} and σ_{Base} describe the modeled behavior of a BLPL with a single-pole filter with input Q as defined by Q_{Base} and noise equivalent bandwidth defined by B_{Base}. Triad System Model interpolates the external BLPL model results and predicts the behavior of a given Triad system configuration.

The following data comes from external BLPL model results printed on 8/13/99 7:34AM for filter Q=116. **Do not alter the values on this page.**

$Q_{Base} := 116$ the input filter quality

$B_{Base} := 1.5685510^{4}$ the input filter noise equivalent bandwidth

$A := 1$ the unmodulated, DSB-RC carrier amplitude at the BLPL input.

$f_s := 9.28 \cdot 10^{6}$ the external BLPL model sampling frequency

$$\sigma_{Base} := \begin{bmatrix} 0.032 \\ 0.032 \\ 0.032 \\ 0.032 \\ 0.032 \\ 0.033 \\ 0.033 \\ 0.034 \\ 0.035 \\ 0.037 \\ 0.040 \\ 0.046 \\ 0.051 \\ 0.068 \\ 0.071 \\ 0.086 \\ 0.101 \\ 0.131 \\ 0.153 \\ 0.196 \\ 0.228 \\ 0.313 \\ 0.531 \end{bmatrix} \quad \rho_{Base} := \begin{bmatrix} 0.0 \\ -5.0 \\ -8.5 \\ -11.5 \\ -13.5 \\ -15.5 \\ -16.5 \\ -17.5 \\ -18.0 \\ -18.5 \\ -19.0 \\ -19.5 \\ -20.0 \\ -20.5 \\ -21.0 \\ -21.5 \\ -22.0 \\ -22.5 \\ -23.0 \\ -23.5 \\ -24.0 \\ -25.0 \\ -27.0 \end{bmatrix}$$

$B_{Base} := 3.1326810^{4}$

$k := 0 .. \text{length}\left(\rho_{Base}\right) - 1$

$\sigma rev\ sim_k := \sigma\ Base_{\text{length}\left(\rho_{Base}\right) - k - 1}$ reverse the order of the model phase jitter results

The following functions compute the behavior of the specified Triad system.

$S := \frac{A^2}{2}$ the unmodulated carrier signal power at the BLPL input

$f_N := \frac{f_s}{2}$ the external BLPL model Nyquist frequency

The following function computes the noise power taken at the BLPL input.

$$P_N(\rho) := \frac{S}{\rho}$$

The following function computes the SNR at the BLPL input. Notice that the SNR is a function of the Nyquist frequency and the input filter noise equivalent bandwidth.

$$\rho rev_k := 10 \cdot \log\left[\frac{S \cdot f_s}{\left(2 \cdot P_N\left(10^{\frac{\rho_{Base_{length}(\rho_{Base})} - k - 1}{10}}\right) \cdot B_{Base}\right)}\right]$$

Function cspline computes a vector of cubic spline coefficients to be used by the interpolation function called interp.

$$v_{cs} := cspline\left(\rho rev, \sigma rev_{sim}\right)$$

The following function interpolates the behavior of the BLPL with bandwidth B_{Base} to the specified noise equivalent bandwidth B and signal-to-noise ratio x. It computes the interpolated phase jitter.

$$\sigma_{interp}(x, B) := interp\left(v_{cs}, \rho rev, \sigma rev_{sim}, x + 10 \cdot \log\left(\frac{B_{Base}}{B}\right)\right)$$

The bit error probability of a BPSK receiver is as follows:

$$P_b(snr, \phi) := erfc\left(\sqrt{2 \cdot snr \cdot \cos(\phi)}\right)$$

The phase jitter at the Triad receiver correlator is

$$\sigma_{triad}\left(\rho_{tx}, \rho_{rx}, \Delta, B_i\right) := (1 + \Delta) \cdot \sqrt{\sigma_{interp}\left(\rho_{rx}, B_i\right)^2 + \sigma_{interp}\left(\rho_{tx}, B_i\right)^2}$$

The following parameters describe the Triad system under study. Modify the following parameters to obtain predictions of a desired Triad system configuration.

$\Delta := 0.1$	Triad transceiver carrier frequency offset, i.e., $f_c = (1+\Delta)\cdot f_{RC}$
$Q := 23000$	BLPL input filter quality (optional)
$B_i := 7.9242 \cdot 10^{1}$	BLPL input filter noise equivalent bandwidth
$\rho_{tx} := -25$	DSB-RC broadcast SNR at the data transmitter BLPL input
$\rho_{rx} := -18$	DSB-RC broadcast SNR at the data receiver BLPL input
$\rho_{path} := 6$	DSB-SC, BPSK SNR at the data detector filter input of the receiver

The following graph describes the Triad BLPL performance across a range of SNRs.

$$\rho := \rho prev_0 + 10\cdot\log\left(\frac{B_i}{B_{Base}}\right), \rho prev_0 + 10\cdot\log\left(\frac{B_i}{B_{Base}}\right) + 1 .. \rho prev_{last(\rho prev)} + 10\cdot\log\left(\frac{B_i}{B_{Base}}\right)$$

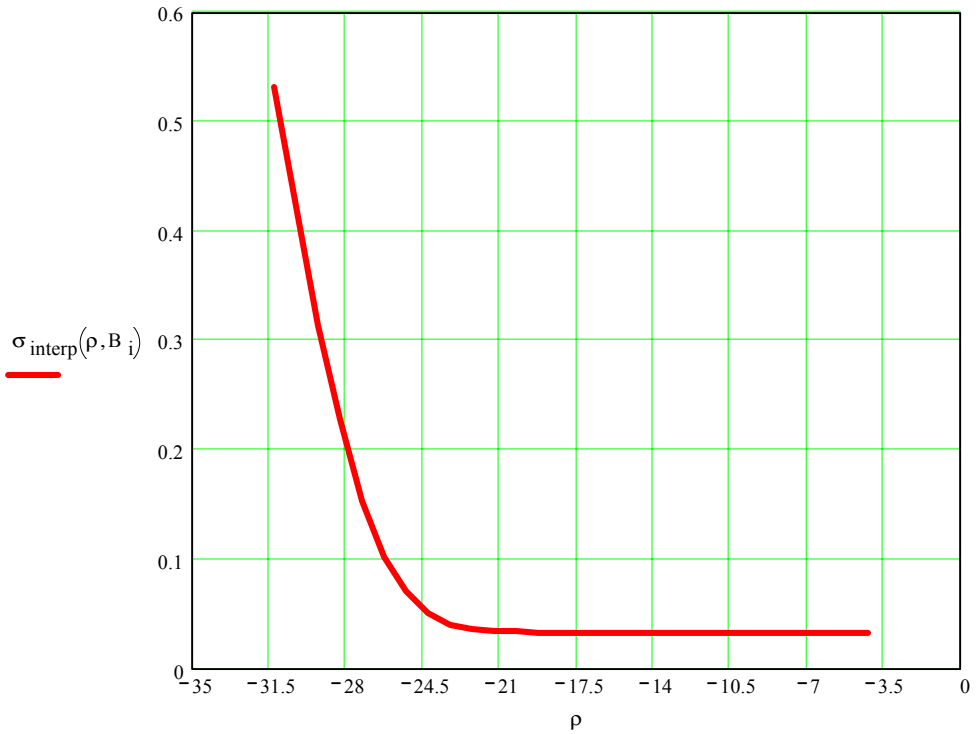

BLPL estimated phase jitter performance

The total phase jitter at the Triad receiver is (radians)

$$\sigma_{triad}\left(\rho_{tx}, \rho_{rx}, \Delta, B_i\right) = 0.084$$

The Triad bit error rate is (errors per bit)

$$P_b\left(10^{\frac{\rho_{path}}{10}}, \sigma_{triad}\left(\rho_{tx}, \rho_{rx}, \Delta, B_i\right)\right) = 6.792 \cdot 10^{-5}$$

APPENDIX B. INTERNALLY-REFERENCED BLSL MODEL

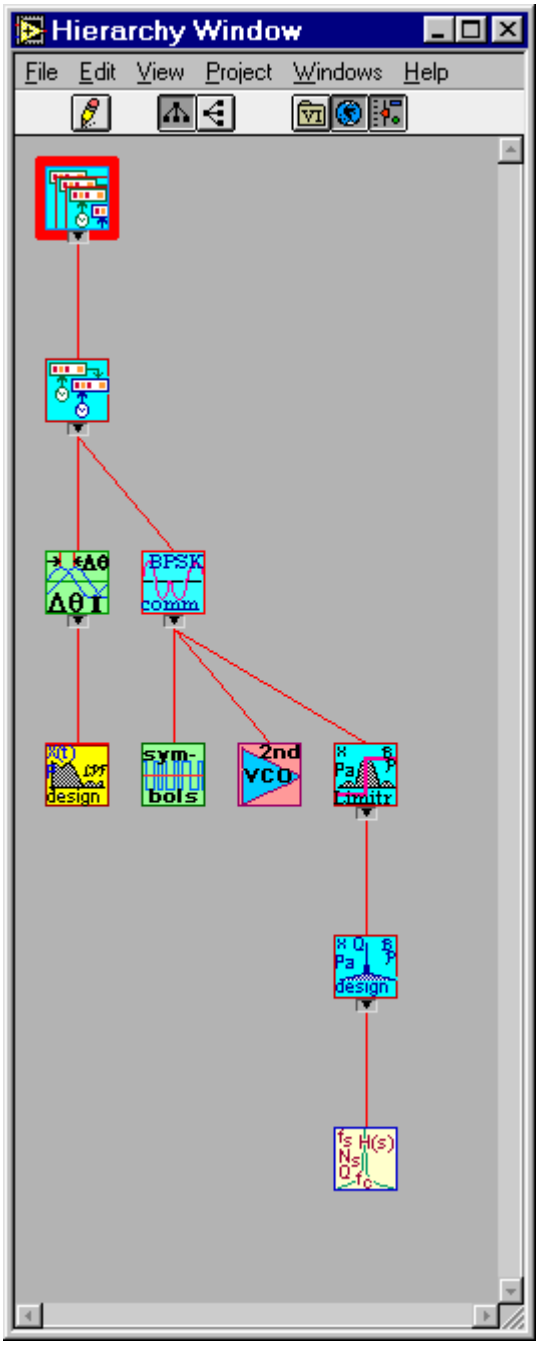

Figure B–1. Internally-Referenced BLSL Model VI Hierarchy.

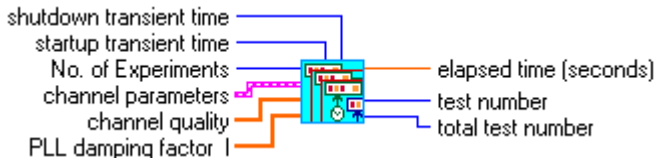

Internal BLSL Iterant Test VI (Figure B–3)

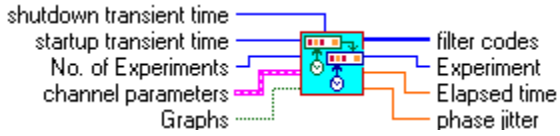

Internal BLSL Model VI (Figure B–5)

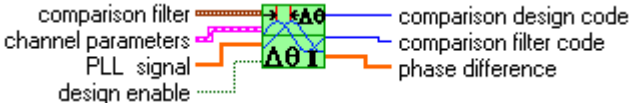

BLSL Phase Comparator VI (Figure B–7)

Design Once Low-pass VI (Figure B–9)

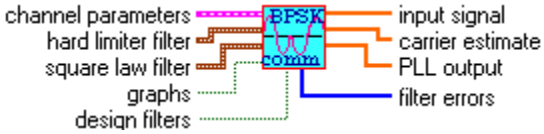

Internal BPSK Channel VI (Figure B–11)

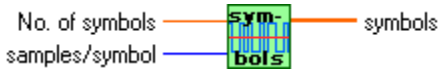

Data Generator VI (Figure B–13)

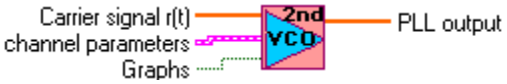

Second-Order Phase Lock Loop VI (Figure B–14)

Figure B–2. Internally-Referenced BLSL Model VI Connector Legend.

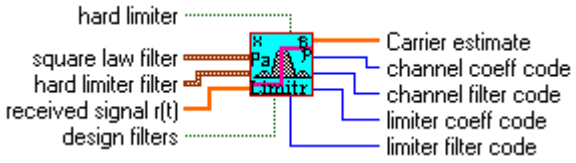

Squaring Bandpass Filter With Hard Limiter VI (Figure B–16)

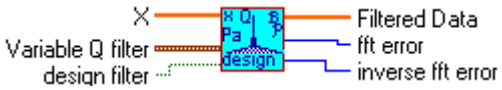

Design Once – Variable *Q* Bandpass Filter (Figure B–18)

Variable *Q* Bandpass Filter Transfer Function VI (Figure B–20)

Figure B–2. (continued)

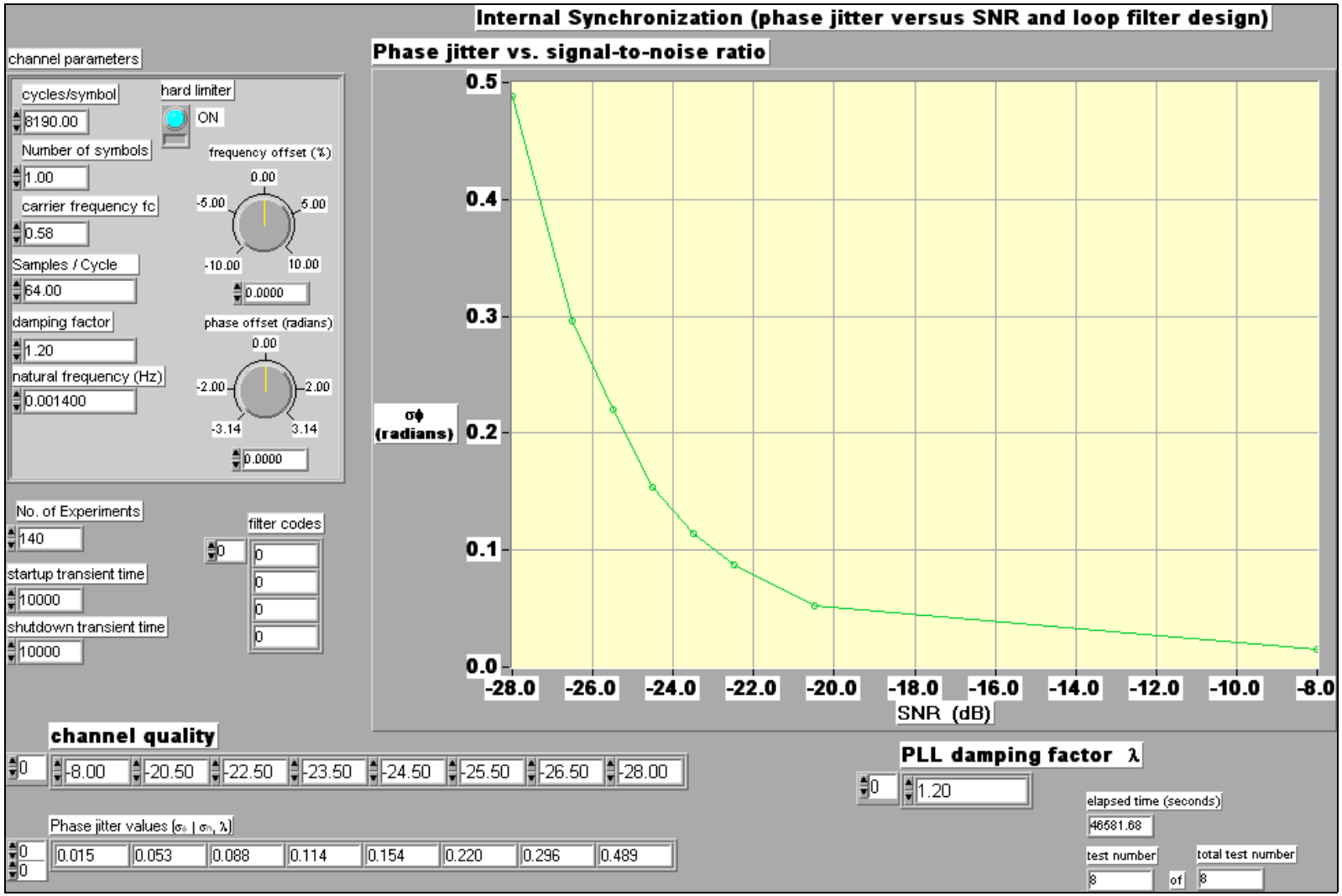

Figure B–3. Internal BLSL Iterant Test VI front panel.

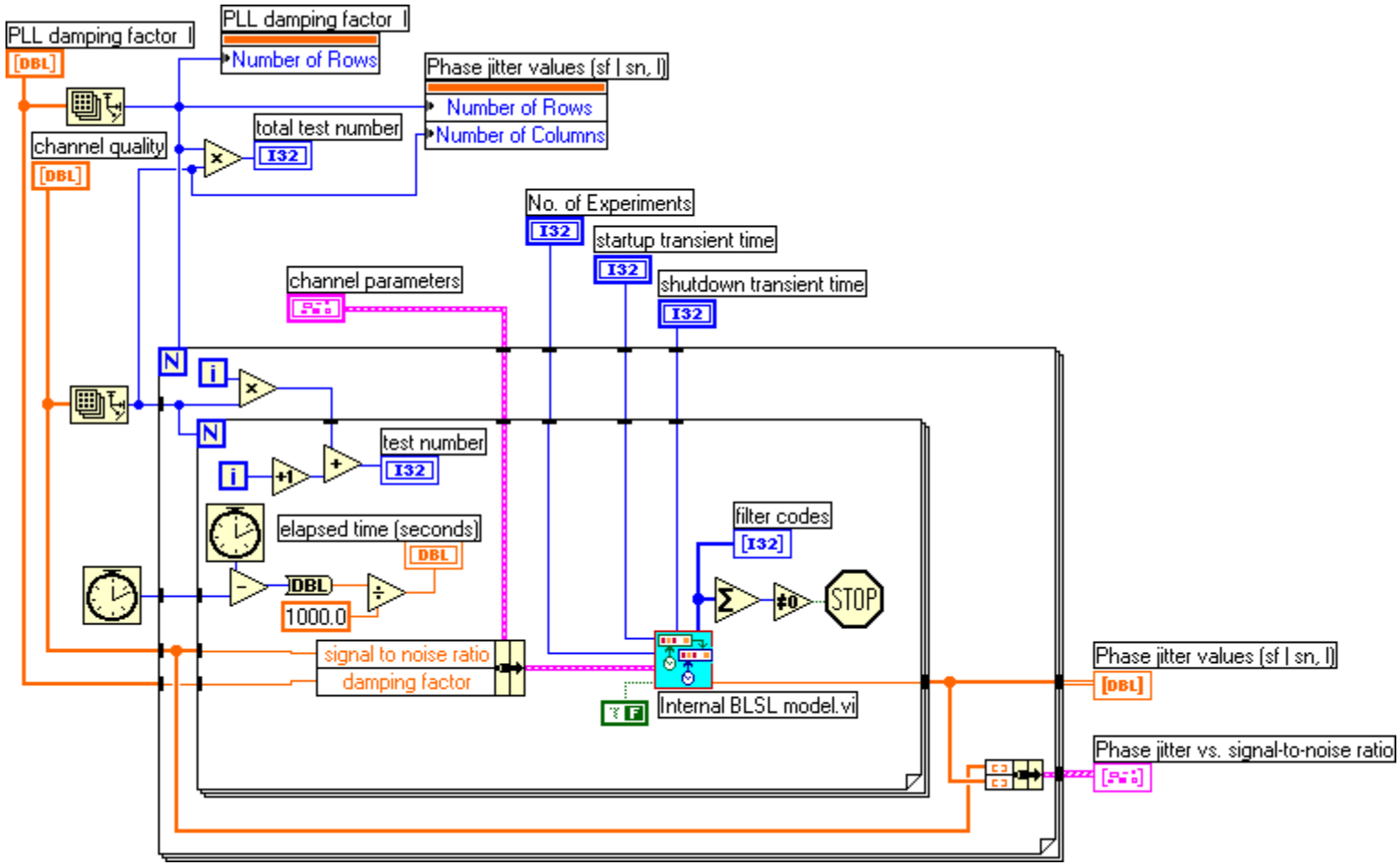

Figure B–4. Internal BLSL Iterant Test VI diagram.

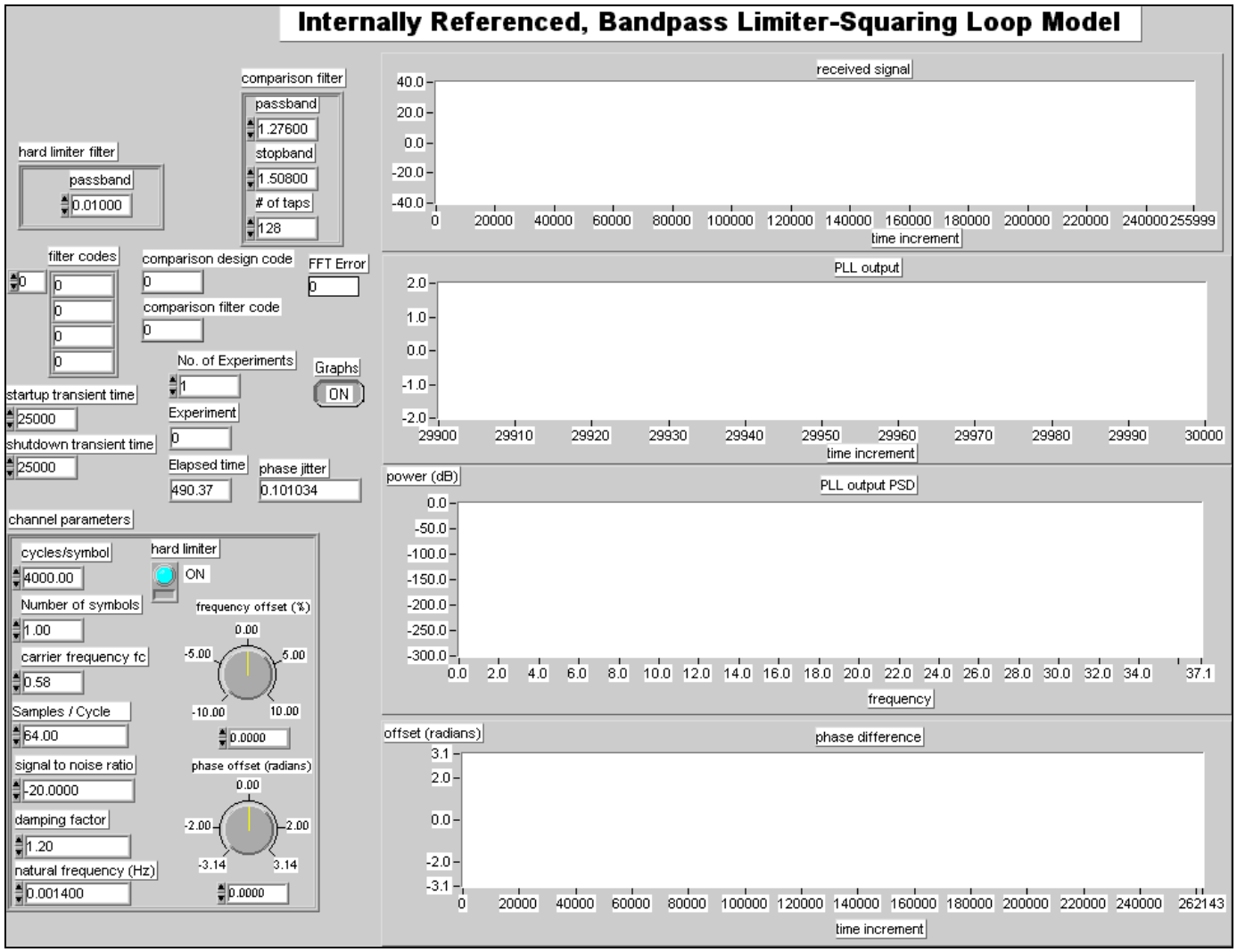

Figure B–5. Internal BLSL Model VI front panel.

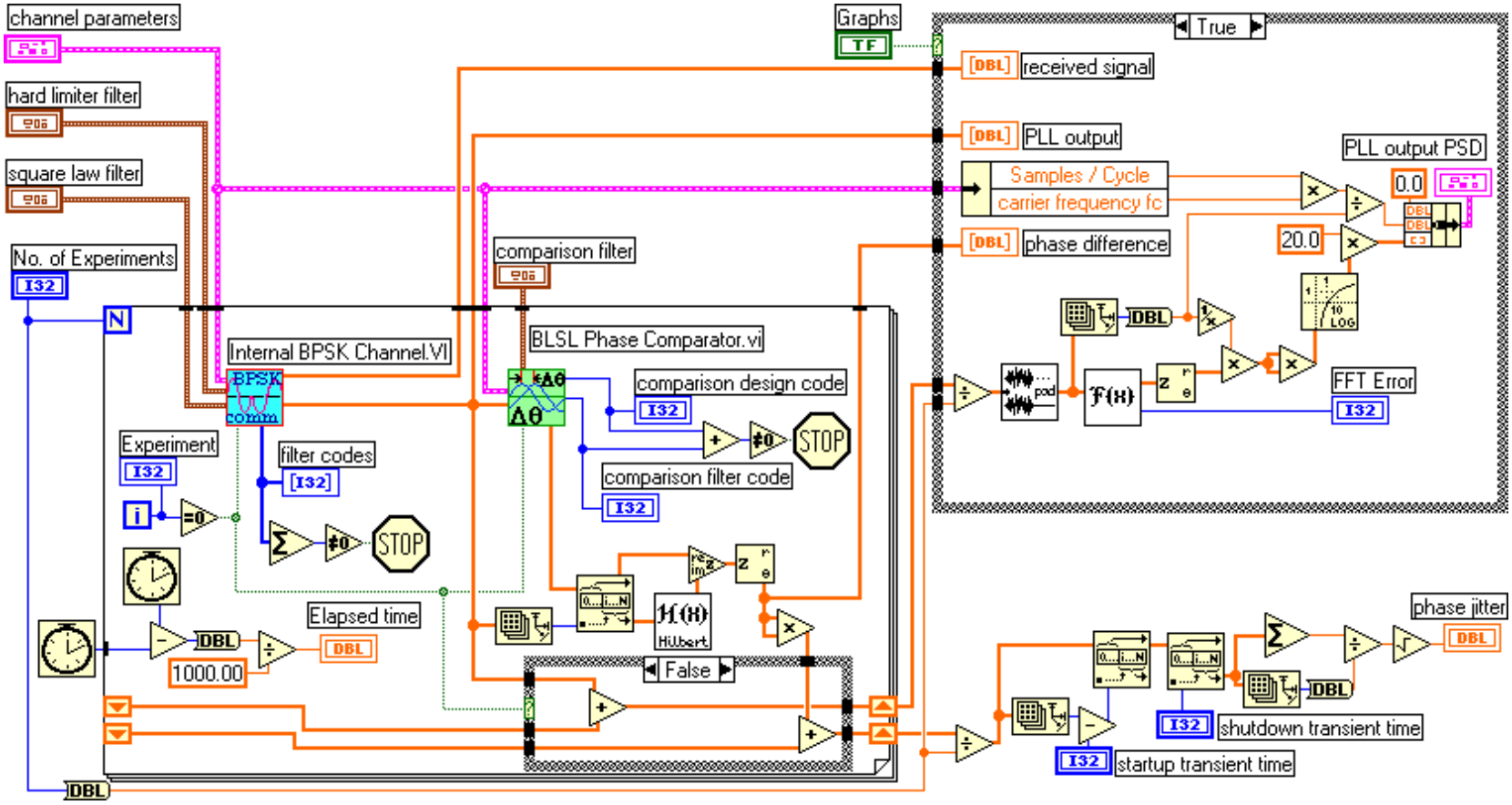

Figure B–6. Internal BLSL Model diagram.

Figure B–6. (continued)

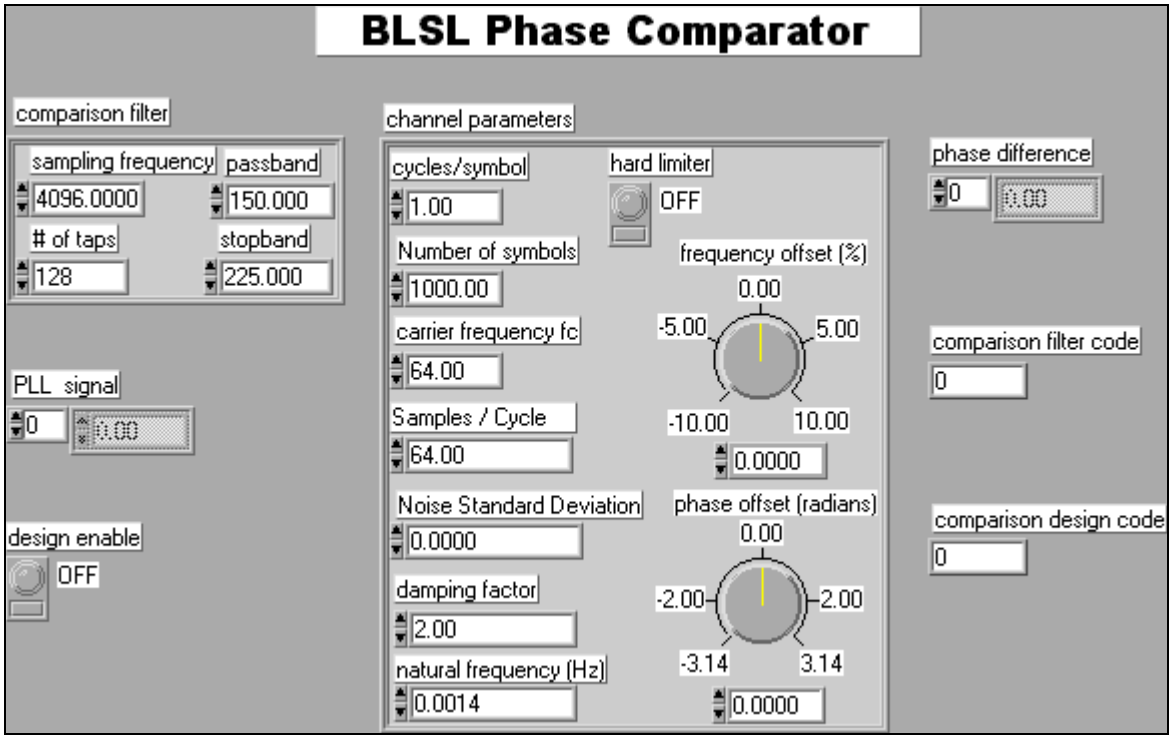

Figure B–7. BLSL Phase Comparator VI front panel.

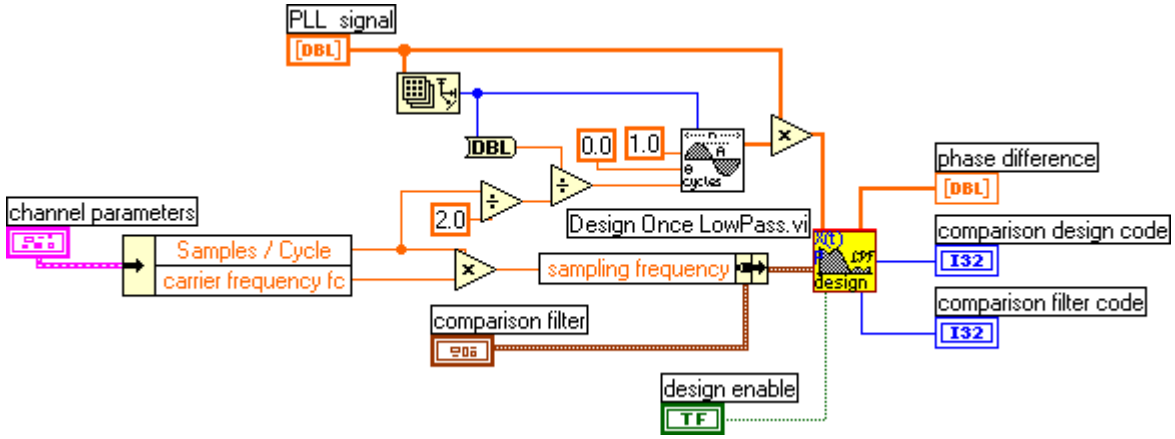

Figure B–8. BLSL Phase Comparator VI diagram.

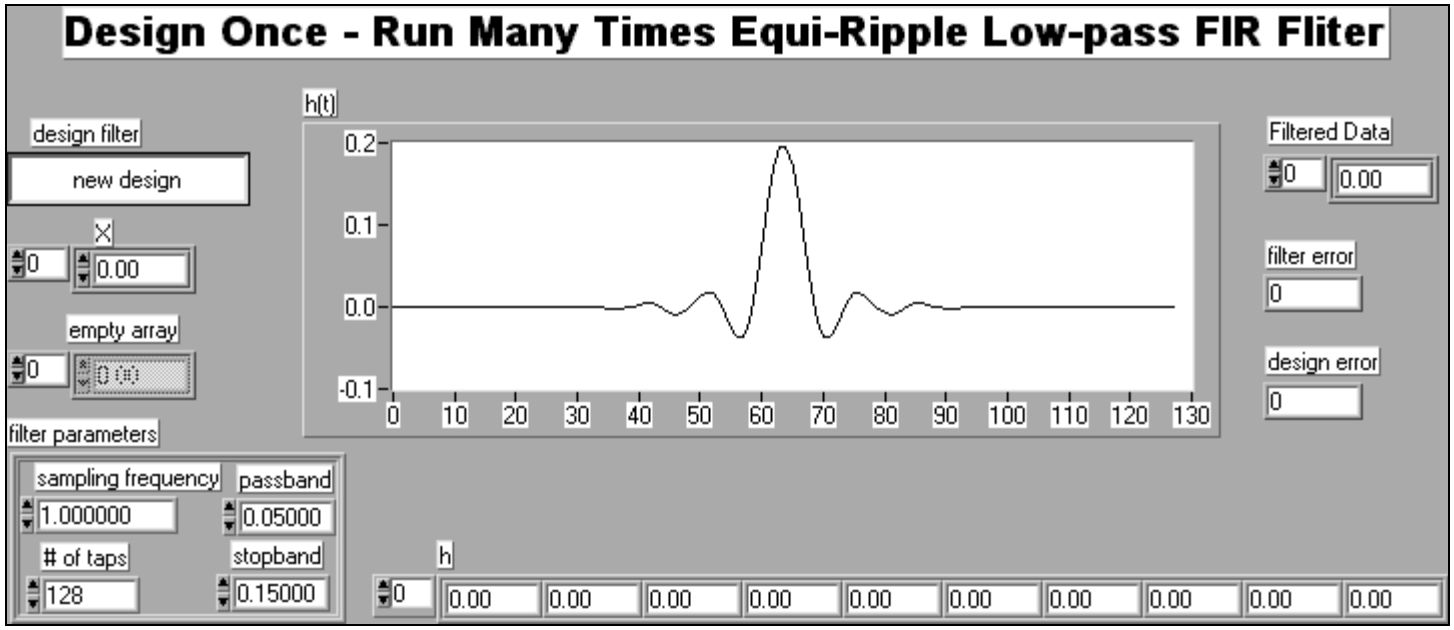

Figure B–9. Design Once Low-pass VI front panel

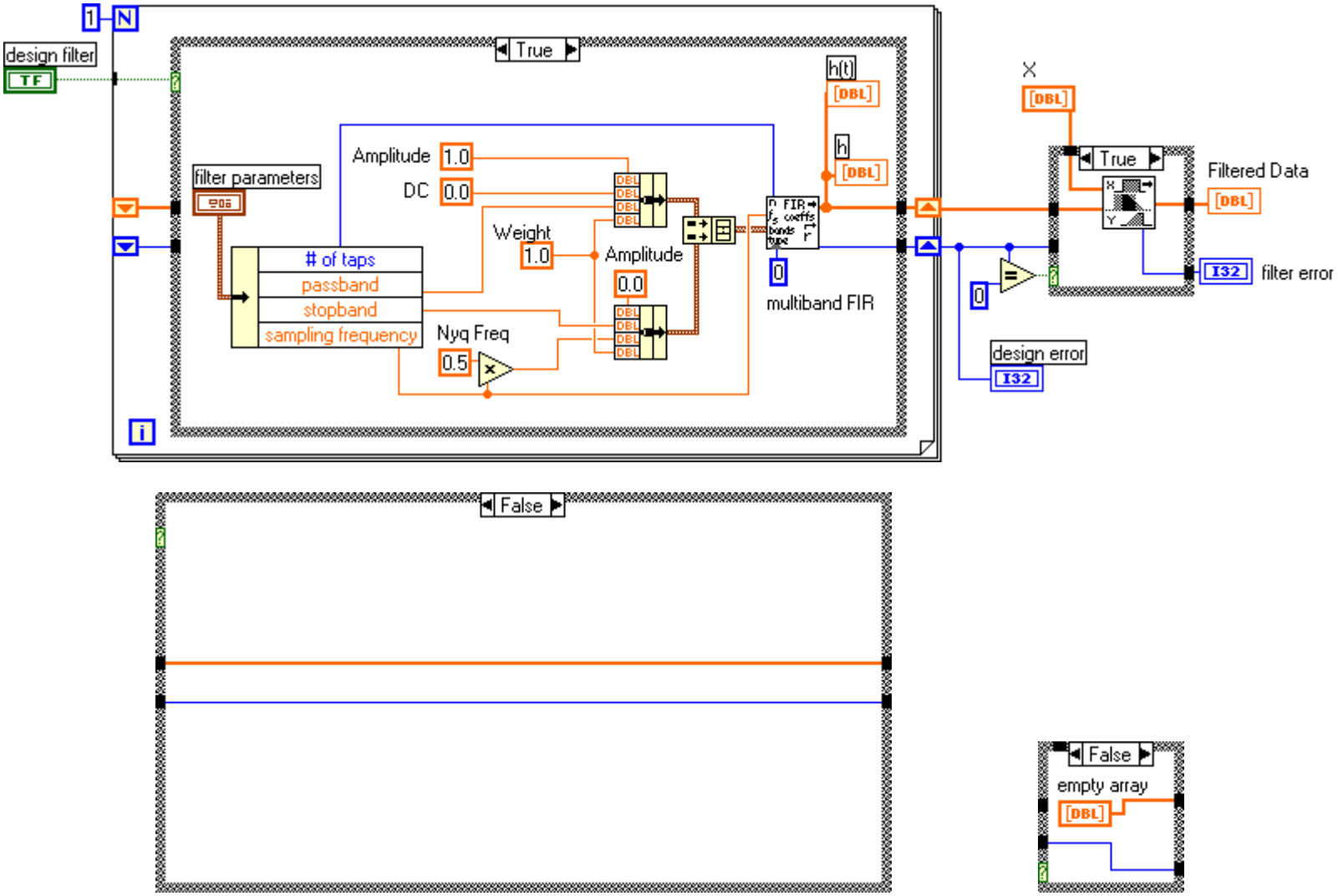

Figure B–10. Design Once Low-pass VI diagram.

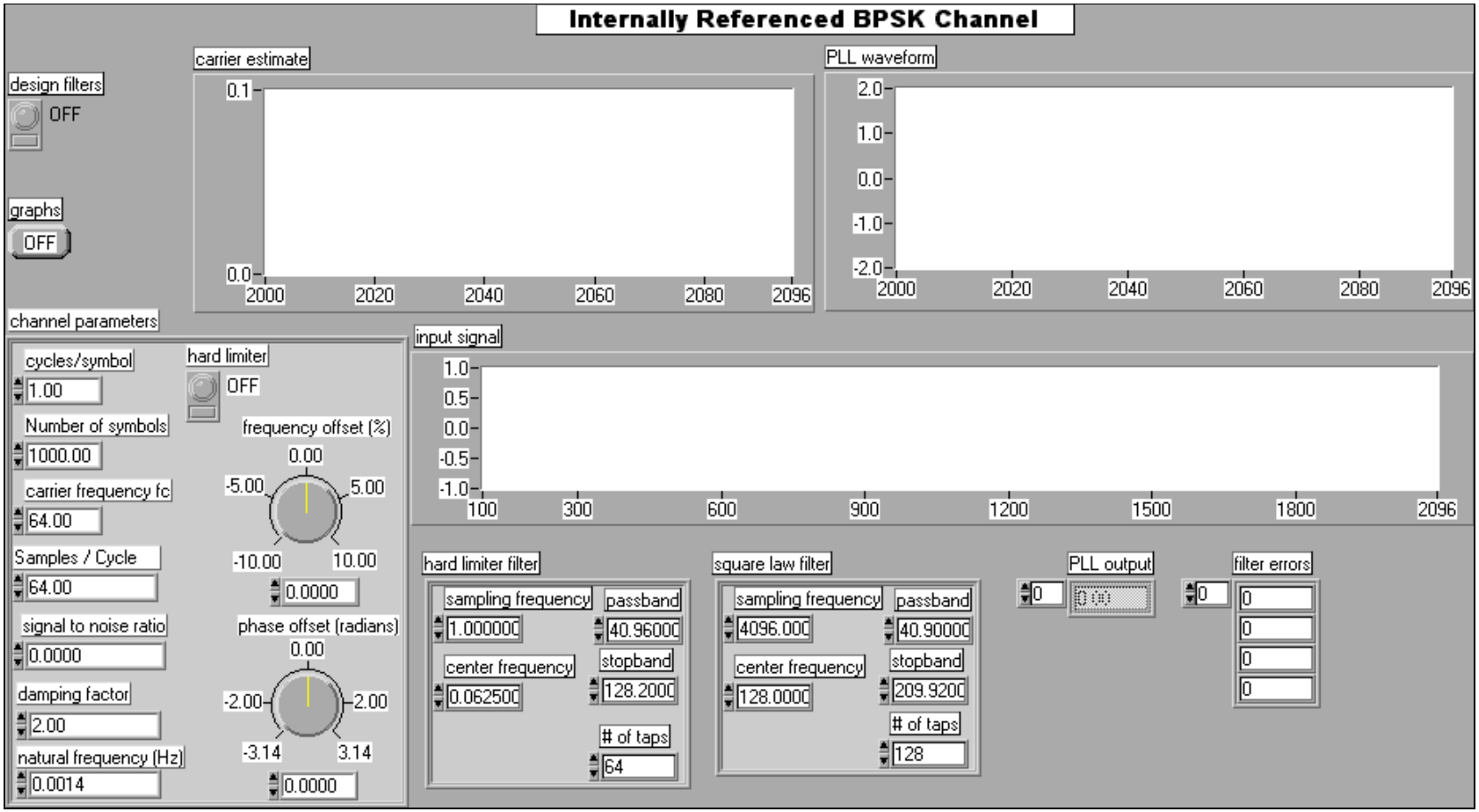

Figure B–11. Internal BPSK Channel VI front panel.

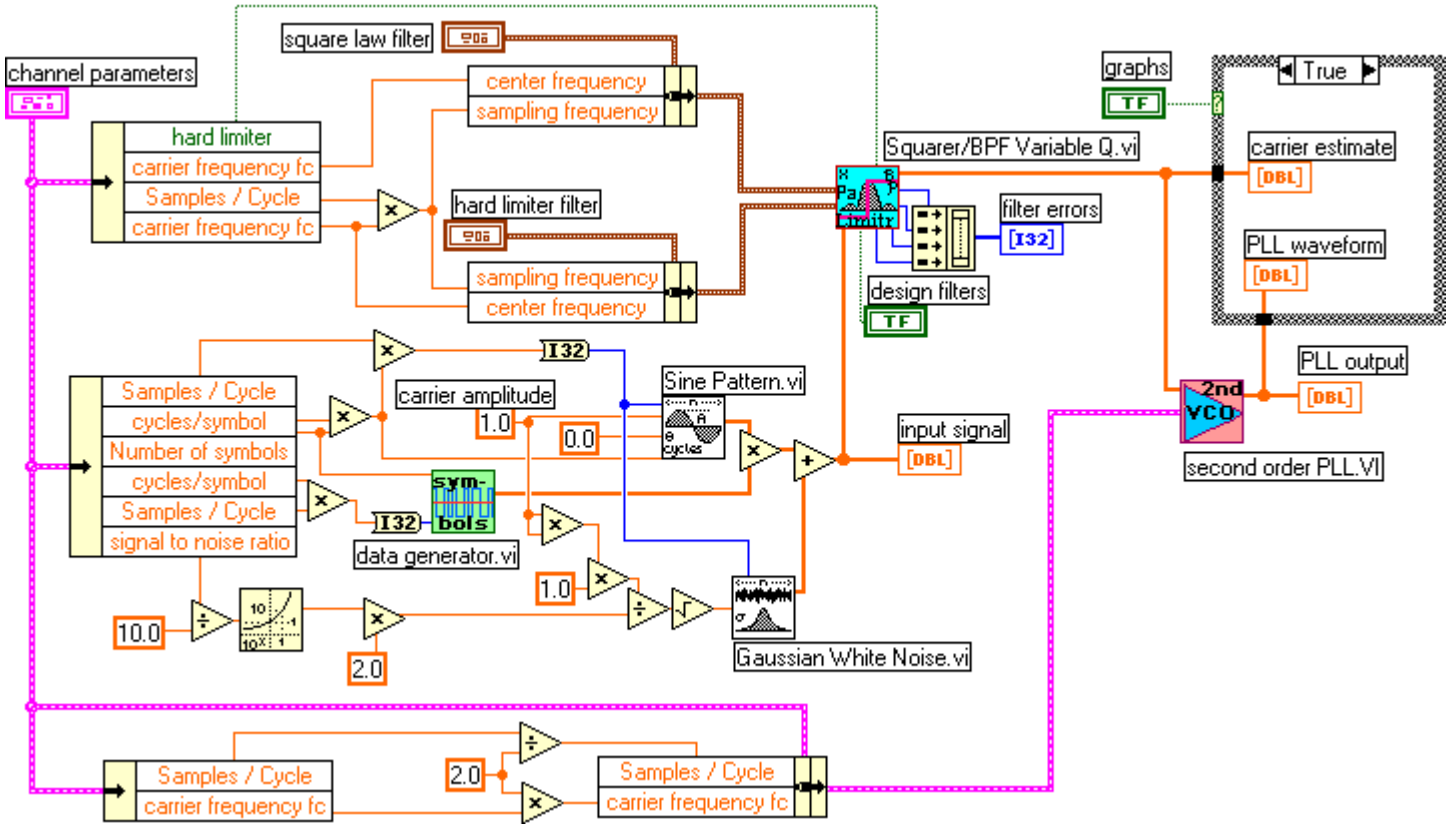

Figure B–12. Internal BPSK Channel VI diagram.

Figure B–12. (continued)

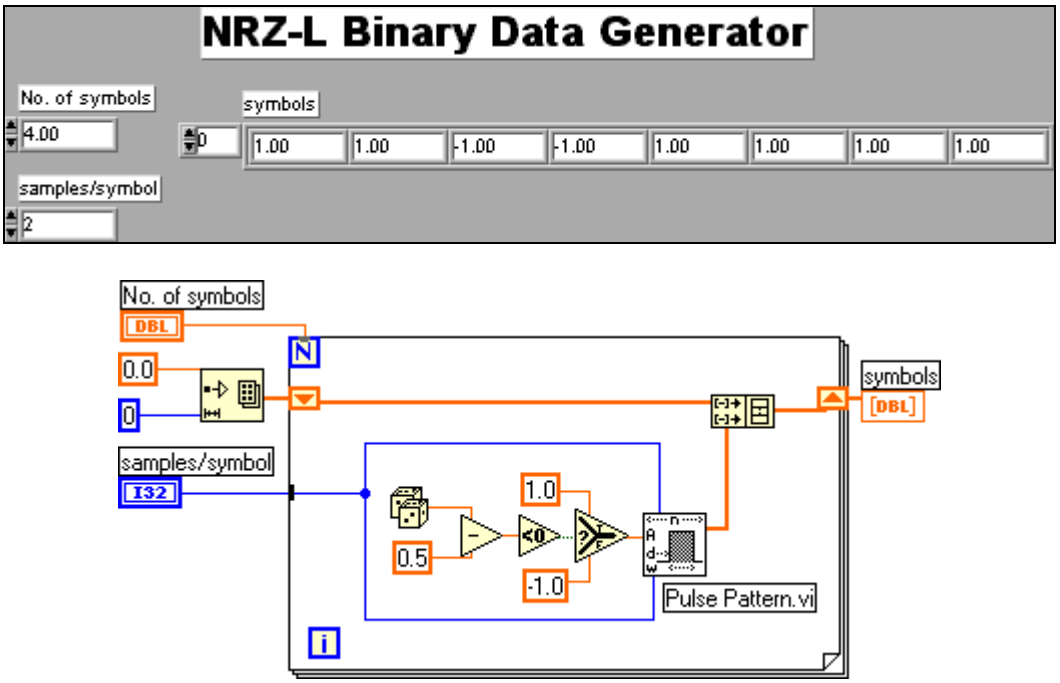

Figure B–13. Data Generator VI.

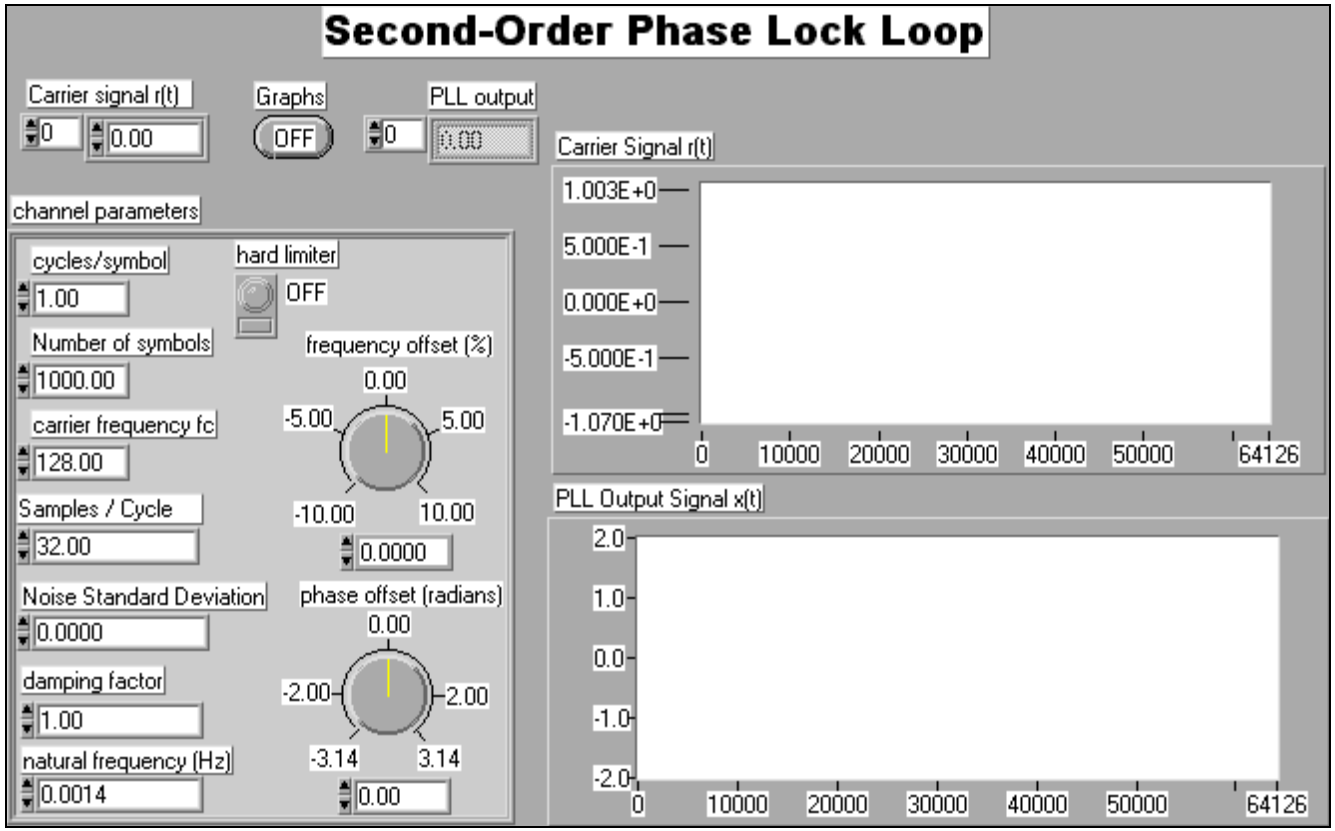

Figure B–14. Second-Order Phase Lock Loop VI front panel.

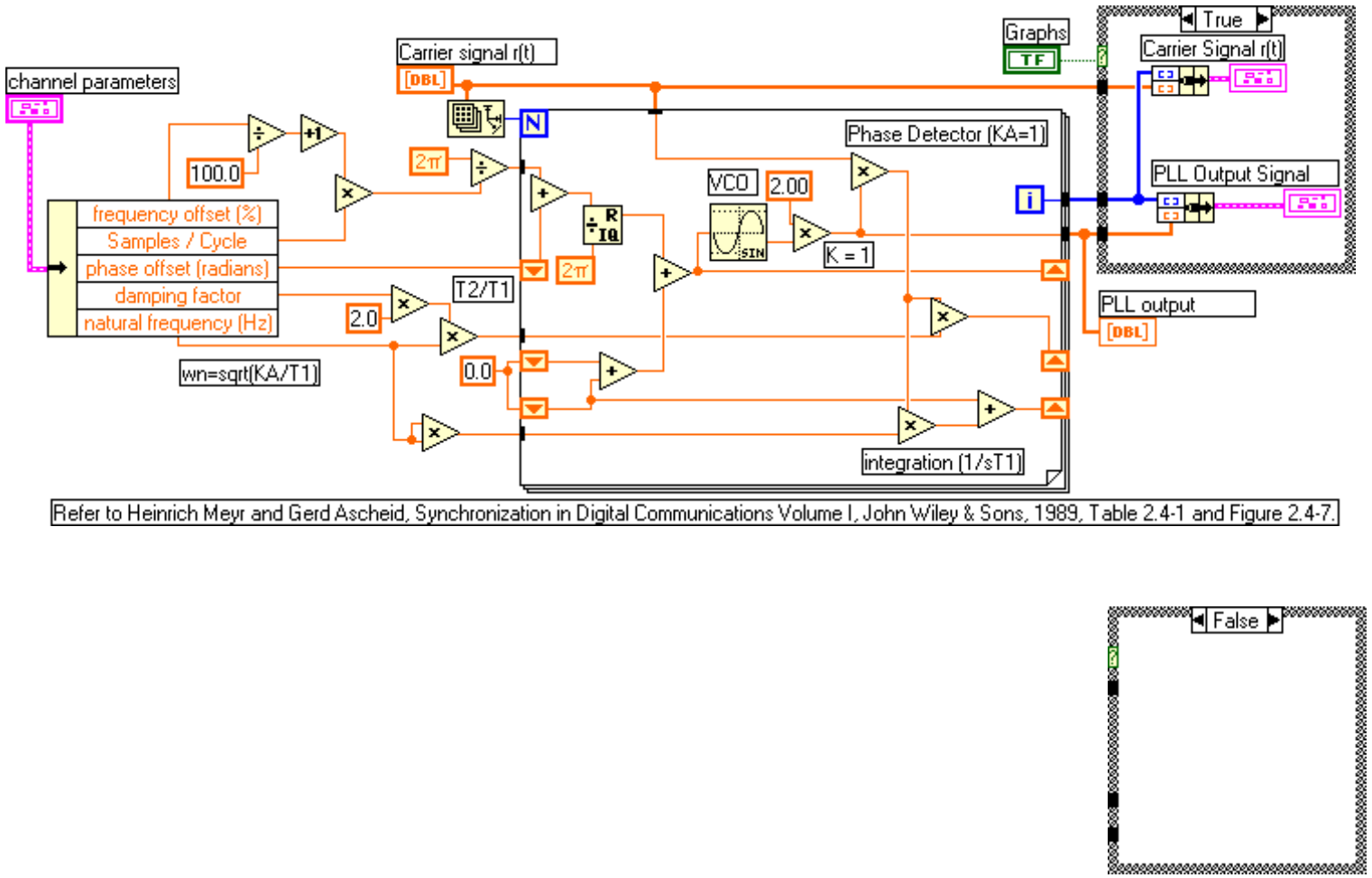

Figure B–15. Second-Order Phase Lock Loop VI diagram.

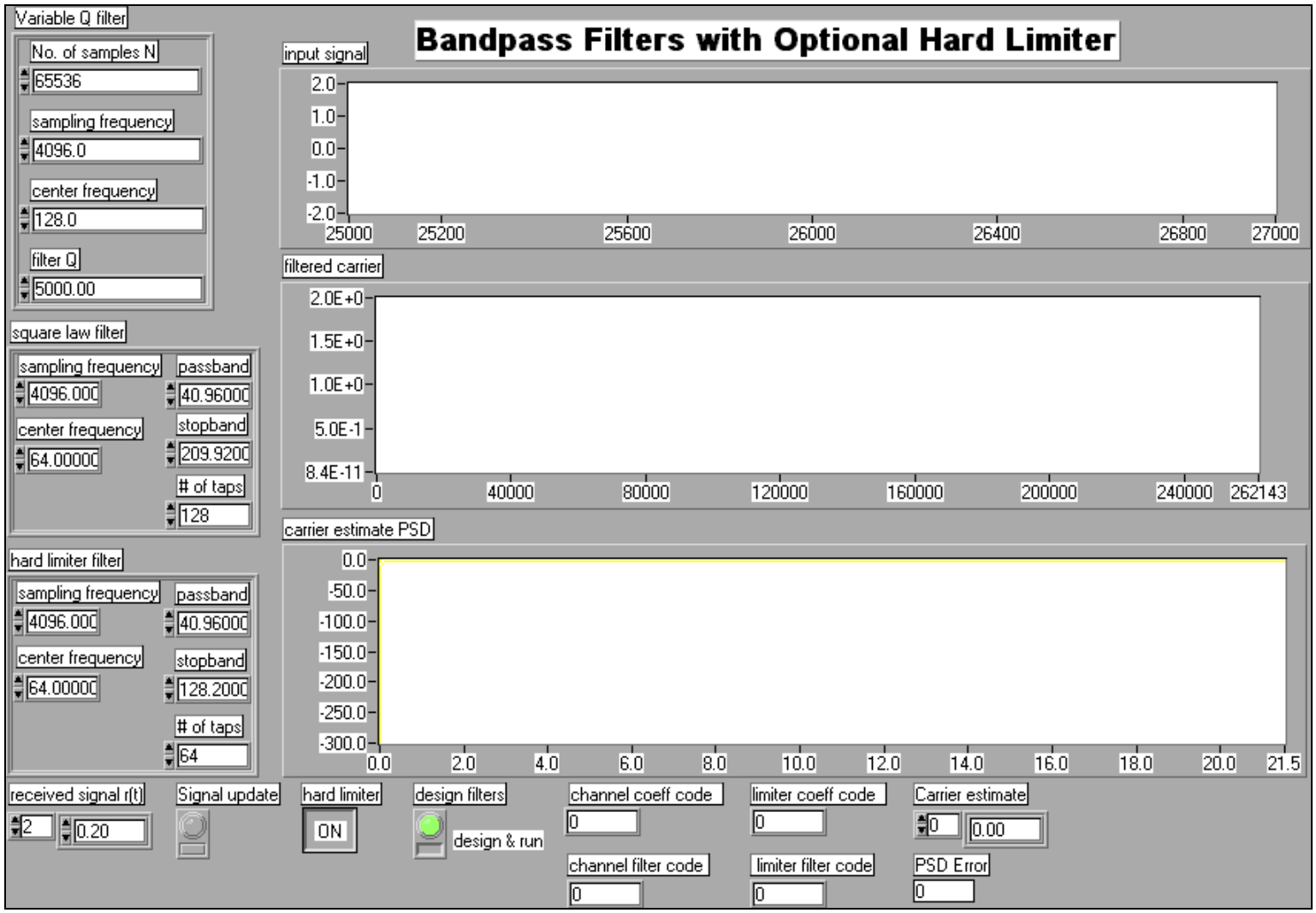

Figure B–16. Squaring Bandpass Filter With Hard Limiter VI front panel.

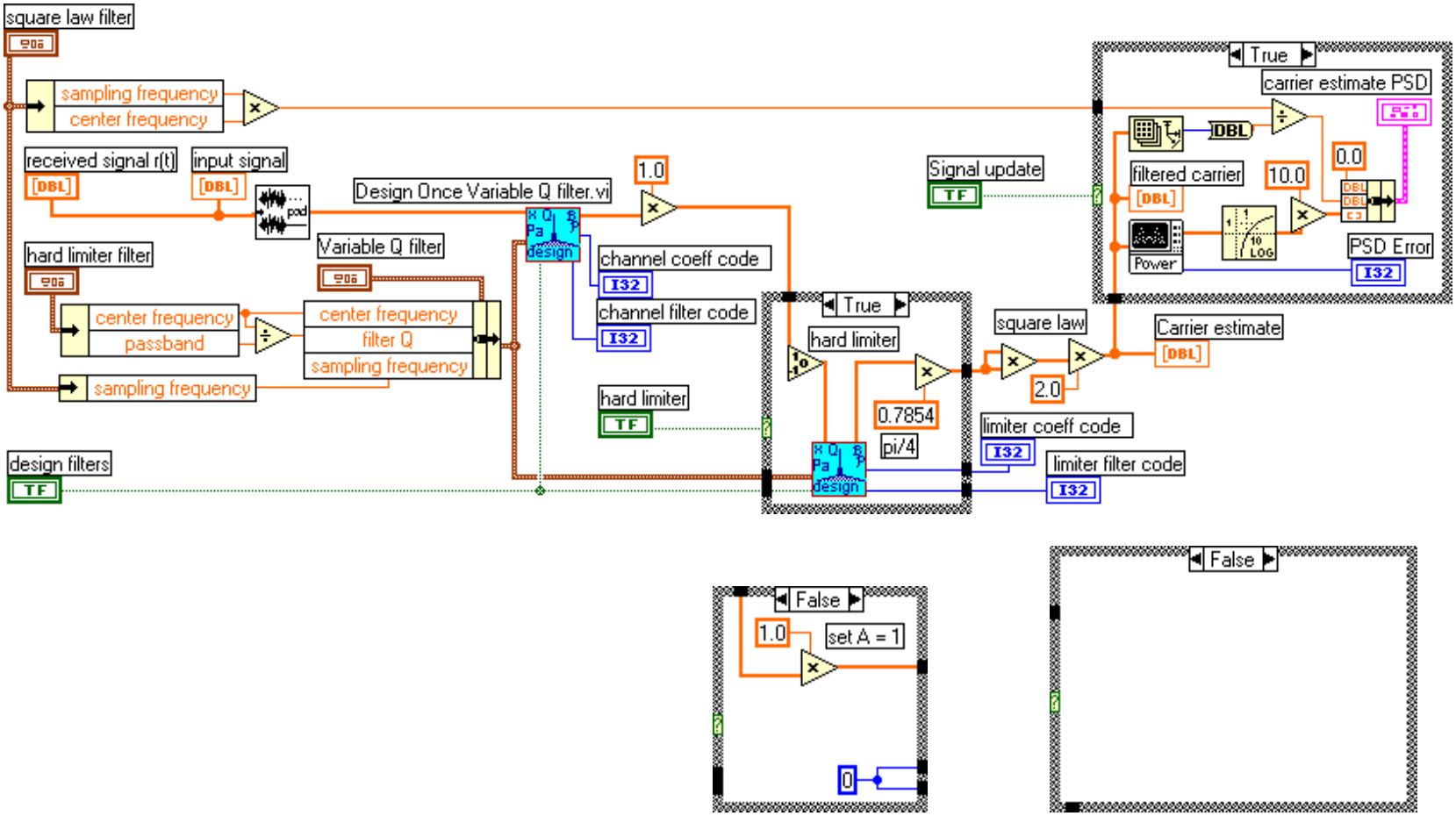

Figure B–17. Squaring Bandpass Filter With Hard Limiter VI diagram.

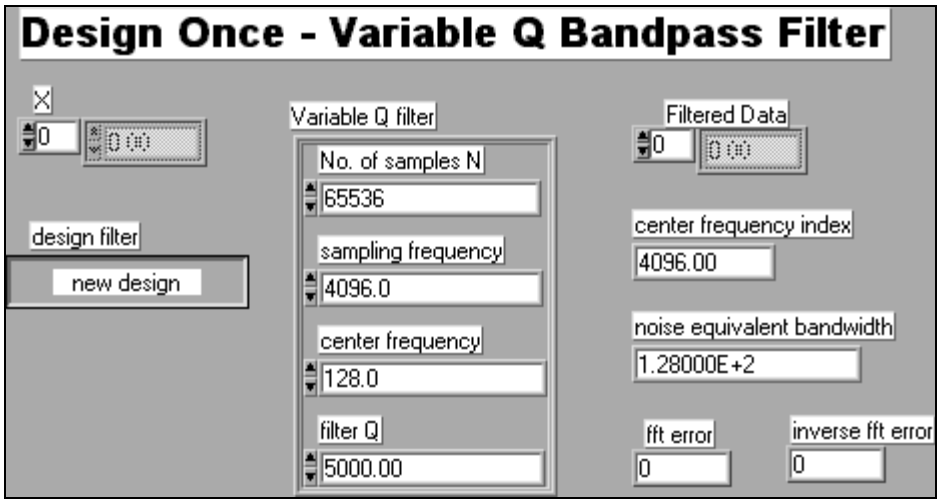

Figure B–18. Design Once – Variable *Q* Bandpass Filter front panel.

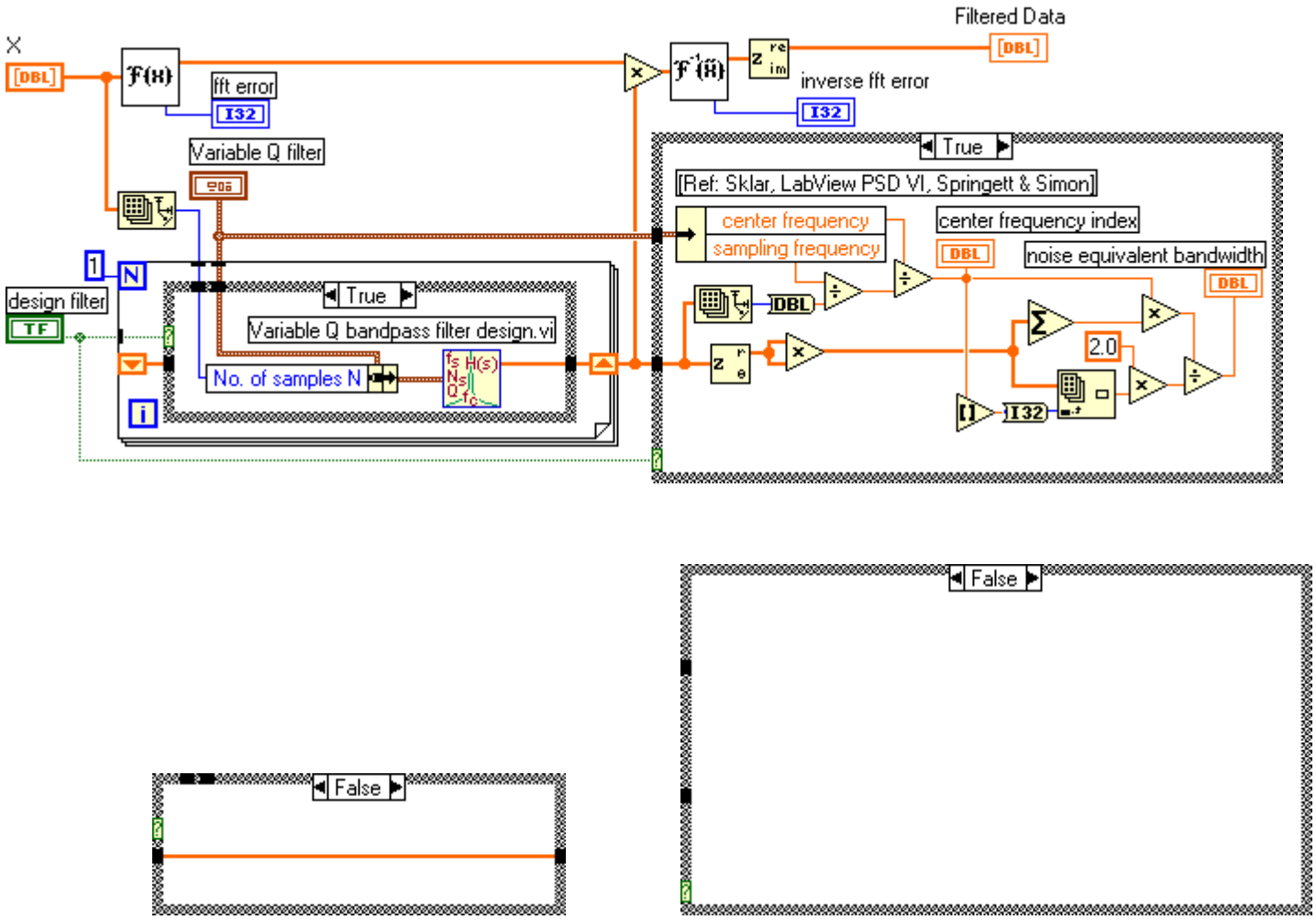

Figure B–19. Design Once – Variable *Q* Bandpass Filter diagram.

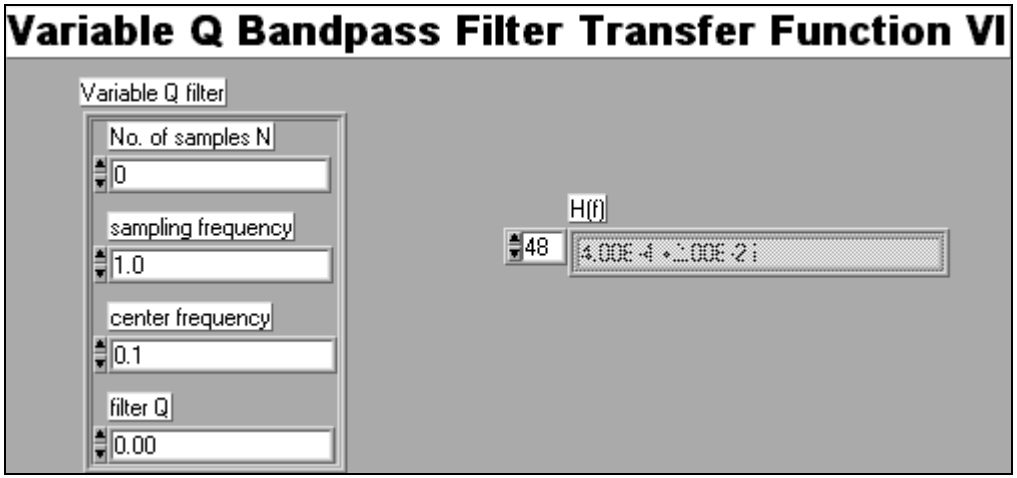

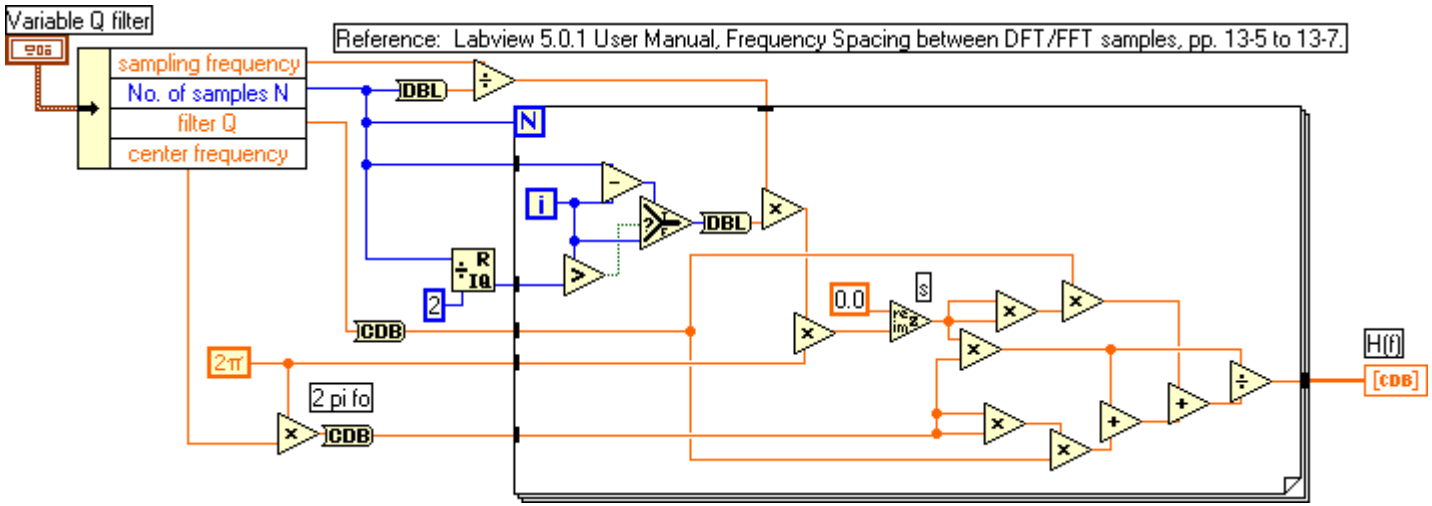

Figure B–20. Variable *Q* Bandpass Filter Transfer Function VI.

APPENDIX C. EXTERNALLY-REFERENCED BLPL MODELS

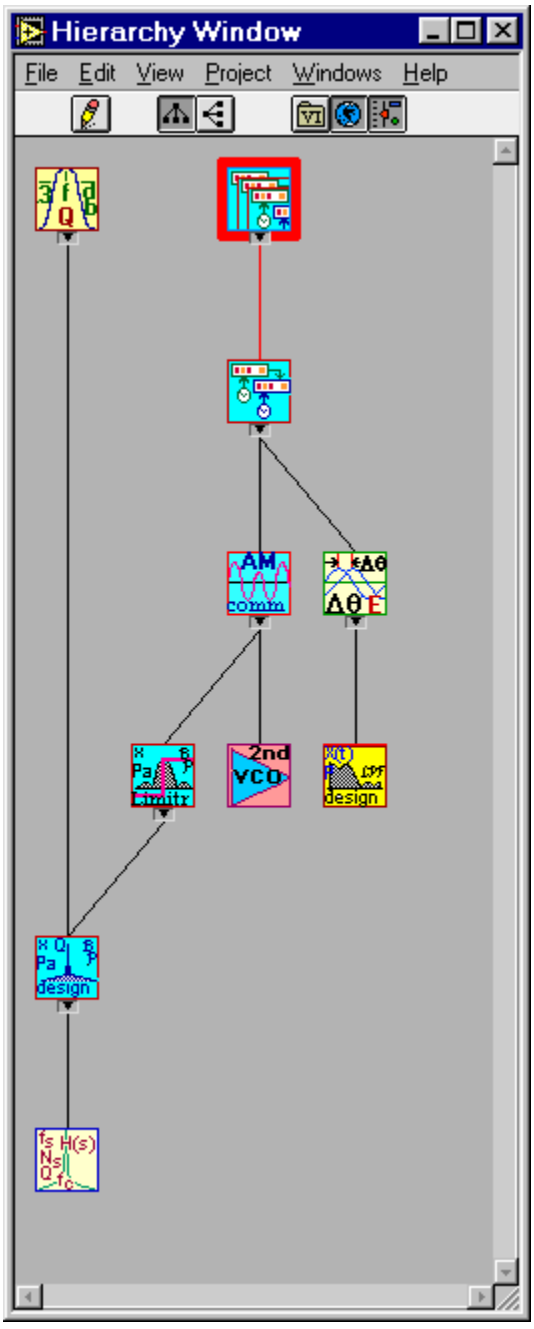

Figure C–1. Externally-Referenced BLPL Model VI Hierarchy.

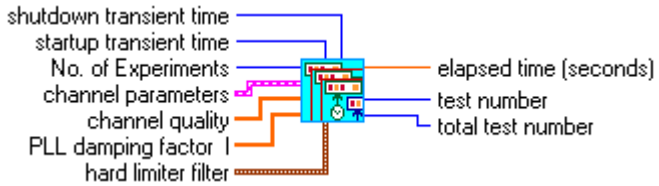

External BLPL Iterant Test VI (Figure C–3)

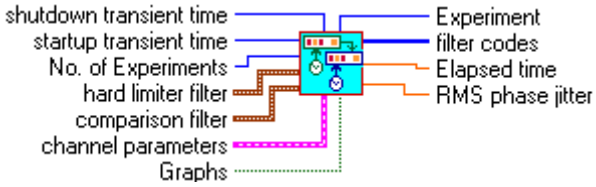

External BLPL Model VI (Figure C–5)

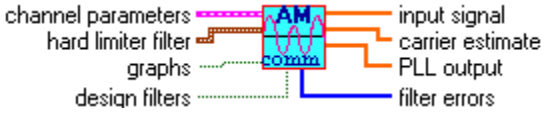

External BLPL DSB-RC Channel VI (Figure C–7)

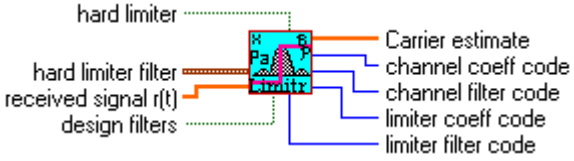

Bandpass Limiter with Variable Q Filter VI (Figure C–9)

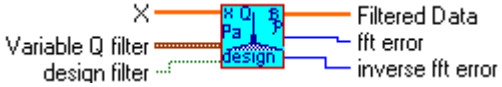

Design Once – Variable *Q* Bandpass Filter (Figure C–11)

Variable *Q* Bandpass Filter Transfer Function VI (Figure C–13)

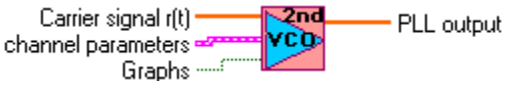

Second-Order Phase Lock Loop VI (Figure C–14)

Figure C–2. Externally-Referenced BLPL Model VI Connector Legend.

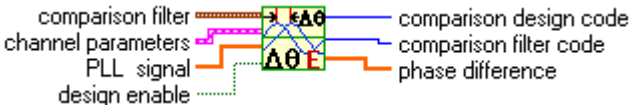

External Reference Phases Comparison VI (Figure C–16)

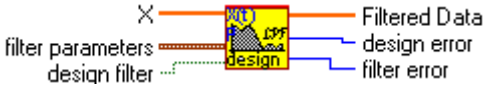

Design Once Low-pass VI (Figure C–18)

Variable *Q* Filter Design VI (Figure C–20)

Figure C–2. (continued)

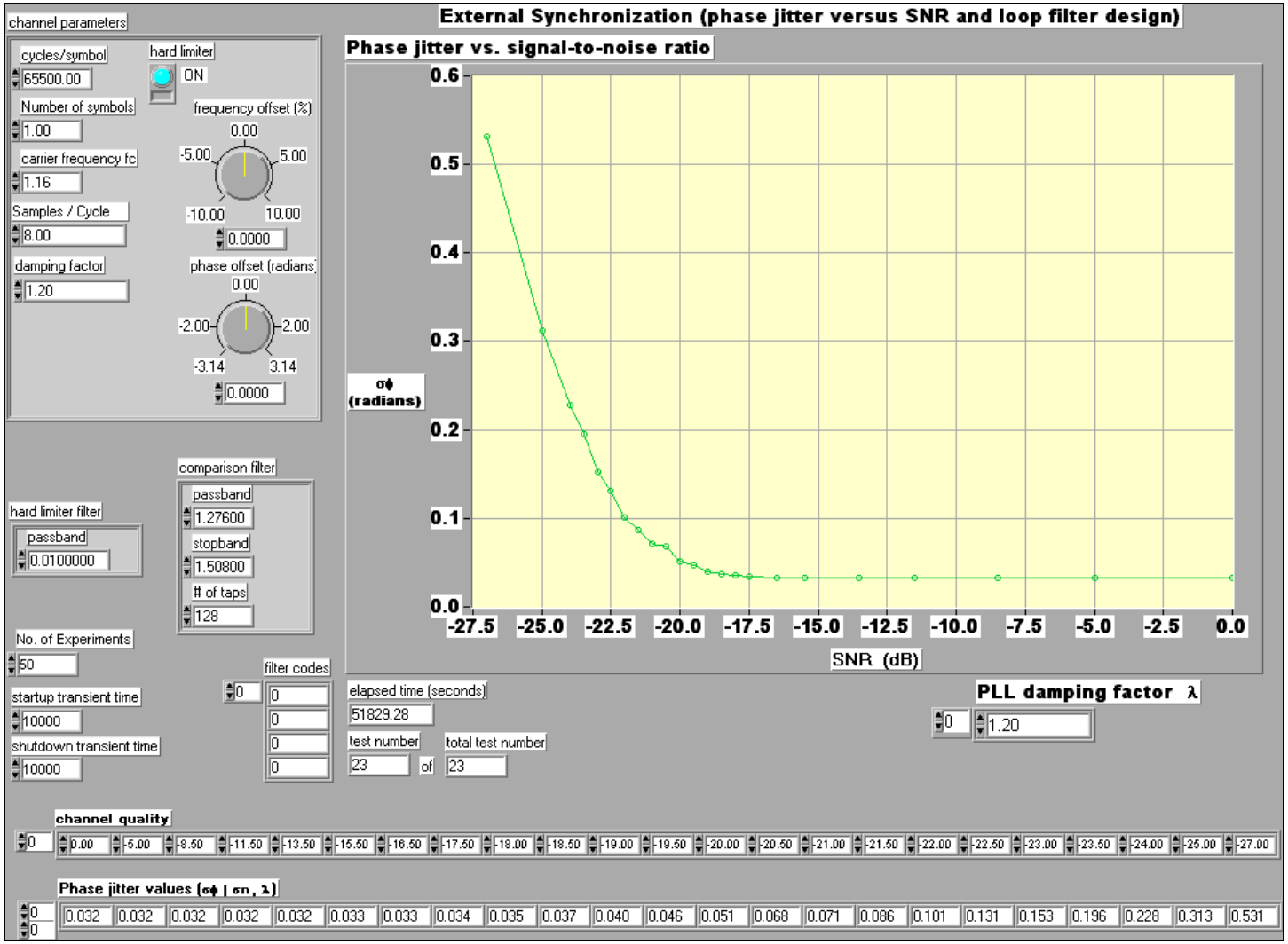

Figure C–3. External BLPL Iterant Test VI front panel.

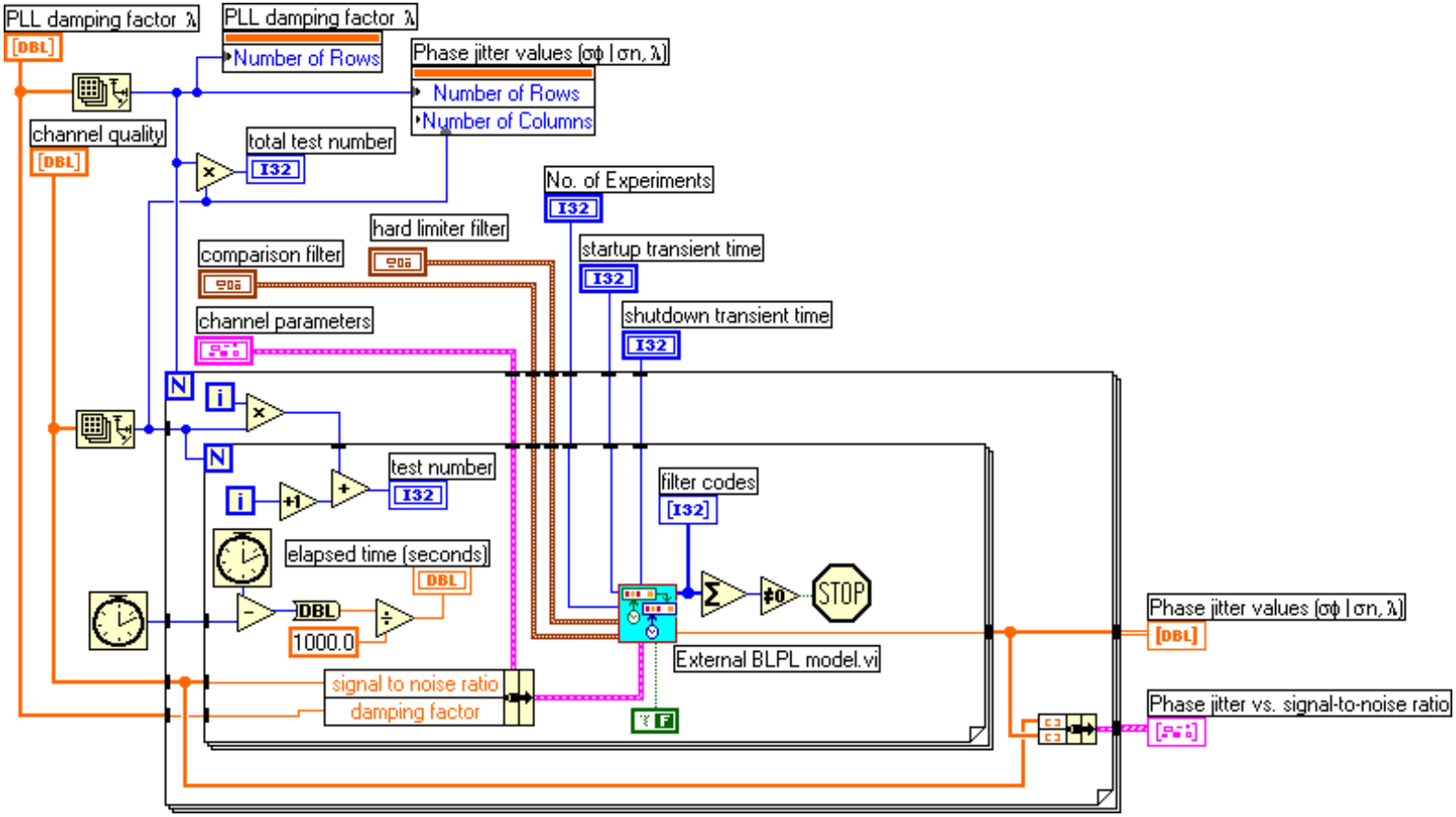

Figure C–4. External BLPL Iterant Test VI diagram.

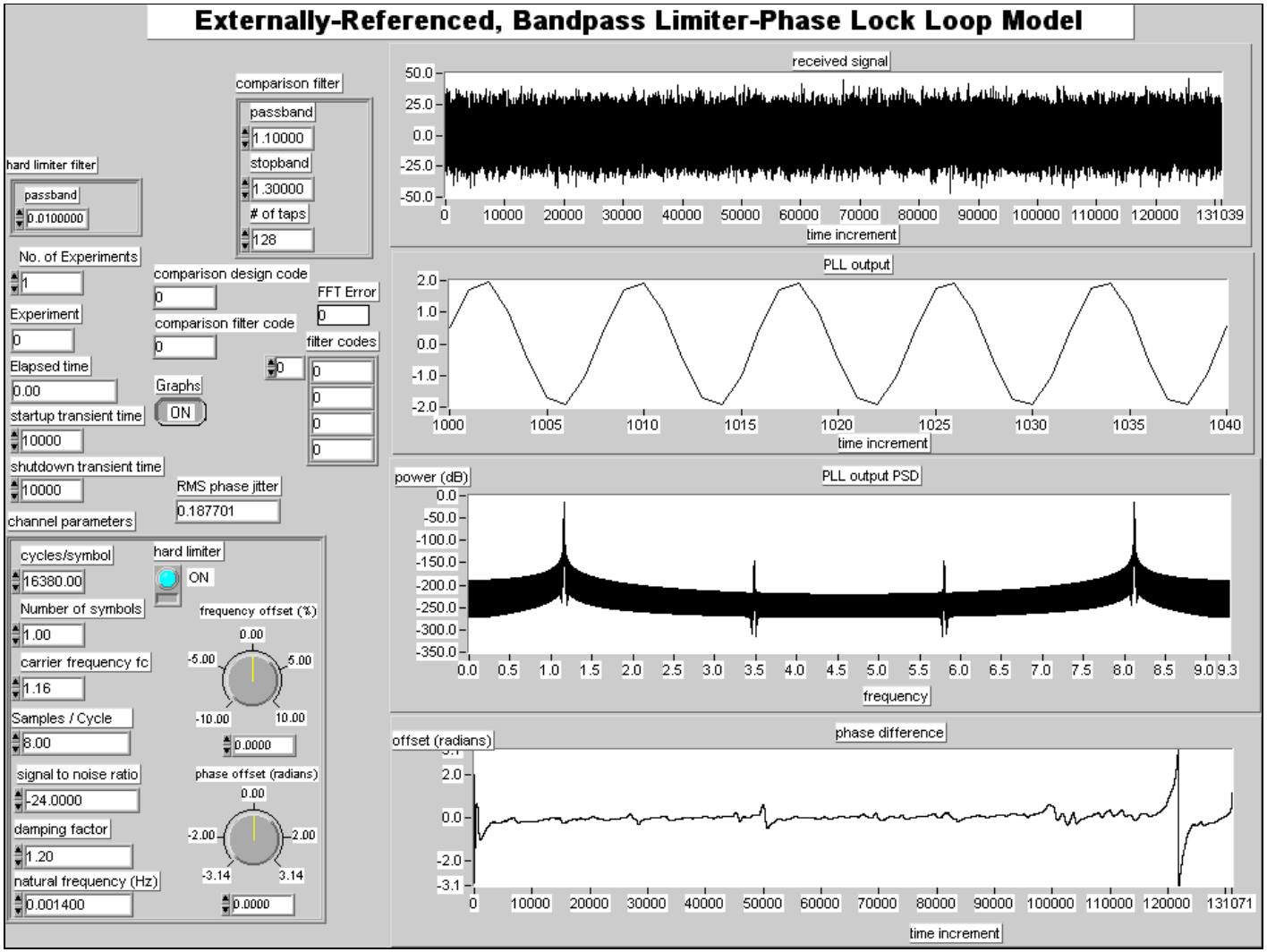

Figure C–5. External BLPL Model VI front panel.

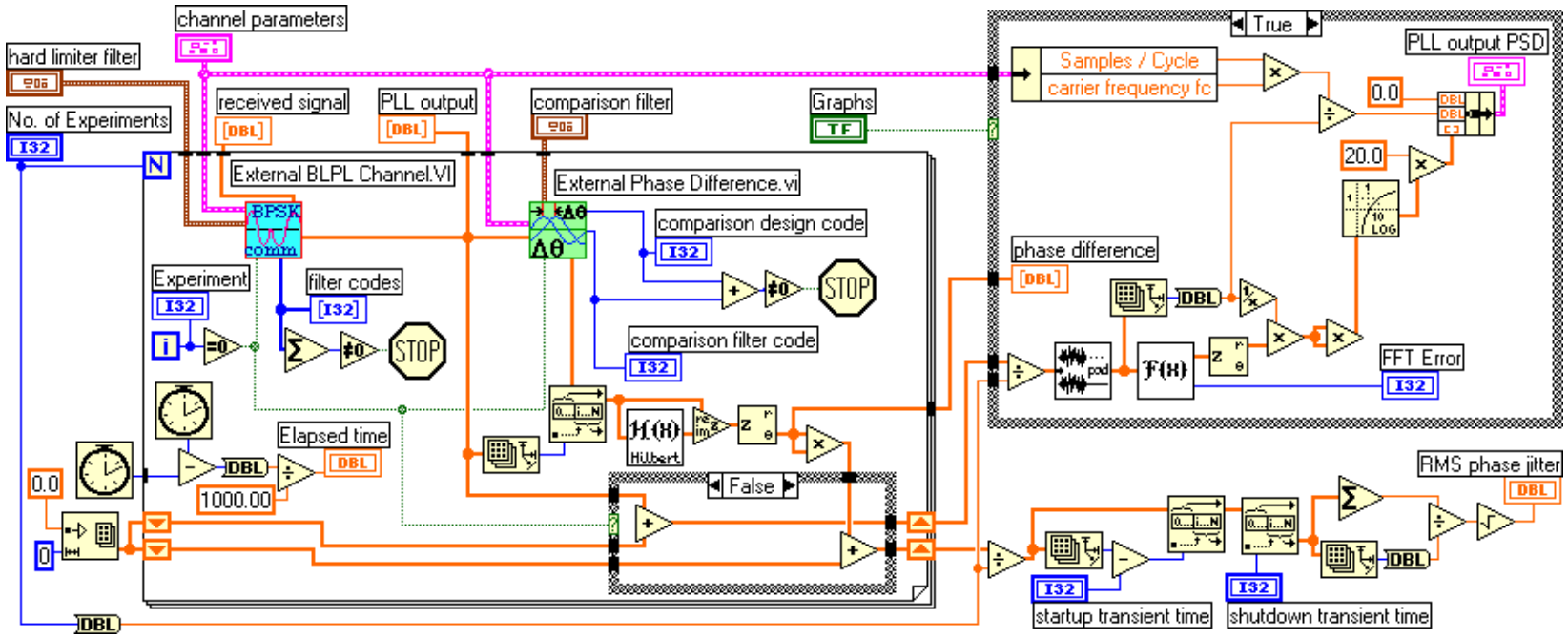

Figure C–6. External BLPL Model VI diagram.

Figure C–6. (continued)

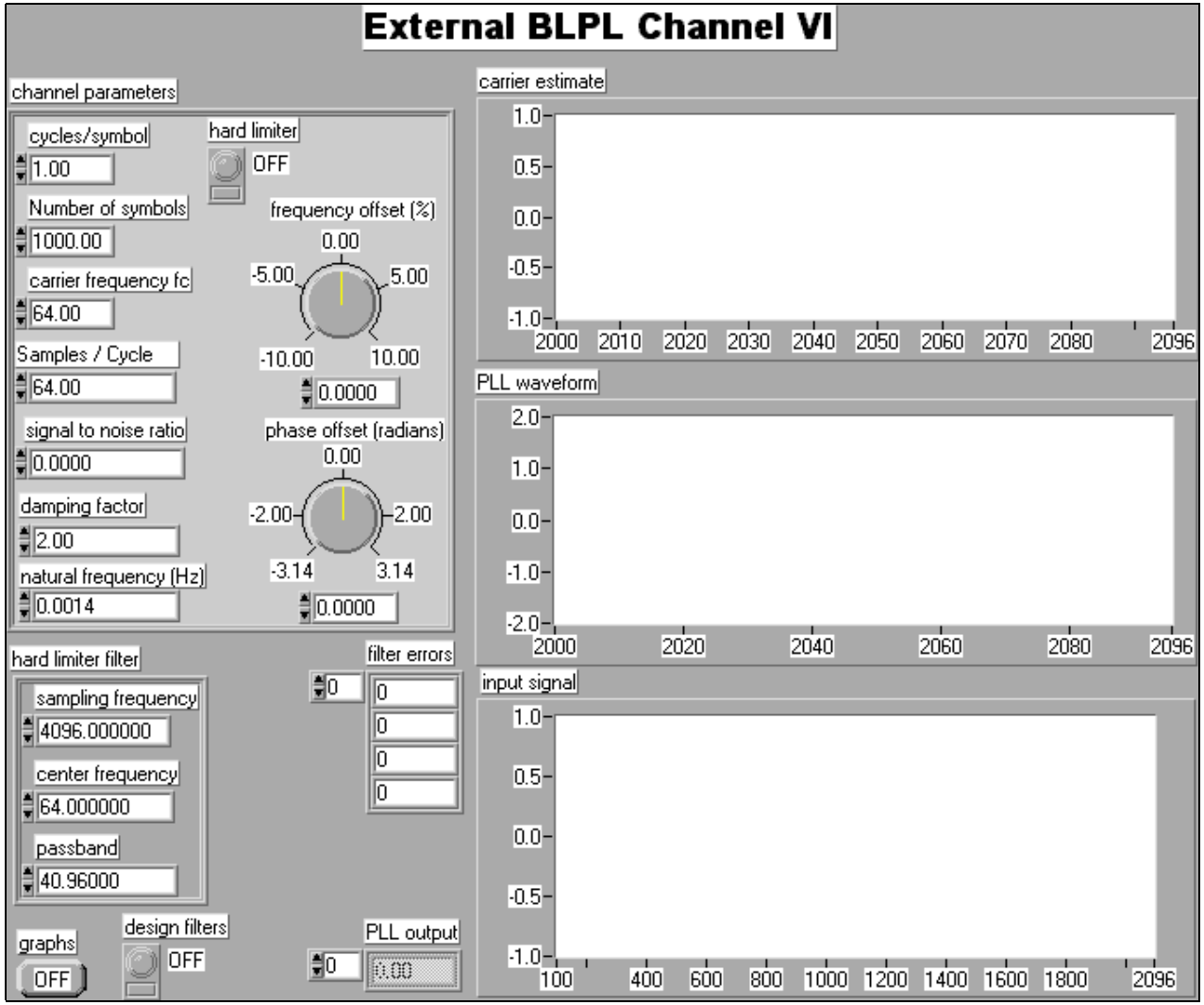

Figure C–7. External BLPL DSB-RC Channel VI front panel.

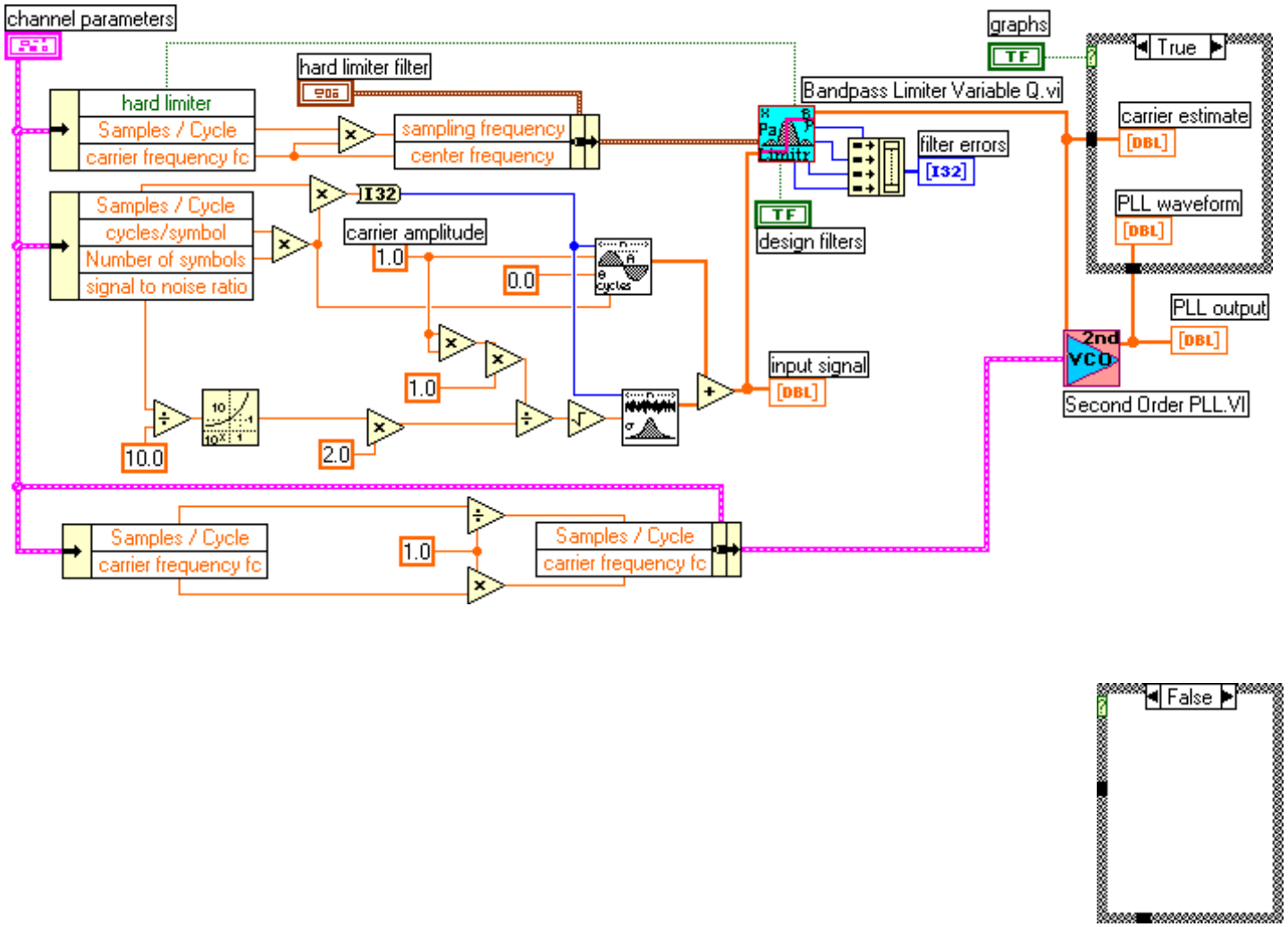

Figure C–8. External BLPL DSB-RC Channel VI diagram.

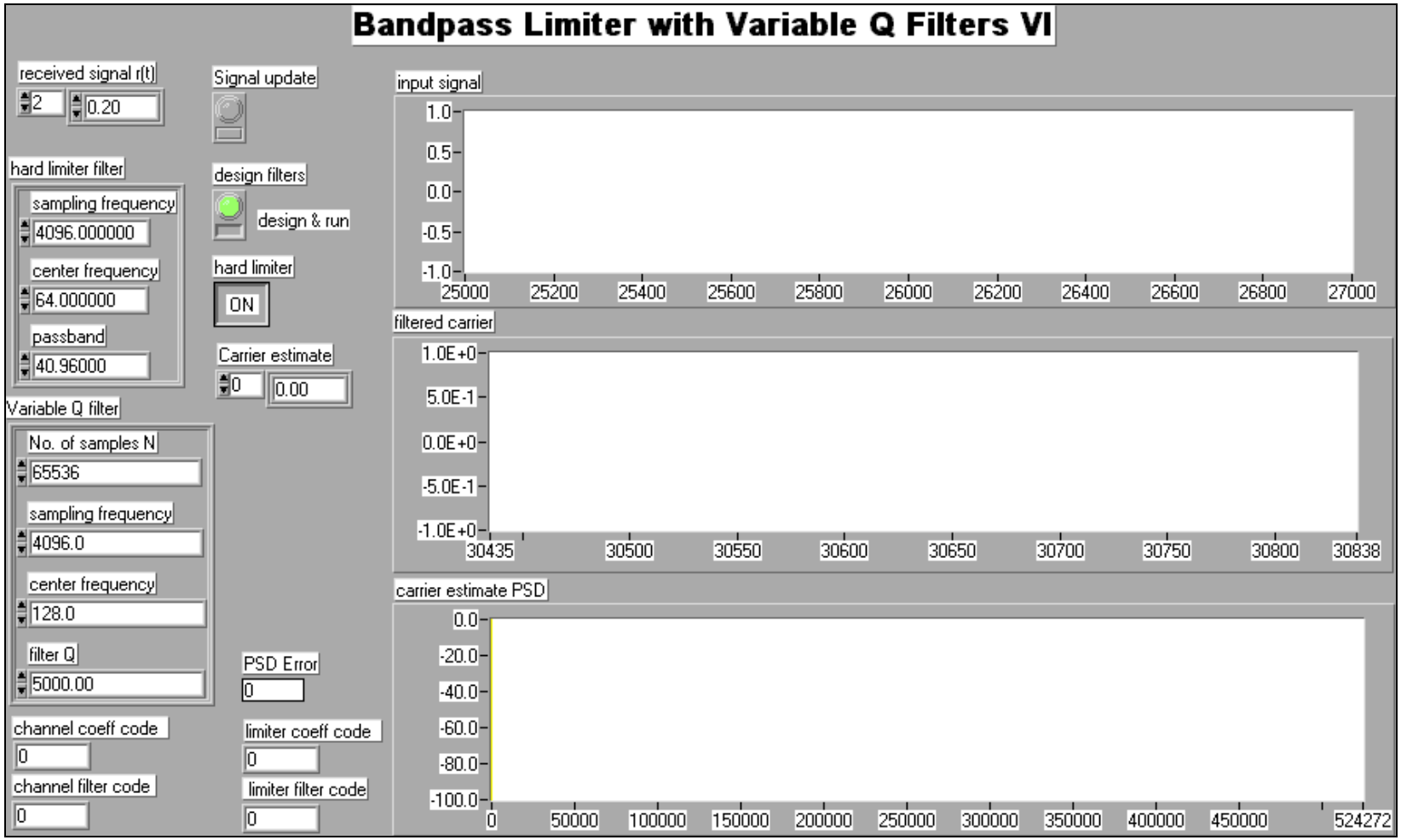

Figure C–9. Bandpass Limiter with Variable Q Filter VI front panel.

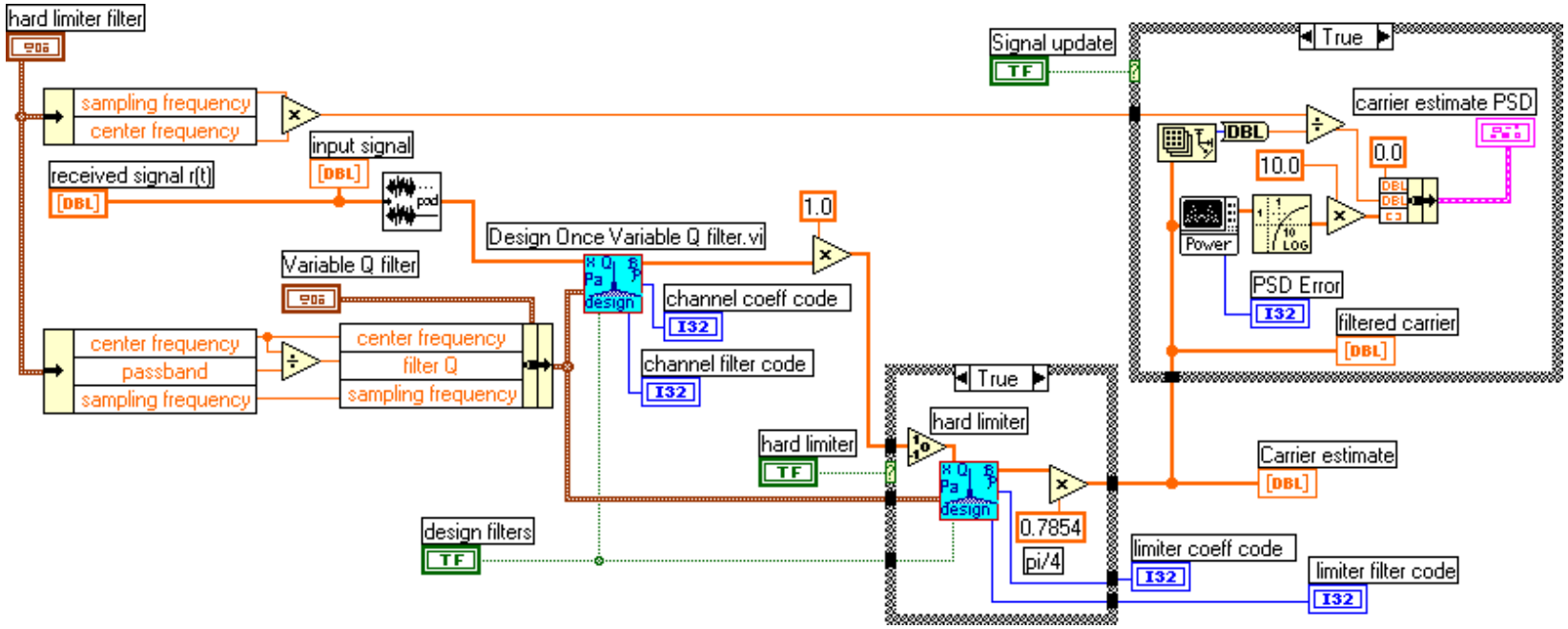

Figure C–10. Bandpass Limiter with Variable Q Filter VI diagram.

Figure C–10. (continued)

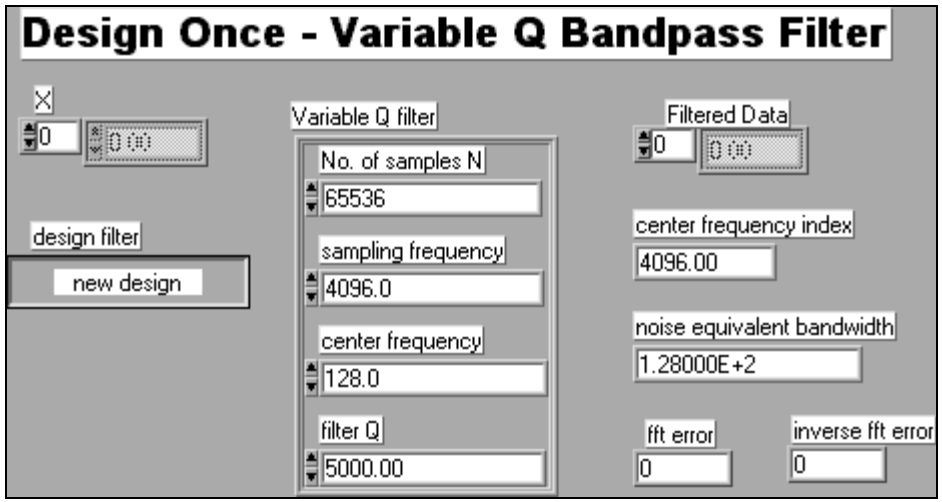

Figure C–11. Design Once – Variable *Q* Bandpass Filter front panel.

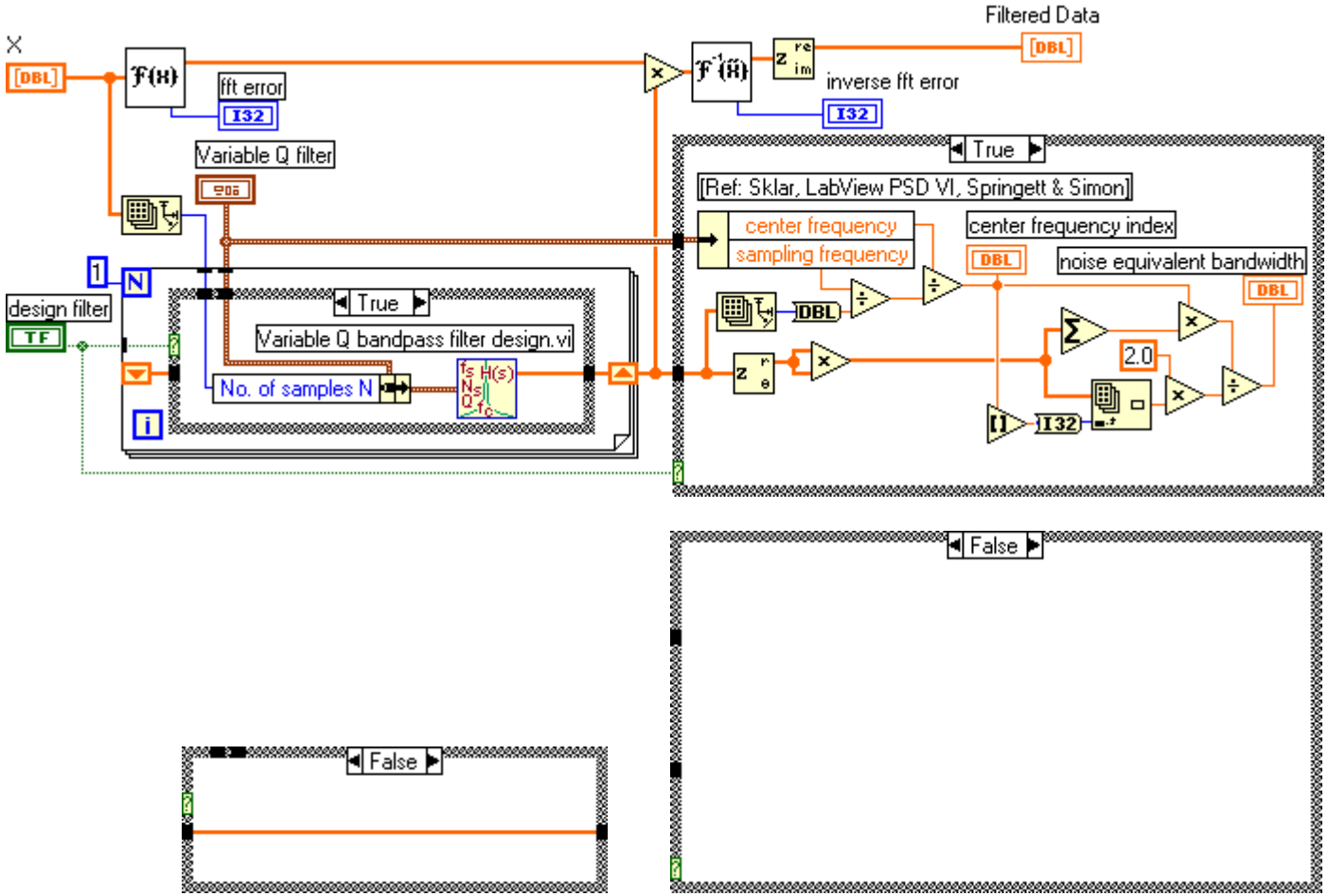

Figure C–12. Design Once – Variable *Q* Bandpass Filter diagram.

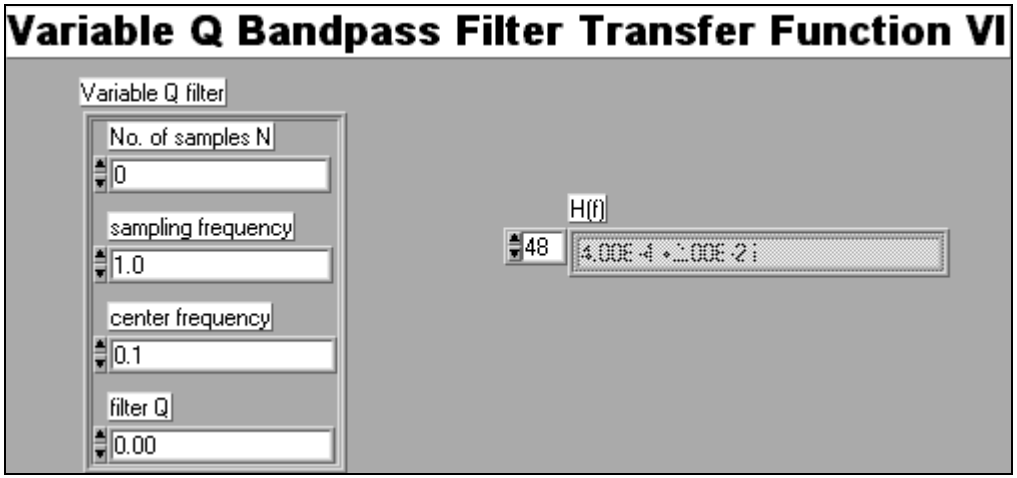

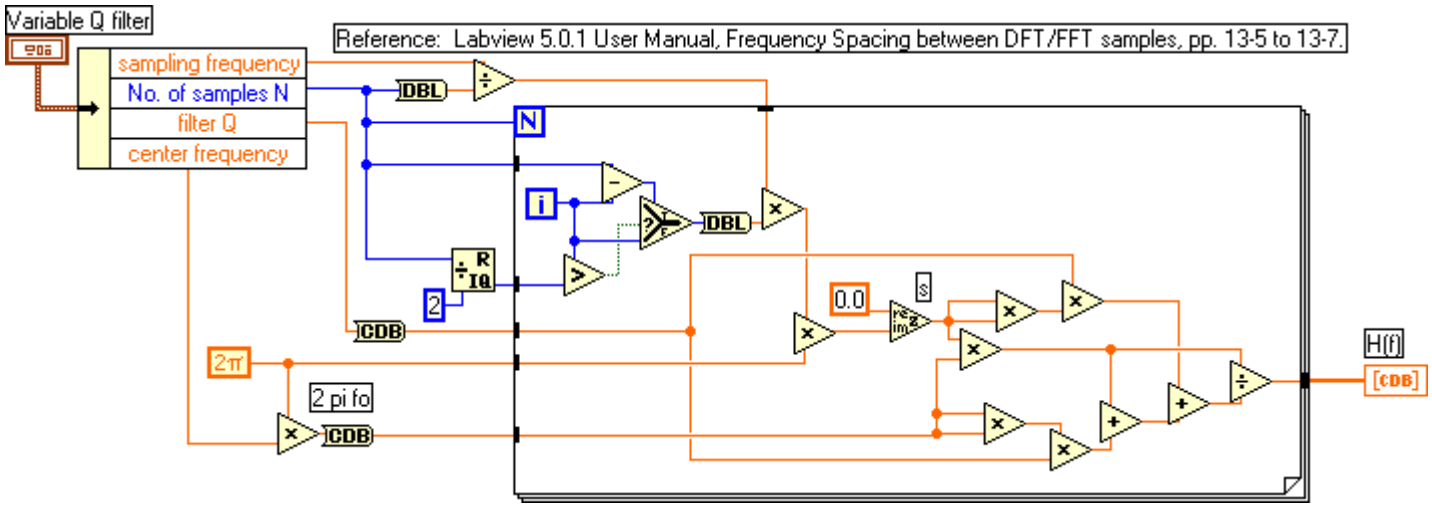

Figure C–13. Variable *Q* Bandpass Filter Transfer Function VI.

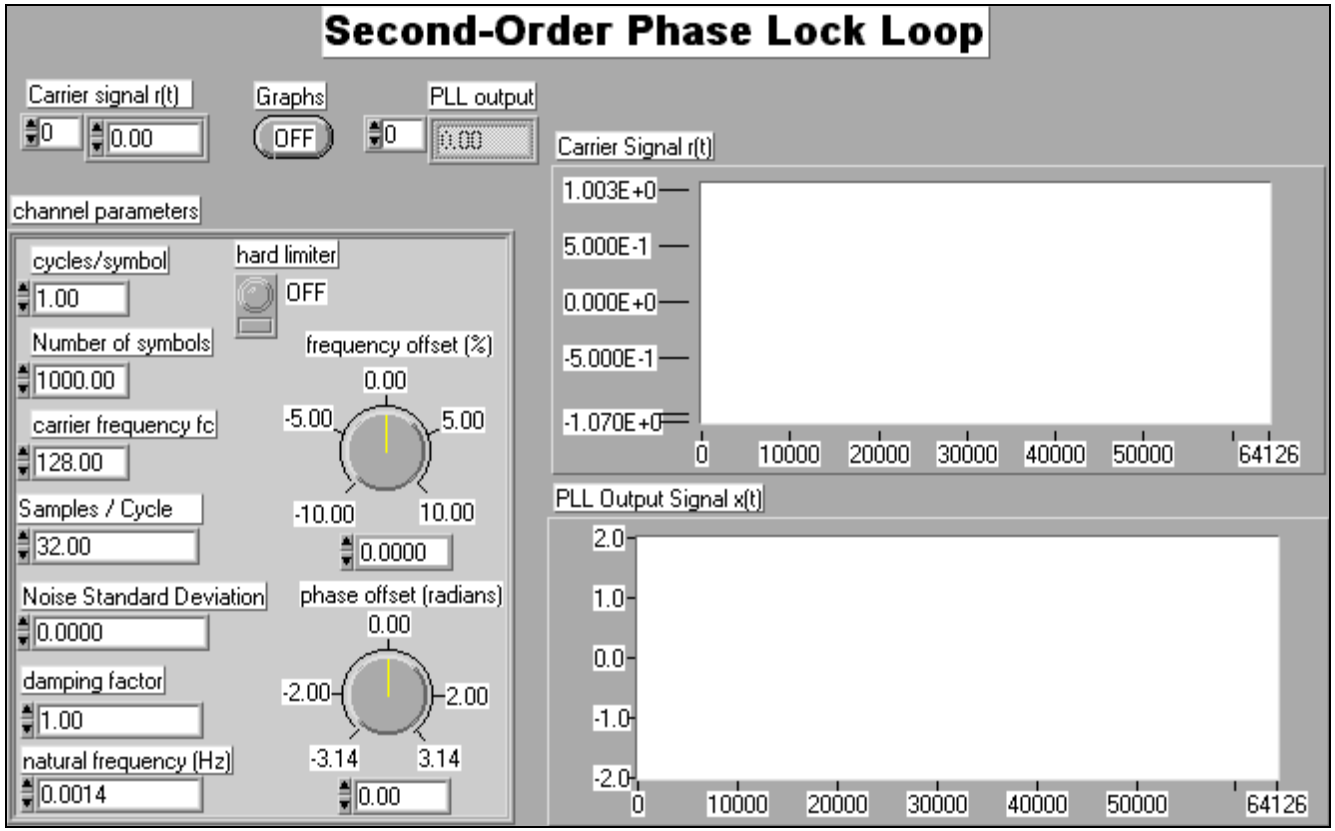

Figure C–14. Second-Order Phase Lock Loop VI front panel.

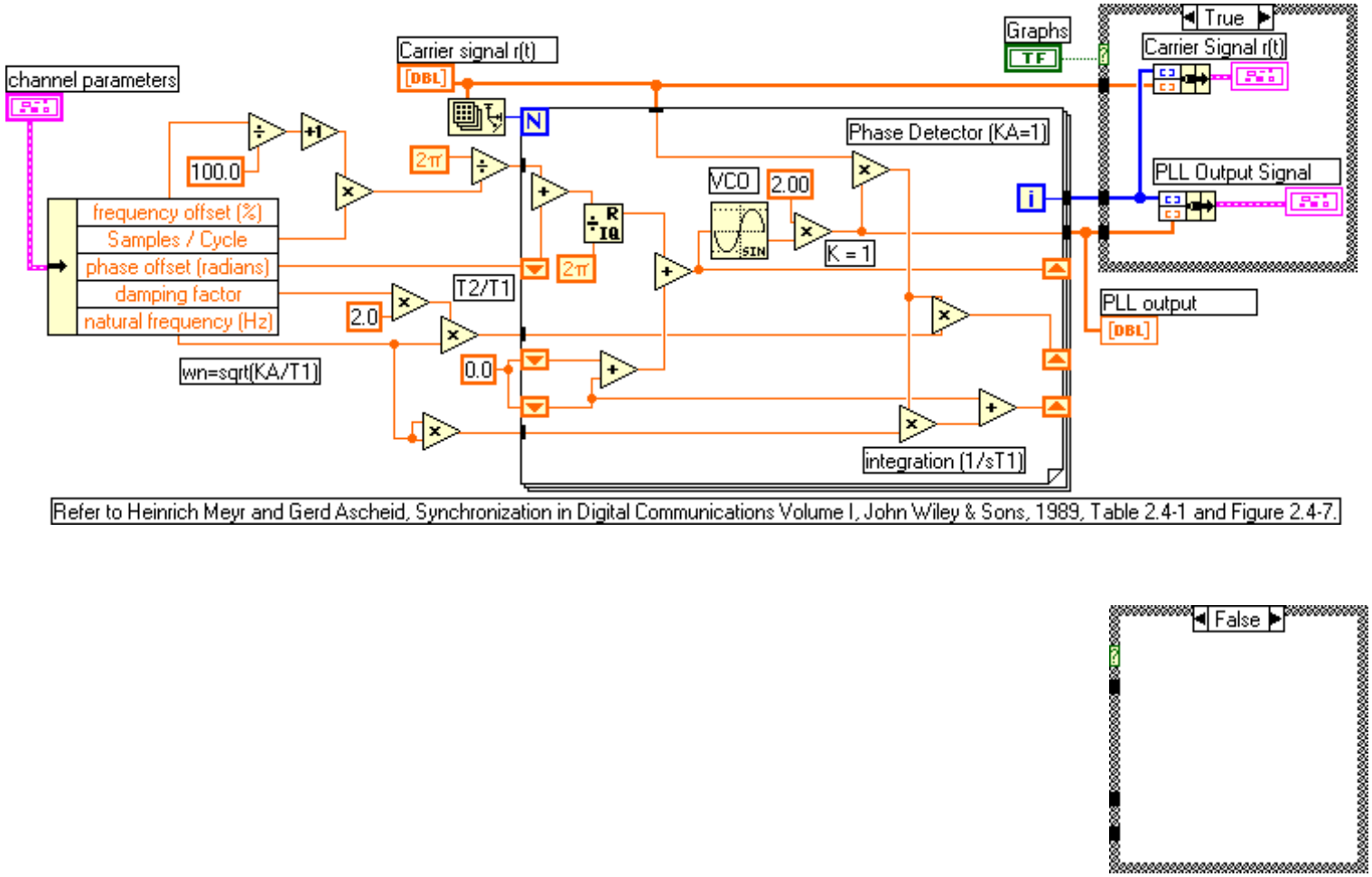

Figure C–15. Second-Order Phase Lock Loop VI diagram.

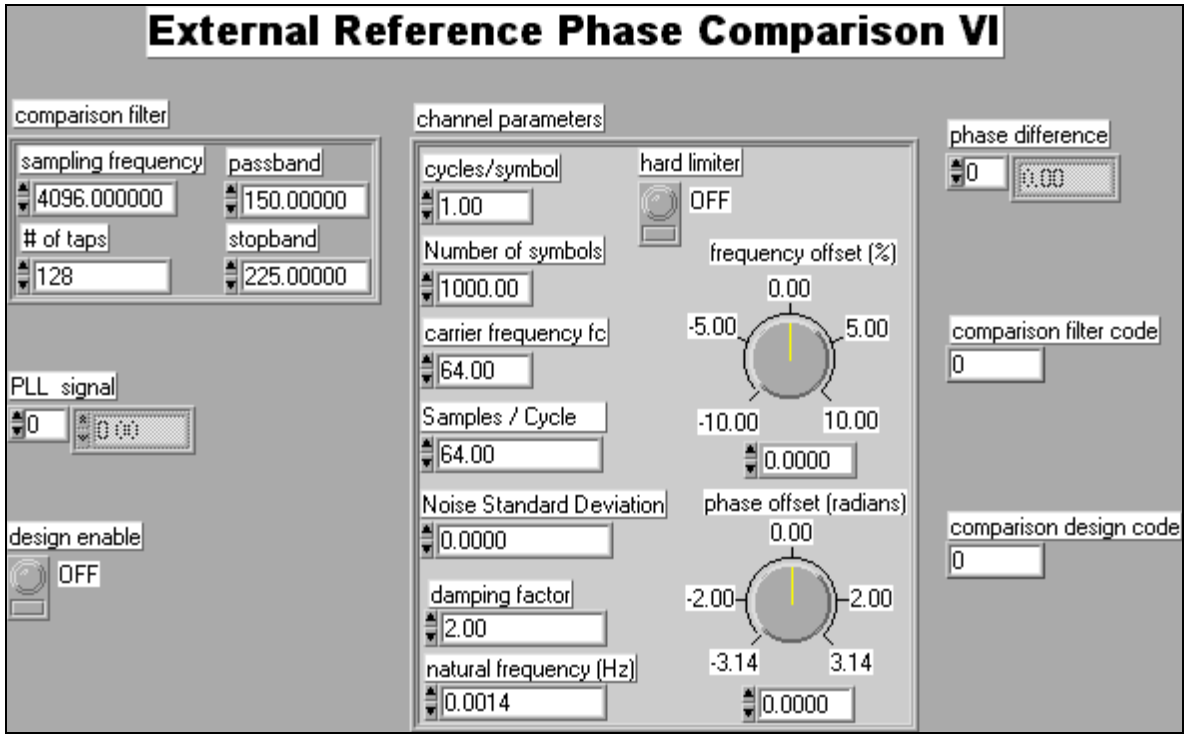

Figure C–16. External Reference Phases Comparison VI front panel.

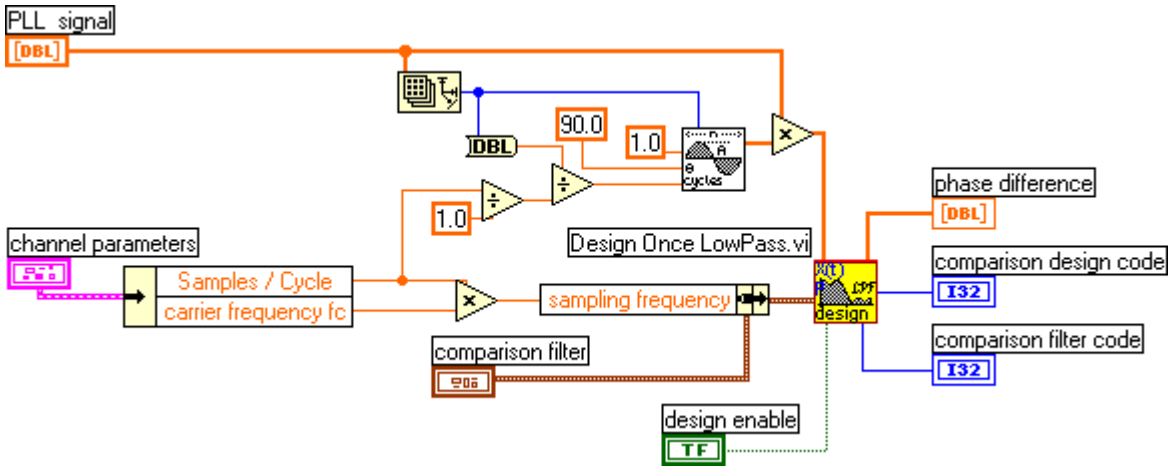

Figure C–17. External Reference Phases Comparison VI diagram.

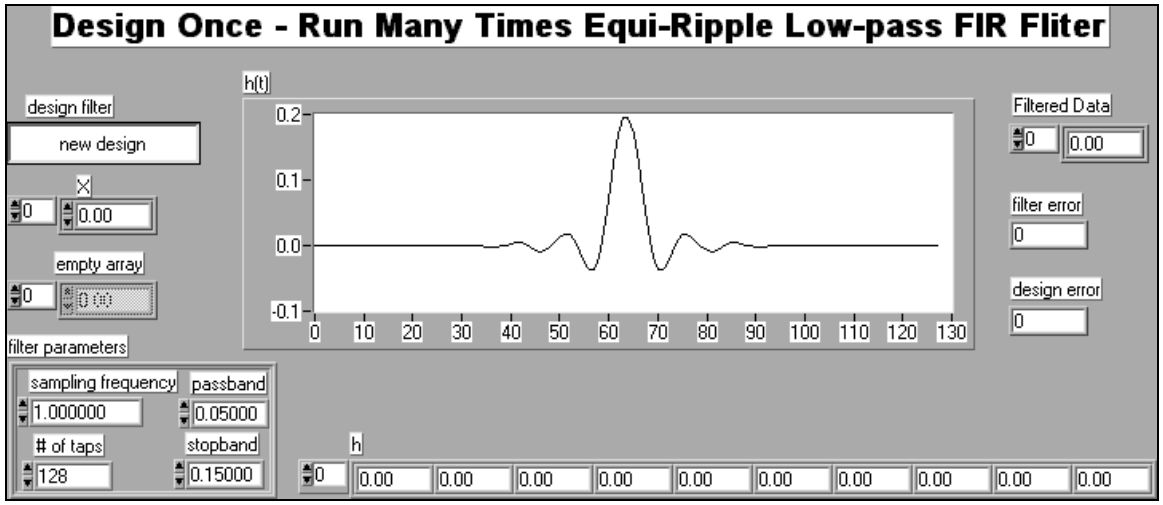

Figure C–18. Design Once Low-pass VI front panel

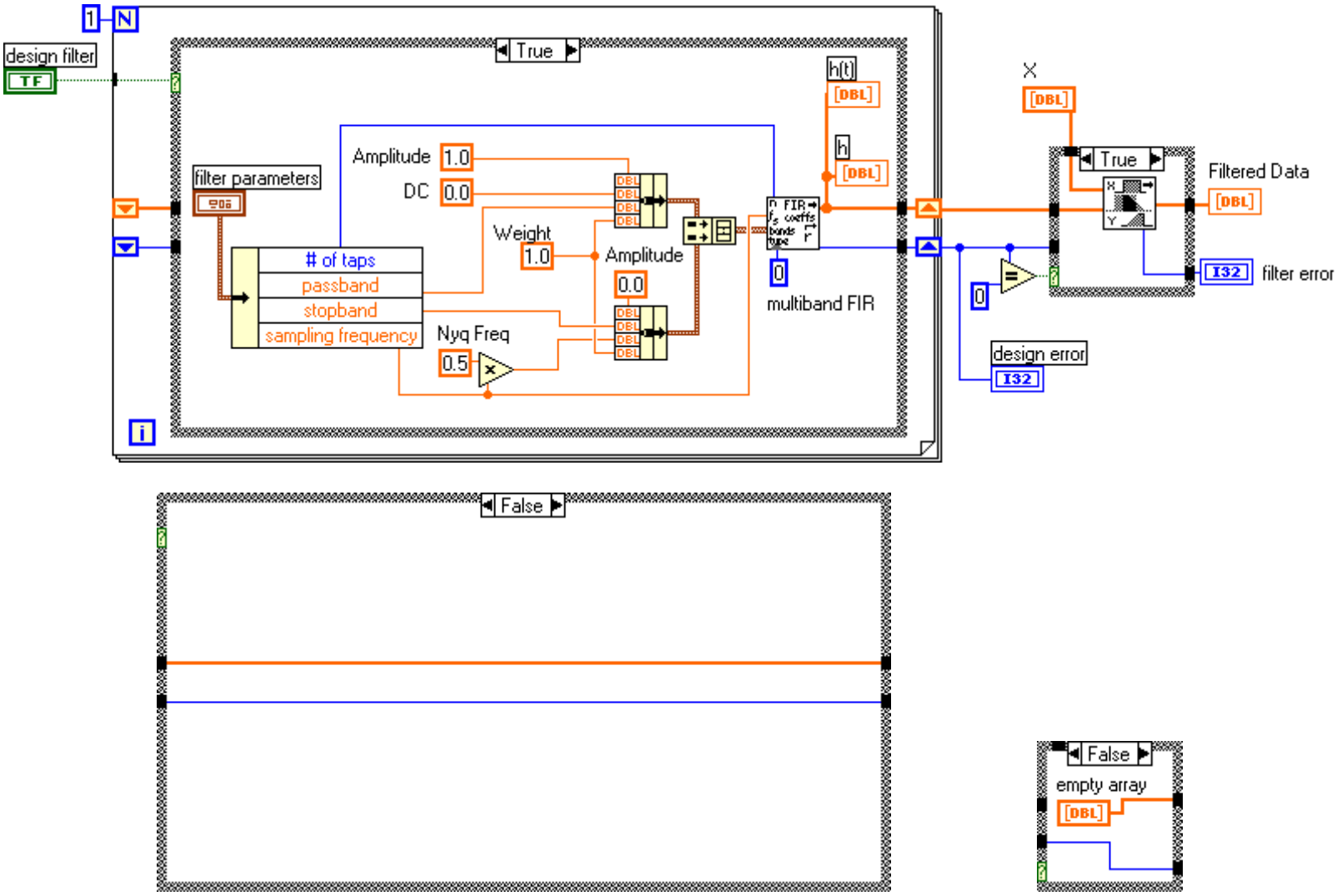

Figure C–19. Design Once Low-pass VI diagram.

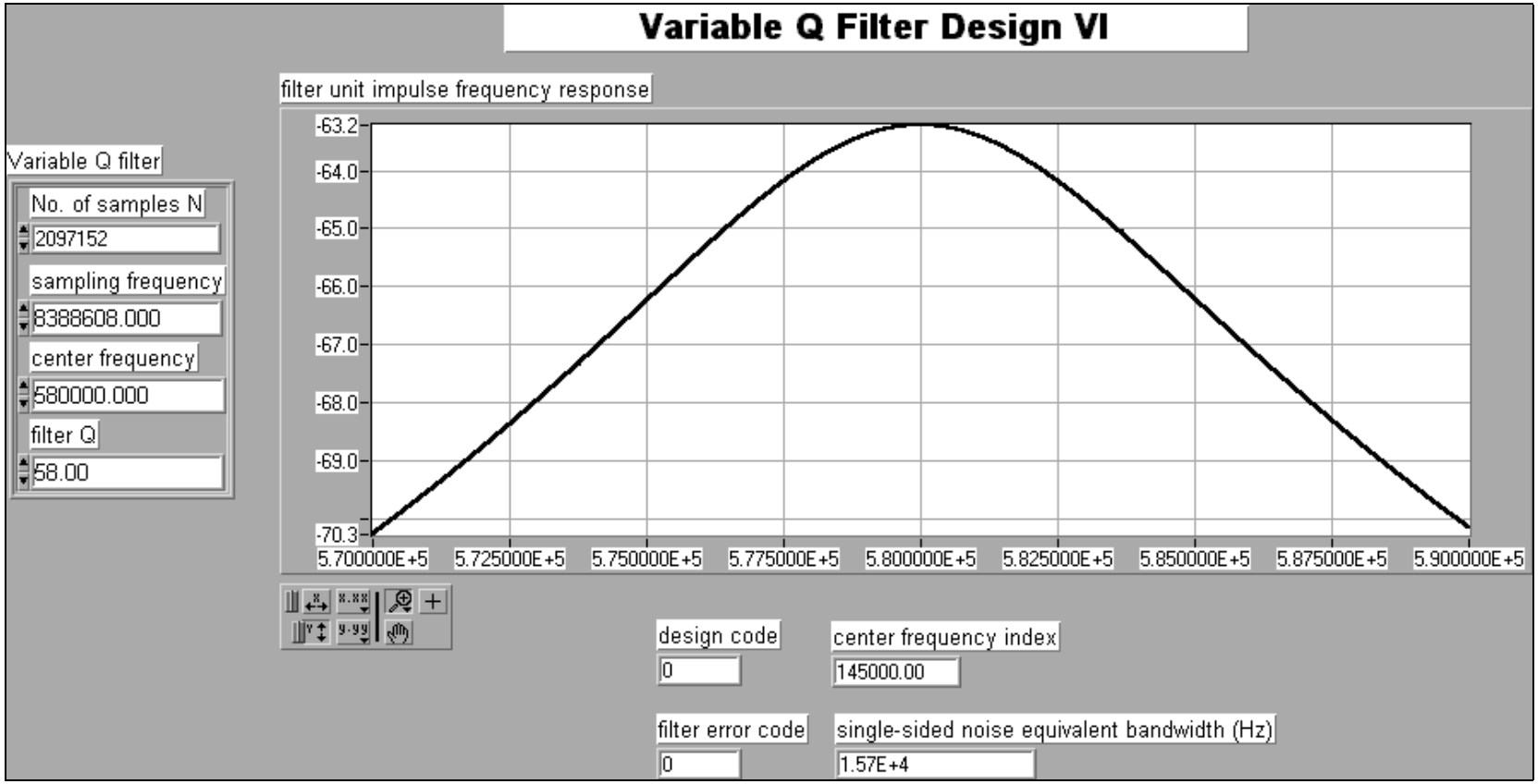

Figure C–20. Variable *Q* Filter Design VI front panel.

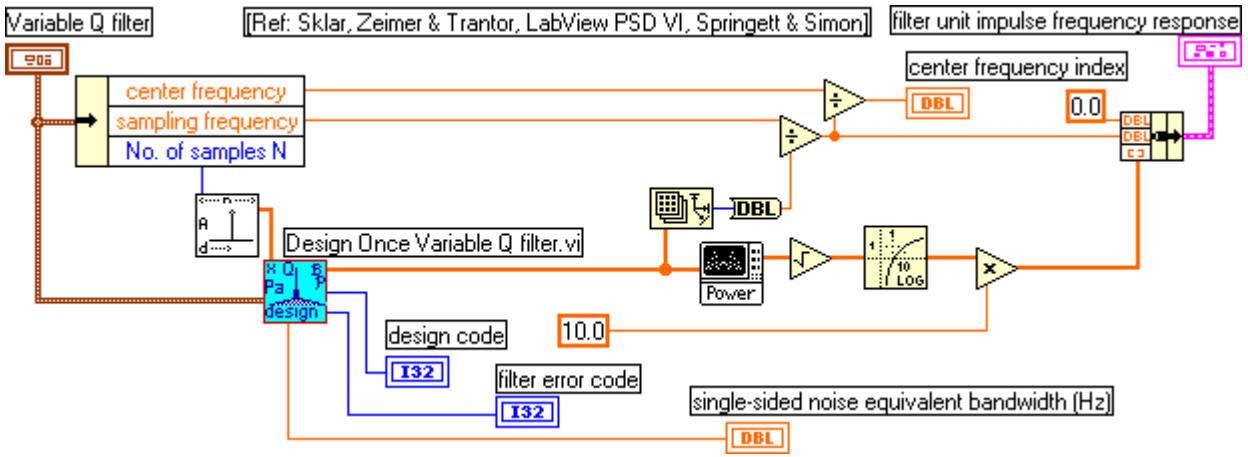

Figure C–21. Variable Q Filter Design VI diagram.

VITA

Gary Lynn Ragsdale was born in Paris, Missouri, on March 7, 1951. He attended elementary school in the Paris R-II School District graduating from Paris High School in May 1969. In September 1969, he enrolled at the University of Missouri, Columbia, and received a Bachelor of Science degree in Electrical Engineering in May 1973.

Mr. Ragsdale practiced as a Design Engineer at the Collins Radio Division, Rockwell International, for nearly five years. He served as a Design Engineer and Engineering Manager at Federal Express Corporation for fifteen years. He currently practices as a Principal Engineer at Southwest Research Institute.

Mr. Ragsdale entered the University of Tennessee, Knoxville, in June 1993. He received a Master of Science degree in Electrical Engineering in May 1995 and a Doctor of Philosophy degree in Electrical Engineering in May 2001.